

12-2009

IDENTIFICATION OF A CONSERVED CLUSTER IN THE RH DOMAIN OF GRK CRITICAL FOR ACTIVATION BY GPCRs

Faiza Baameur

Follow this and additional works at: https://digitalcommons.library.tmc.edu/utgsbs_dissertations



Part of the [Cell Biology Commons](#), and the [Pharmacology Commons](#)

Recommended Citation

Baameur, Faiza, "IDENTIFICATION OF A CONSERVED CLUSTER IN THE RH DOMAIN OF GRK CRITICAL FOR ACTIVATION BY GPCRs" (2009). *The University of Texas MD Anderson Cancer Center UTHealth Graduate School of Biomedical Sciences Dissertations and Theses (Open Access)*. 2.
https://digitalcommons.library.tmc.edu/utgsbs_dissertations/2

This Dissertation (PhD) is brought to you for free and open access by the The University of Texas MD Anderson Cancer Center UTHealth Graduate School of Biomedical Sciences at DigitalCommons@TMC. It has been accepted for inclusion in The University of Texas MD Anderson Cancer Center UTHealth Graduate School of Biomedical Sciences Dissertations and Theses (Open Access) by an authorized administrator of DigitalCommons@TMC. For more information, please contact digitalcommons@library.tmc.edu.

**IDENTIFICATION OF A CONSERVED CLUSTER IN THE RH DOMAIN OF GRK
CRITICAL FOR ACTIVATION BY GPCRs**

by

Faïza Baameur, M.S.

APPROVED:

RICHARD B. CLARK, Ph.D

CARMEN W. DESSAUER, Ph.D

JEFFREY A. FROST, Ph.D

OLIVIER LICHTARGE, M.D., Ph.D

JOHN S. McMURRAY, Ph.D

APPROVED:

Dean, The University of Texas
Graduate School of Biomedical Sciences at Houston

IDENTIFICATION OF A CONSERVED CLUSTER IN THE RH DOMAIN OF GRK
CRITICAL FOR ACTIVATION BY GPCRs

A DISSERTATION

Presented to the Faculty of
The University of Texas
Health Science Center at Houston
and
The University of Texas
M. D. Anderson Cancer Center
Graduate School of Biomedical Sciences
in Partial Fulfillment
of the Requirements
for the Degree of

DOCTOR OF PHILOSOPHY

By

Faïza Baameur, B.S., M.S.

Houston, Texas

December, 2009

DEDICATION

To Yamina Kerzabi

My grandmother, the only Mother I have known

ACKNOWLEDGEMENTS

My profound gratitude goes to “Docteur” Clark or “Dicky” for being the savior of lost souls. He took me under his wing despite my lack of proficiency in English and Biology. He supported, encouraged, guided, and helped me through my ups and downs. He is the best “Teacher”.

To Carmen Dessauer “The Queen” for being a great source of encouragement and inspiration, to Jeff Frost for all his suggestions and helpful tips over the years; thanks to both of them.

To Olivier Lichtarge, John McMurray, Kevin Ridge, Agnes Schonbrunn, Jian Kuang, David Loose, Mike Blackburn, and Thomas Rich, thanks for your guidance and support.

I would like to acknowledge Kevin Ridge for generously providing us with purified ROS and letting me use his equipment.

Thanks to Rasmus Jorgensen for providing us with all the human WT-GRK DNA plasmids; Daniel Morgan and Hui Yao for the trace analyses; and Richard Hammitt for making the peptides.

Thanks to my Clark family: Jackie Friedman for guiding me through my first steps in the lab and being so patient with me; Tuan Tran “Tuani” for helping and encouraging me through the years; Sharat Vayttaden “Vaytty” for being who you are, a wonderful friend.

Special thanks for my lab meeting group “the Dessauers and Frosts”, and the CRB and IBP family for all the help and support.

To Karolina Mueller, Julie Hauptman, Kendra “Kendy Girr” Carmon, Leslie Piggott, Humam Kadara, Heather Carr, Bao Nguyen, Rachna Sadana, Christina Papke, Kedryn Baskin, and Romain Harmancey, thanks for your friendship.

To the Marzoukis, my Houstonian “adoptive” family, I want to extend my gratitude.

Finally, I am so grateful to have such a wonderful family: Maryvonne and Elias Kerzabi the best aunt and uncle in the world and their sons, without whom I would have never made it to the US; Nabila Boukelmoune “Bilo” my sistah; Meriem, Saliha and Bachir Kerzabi for their love, support, and always being there for me.

IDENTIFICATION OF A CONSERVED CLUSTER IN THE RH DOMAIN OF GRK CRITICAL FOR ACTIVATION BY GPCRs

Publication No. _____

Faiza Baameur, B.S., M.S.

Supervisory Professor: Richard B. Clark, Ph.D.

One of the most critical aspects of G Protein Coupled Receptors (GPCRs) regulation is their rapid and acute desensitization following agonist stimulation. Phosphorylation of these receptors by GPCR kinases (GRK) is a major mechanism of desensitization. Considerable evidence from studies of rhodopsin kinase and GRK2 suggests there is an allosteric docking site for the receptor distinct from the GRK catalytic site. While the agonist-activated GPCR appears crucial for GRK activation, the molecular details of this interaction remain unclear. Recent studies suggested an important role for the N- and C-termini and domains in the small lobe of the kinase domain in allosteric activation; however, neither the mechanism of action of that site nor the RH domain contributions have been elucidated. To search for the allosteric site, we first identified evolutionarily conserved sites within the RH and kinase domains presumably deterministic of protein function employing evolutionary trace (ET) methodology and crystal structures of GRK6. Focusing on a conserved cluster centered on helices 3, 9, and 10 in the RH domain, key residues of GRK5 and 6 were targeted for mutagenesis and functional assays. We found that a number of double mutations within helices 3, 9, and 10 and the N-terminus markedly reduced (50-90%) the constitutive phosphorylation of the β -2 Adrenergic Receptor (β 2AR) in intact cells

and phosphorylation of light-activated rhodopsin (Rho*) in vitro as compared to wild type (WT) GRK5 or 6. Based on these results, we designed peptide mimetics of GRK5 helix 9 both computationally and through chemical modifications with the goal of both confirming the importance of helix 9 and developing a useful inhibitor to disrupt the GPCR-GRK interaction. Several peptides were found to block Rho* phosphorylation by GRK5 including the native helix 9 sequence, Peptide Builder designed-peptide preserving only the key ET residues, and chemically locked helices. Most peptidomimetics showed inhibition of GRK5 activity greater than 80 % with an IC_{50} of $\sim 30 \mu M$. Alanine scanning of helix 9 has further revealed both essential and non-essential residues for inhibition. Importantly, substitution of Arg 169 by an alanine in the native helix 9-based peptide gave an almost complete inhibition at $30 \mu M$ with an IC_{50} of $\sim 10 \mu M$. In summary we report a previously unrecognized crucial role for the RH domain of GRK5 and 6, and the subsequent identification of a lead peptide inhibitor of protein-protein interaction with potential for specific blockade of GPCR desensitization.

LAY SUMMARY

STUDY OF THE ADRENERGIC RECEPTOR DESENSITIZATION

Faiza Baameur, B.S., M.S.

In the Fight or Flight response to danger, the autonomic nervous system releases a flood of adrenaline and noradrenaline (also termed epinephrine and norepinephrine) that triggers many important biological reactions. One key response is the relaxation of bronchial smooth muscles through binding of adrenaline to the beta 2 adrenergic receptor; this leads to an increase of air flow into the lungs. Drugs that mimic this action, termed agonists, are clinically very important in the treatment of asthma and other diseases. As with most biological processes the effect of the drugs is limited by the desensitization process that involves enzymes (protein kinases) which modify the receptor making it less responsive. Our studies are aimed at identifying key structural hotspots on the kinases that are involved in activation by the beta 2 adrenergic receptor, and based on that knowledge the development of specific inhibitors of desensitization that could prolong the action of clinically important drugs. In the present study we have found one of the hotspots responsible for adrenaline activation of the kinases and based on this discovery developed an inhibitor that blocks the process of desensitization.

TABLE OF CONTENTS

APPROVAL PAGE	i
TITLE PAGE	ii
DEDICATION	iii
ACKNOWLEDGEMENTS	iv
ABSTRACT	v
LAY ABSTRACT	vii
TABLE OF CONTENTS	viii
LIST OF FIGURES	xi
LIST OF TABLES	xiii
ABBREVIATIONS	xiv
CHAPTER 1.	
INTRODUCTION	1
1.1 THE β2AR: STRUCTURE AND FUNCTION	2
1.2 β2AR REGULATION AND DESENSITIZATION	5
<i>1.2.1 The heterologous desensitization pathway</i>	5
<i>1.2.2 The homologous desensitization pathway</i>	5
1.3 THE GRKs: STRUCTURE, FUNCTION, AND REGULATION	7
1.4 SPECIFICITY OF GRKs IN β2AR DESENSITIZATION	10
1.5 EVIDENCE FOR GPCR-GRK INTERACTION	11
1.6 PEPTIDE MODULATORS OF GRK ACTIVITY	15
CHAPTER 2.	
FUNCTIONAL STUDIES OF THE GRK RH DOMAIN	18

2.1 INTRODUCTION	19
2.2 MATERIALS AND METHODS	20
<i>2.2.1 Cell culture</i>	20
<i>2.2.2 Evolutionary trace analysis</i>	21
<i>2.2.3 Mutagenesis of top-ranked residues</i>	22
<i>2.2.4 Intact-cell phosphorylation of the β2AR by WT or mutant GRK5/6</i>	24
<i>2.2.5 Preparation of GRK5/6 from 21K membrane fractions</i>	25
<i>2.2.6 Purification of GRK5 on SP-sepharose</i>	25
<i>2.2.7 In-vitro phosphorylation of light-activated rhodopsin by WT or mutant GRK5/6</i>	26
2.3 RESULTS	27
<i>2.3.1 Evolutionary Trace Analyses</i>	27
<i>2.3.2 Mutagenesis of top ranked residues in GRK RH domain</i>	32
<i>2.3.3 Constitutive phosphorylation of the β2AR</i>	33
<i>2.3.3.1 Effects of mutant KHE-GRK5</i>	34
<i>2.3.3.2 Effects of WT and mutant GRK5</i>	36
<i>2.3.3.3 Effects of WT and mutant GRK6</i>	42
<i>2.3.4 Phosphorylation of light- activated rhodopsin</i>	44
<i>2.3.4.1 Effects of WT and mutant GRK5</i>	44
<i>2.3.4.2 Effects of WT and mutant GRK6</i>	46
2.4 DISCUSSION	48
CHAPTER 3.	
DEVELOPMENT OF PEPTIDE INHIBITORS OF THE GPCR-GRK INTERACTION	52
3.1 INTRODUCTION	53

3.2 METHODS	53
<i>3.2.1 Computational design of peptides</i>	53
<i>3.2.2 Synthesis of chemically modified peptides</i>	56
<i>3.2.3 In-vitro peptide assay</i>	58
3.3 RESULTS	59
<i>3.3.1 Peptide inhibition of GRK5 phosphorylation of light-activated Rhodopsin</i>	59
<i>3.3.2 Kinetic analysis of peptide inhibition</i>	61
<i>3.3.3 Specificity of peptide inhibition</i>	62
<i>3.3.4 Effects of mutant peptide on GRK5 phosphorylation of Rho*</i>	63
<i>3.3.5 Effects of truncated peptide on GRK5 phosphorylation of Rho*</i>	65
3.4 DISCUSSION	66
CHAPTER 4.	
GENERAL SUMMARY	70
4.1 CONCLUSIONS	71
4.2 FUTURE DIRECTIONS	74
APPENDIX	77
1 EVOLUTIONARY TRACE RESULTS	78
2 LIST OF OLIGONUCLEOTIDE PRIMERS	102
3 SEQUENCE ALIGNMENT OF THE GRKs N-TERMINUS AND HELICES 3, 9, AND 10	104
BIBLIOGRAPHY	105
VITA	126

LIST OF FIGURES

CHAPTER 1.

Figure 1. Diagram of the β 2AR	3
Figure 2. Model of β 2AR desensitization	4
Figure 3. Structure of GRKs	8
Figure 4. Venn diagram of hypothetical contact sites between β 2AR and G protein, GRK, and β -arrestin	17

CHAPTER 2.

Figure 5. ET of the RH domain	28
Figure 6. ET of the Kinase domain	29
Figure 7. ET analysis mapped onto GRK6	31
Figure 8. Surface representation of ET residues mapped onto GRK6	32
Figure 9. β 2AR constitutive phosphorylation by overexpression of GRKs	34
Figure 10. Effect of the KHE-GRK5 mutations on constitutive β 2AR GRK site phosphorylation	35
Figure 11. Effect of GRK5 mutations on constitutive β 2AR GRK site phosphorylation	37
Figure 12. Expression levels and locale of mutant GRK5	38
Figure 13. Effect of GRK5 mutations on ISO-stimulated β 2AR GRK site phosphorylation	41
Figure 14. Effect of mutant GRK5 (S484A-T485A) on β 2AR and Rho* phosphorylation	42
Figure 15. Effect of GRK6 mutations on constitutive β 2AR GRK site phosphorylation	43
Figure 16. Effect of GRK5 mutations on Rho* phosphorylation	45

Figure 17. Effect of increased Rho and GRK5 concentrations on Rho* phosphorylation	46
Figure 18. Effect of GRK6 mutations on Rho* phosphorylation	47
Figure 19. Representation of the interaction between residues R68 and D85	51

CHAPTER 3.

Figure 20. Model of the Peptide Builder designed peptides	56
Figure 21. Sequence of chemically modified GRK5 helix 9 peptidomimetics	58
Figure 22. Peptide inhibition of GRK5 phosphorylation of Rho*	61
Figure 23. Kinetic analysis of peptide 6 inhibition of GRK5 phosphorylation of Rho*	62
Figure 24. Peptides 4 and 6 inhibition of GRK phosphorylation of Rho*	63
Figure 25. Mutant peptide inhibition of GRK5 phosphorylation of Rho*	65
Figure 26. Truncated peptide inhibition of GRK5 phosphorylation of Rho*	66

LIST OF TABLES

CHAPTER 1.

Table 1. Summary of effects of GRKs 1, 2, and 5 mutations	13
---	----

CHAPTER 2.

Table 2. List of mutations	23
----------------------------	----

CHAPTER 3.

Table 3. Sequences and modifications of the helix 9, GRK5/6 N-Terminus, and il-1 β 2AR peptides	54
---	----

APPENDIX.

Table A. ET analysis of the RGS superfamily	78
Table B. ET analysis of the RH domain of the GRK subfamily	82
Table C. ET analysis of the AGC kinases superfamily	86
Table D. ET analysis of the kinase domain of the GRK subfamily	93

ABBREVIATIONS

AC	Adenylyl cyclase
AGC Kinase	Protein kinase A, G, and C
AMPPNP	5'-adenylyl β,γ -imidodiphosphate
AT	ascorbate / thiourea
ATP	Adenosine triphosphate
β ARK	β Adrenergic receptor kinase
β 2AR	β 2 Adrenergic receptor
BRET	Bioluminescence Resonance Energy Transfer
cAMP	cyclic adenosine monophosphate
GDP/GTP	Guanosine diphosphate/triphosphate
COPD	Chronic obstructive pulmonary disease
DTT	Dithiothreitol
DMSO	Dimethyl sulfoxide
DMF	N, N-dimethylformamide
EC ₅₀	Half maximum effective concentration
EDTA	Ethylenediaminetetraacetic acid
EPAC	Exchange protein activated by cAMP
ET	Evolutionary Trace
DMEM	Dulbecco's modified Eagle's medium
FRET	Fluorescence Resonance Energy Transfer
GFP	Green Fluorescent Protein

GPCR	G protein-coupled receptor
GRK	G protein-coupled receptor kinase
GST	Glutathione S-transferase
HEK	Human embryonic kidney
HPLC	High performance liquid chromatography
IC ₅₀	Half maximum inhibitory concentration
il-1	intracellular loop 1
ISO	Isoproterenol
MAPK	Mitogen activated protein kinase
mGluR1	Metabotropic Glutamate receptor 1
PAGE	Polyacrylamide gel electrophoresis
PBS	Phosphate-buffered saline
PDB	Protein data base
PDE4D	Phosphodiesterase type 4D
PGE1	Prostaglandin E1
PH	Plextrin homology
PIP ₂	Phosphatidylinositol 3,4-bisphosphate
PI3K	Phosphoinositide 3-Kinase
PKA	Protein kinase A
PKC	Protein kinase C
PL-DMA	Polydimethylacrylamide base
PNGaseF	Peptide N-glycosidase F
RGS	Regulator of G protein signaling

RH	RGS homology
Rho	Rhodopsin
ROS	Rod outer segments
SDS	Sodium dodecyl sulfate
TFA	Trifluoroacetic acid
U2-OS	U2-Osteosarcoma
WT	Wild type

CHAPTER 1
INTRODUCTION

1.1 THE β 2AR: STRUCTURE AND FUNCTION

The adrenergic receptors are members of the G Protein-Coupled Receptors (GPCR) family, the largest superfamily of proteins encoded in the human genome. Structurally, the GPCRs consist of seven transmembrane α -helical domains connecting an extracellular N-Terminus and an intracellular C-Terminus through three extracellular and three intracellular loops (Figure 1). They are divided into subclasses based on sequence homology and pharmacology. The adrenergic receptors (AR) are class A GPCRs (Rhodopsin-like receptors), the most extensively studied class (1). ARs are targets for endogenous catecholamines (epinephrine and norepinephrine) and for many medications, leading to either their activation or blockade. The ARs are widely distributed in the body, and the binding of an agonist generally causes a “fight or flight” response. There are nine adrenergic receptors which are divided into two subfamilies, the α 1- and α 2-receptors (three of each) and the β -receptors (β AR) of which there are three subtypes (β 1, β 2, and β 3) (2). Our research group focuses on the understanding of the mechanisms of the β 2AR activation and desensitization.

The β 2AR is expressed in many tissues and it plays a central role in relaying signals from the autonomic sympathetic nervous system to, most notably, the cardiovascular and pulmonary systems where β 2AR activation causes an increase in heart contraction, and relaxation of lung tracheal smooth muscle (3). Numerous agonists of the β 2AR such as albuterol, salmeterol and formoterol are used in the treatment of asthma and chronic obstructive pulmonary disease (COPD) causing vasodilation of tracheal smooth muscle.

β AR antagonists such as metoprolol and propranolol used in the treatment of hypertension, though mainly acting on β 1ARs also inactivate the β 2AR (3, 4).

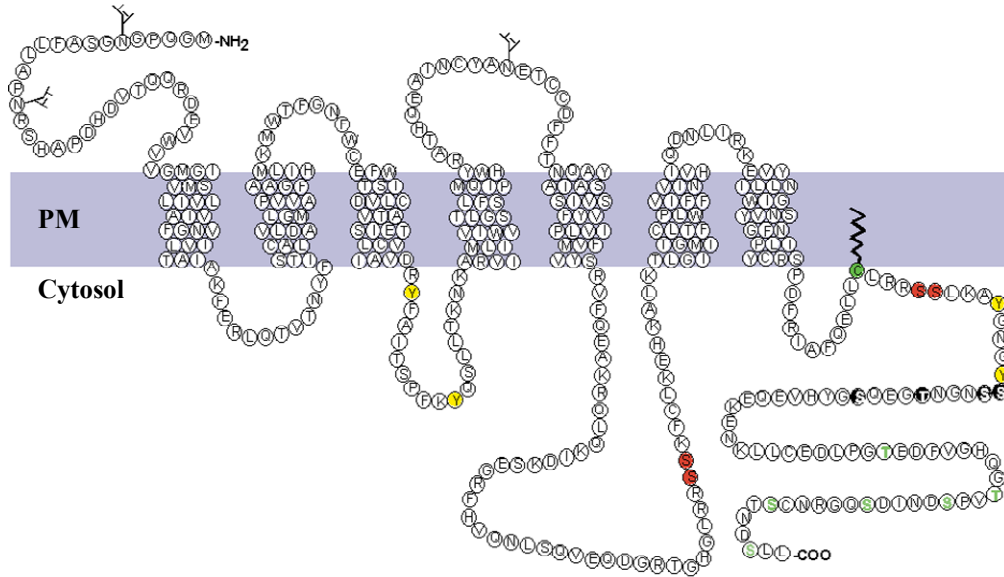


Figure 1. Diagram of the β 2AR. The figure shows the amino acid sequence of the receptor. The plasma membrane is represented in blue. GRK phosphorylation sites (S355, S356, T360, S364), PKA (and PKC) phosphorylation sites (S261, S262, S345, S346) are highlighted in black and red respectively. Yellow residues are tyrosine phosphorylation sites (5, 6). Palmitoylation site C341 is shown in green (7). Residues shown in green letters were previously reported as GRK phosphorylation sites (8), but subsequent studies showed these were not correct (9, 10).

Agonist binding to and activation of the β 2AR promotes its signaling and desensitization through complex cellular events (11). The mechanism of β 2AR activation of adenylyl cyclase occurs through activation of the stimulatory G protein (G_s) which releases GDP and binds GTP upon agonist-activation of the receptor. G_s is a heterotrimeric protein comprised of the subunits ($\alpha\beta\gamma$), which upon activation stimulates in a complex manner

various isoforms of adenylyl cyclase (AC). AC activation in turn generates cyclic adenosine monophosphate (cAMP) that activates Protein Kinase A (PKA), ion channels, and EPAC regulating many downstream pathways (12). Agonist activation of the β 2AR leads essentially to two desensitization pathways known as the heterologous PKA-dependent pathway which is a G protein dependent pathway (13), and the homologous G Protein-Coupled Receptor Kinase (GRK)-dependent, a G protein-independent pathway (14, 15). Figure 2 illustrates these pathways. However, other studies also involve the β 2AR-induced activation of the Mitogen Activated Protein kinase (MAPK) (16) a G protein-independent pathway; as well as a tyrosine kinase Src-dependent pathway (17).

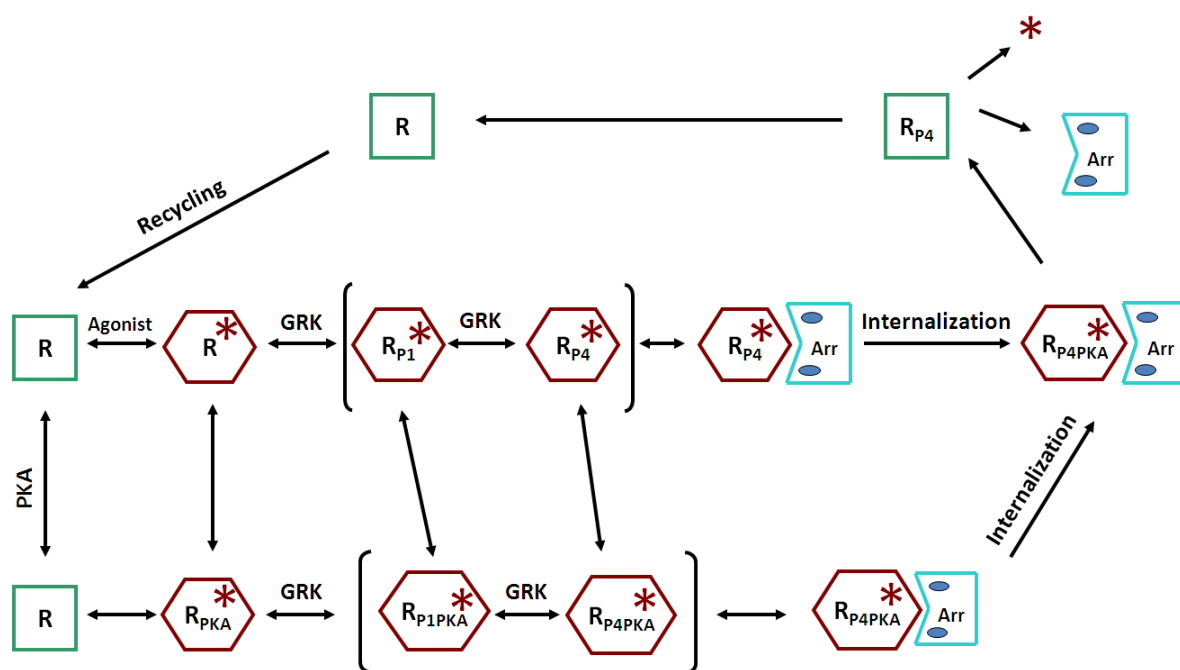


Figure 2. Model of β 2AR desensitization. Both heterologous (PKA-dependent) and homologous (GRK-dependent) pathways are represented. R: receptor; Arr: β -arrestin. P1PKA: p-S262; P4: p-S 355, 356, 364 and p-T 360.

1.2 β 2AR REGULATION AND DESENSITIZATION

1.2.1 The heterologous desensitization pathway

Original studies of the β 2AR in wild type (WT) S49 lymphoma cells showed that β 2AR agonist or PGE₁ activation caused a two- to three-fold increase in the EC₅₀ for epinephrine stimulation of AC, while no change was observed in cells lacking either PKA or AC (18). This process known as heterologous desensitization was attributed to elevated intracellular cAMP and subsequent activation of PKA. Our group found that the activated PKA phosphorylates the β 2AR primarily at serine 262 in intracellular loop 3 (13, 19), although there is some indirect evidence for phosphorylation of residue S346 in the C-terminus (20). Both are sites compatible with the consensus pattern for phosphorylation by PKA (RRxSR/K). In addition to regulation of the β 2AR, PKA has been shown in many systems to activate phosphodiesterase (PDE4D subtype in our system). This action along with receptor phosphorylation, combine to generate a negative feedback on β 2AR function (21, 22).

1.2.2 The homologous desensitization pathway

In an early study our group demonstrated that saturating levels of epinephrine stimulation of the β 2AR caused desensitization of the receptor in S49 lymphoma cell that lacked AC, suggesting that neither Gs nor increased cAMP levels were required in this process (15, 18). This mode of desensitization is known as the homologous desensitization (23), as it depends on relatively high occupancy of the receptor by a strong agonist (EC₅₀ = 30-50 nM), and is closely correlated with the internalization of the receptor. Stimulation of

the receptor causes the rapid activation of GRK in a G protein-independent manner. GRK in turn phosphorylates at least three serine residues in the proximal C-terminus of the receptor, namely S355, S356, and S364. Identification of these three residues for GRK-mediated desensitization was shown through mutagenesis studies. Substitution of these residues with alanine, singly and in various combinations, in a receptor lacking the PKA consensus sites severely impaired desensitization (9). The S-(355, 356) site has been further characterized by the use of a phosphosite-specific antibody directed against pS-(355,356) (10). The EC₅₀ for epinephrine-induced phosphorylation of the GRK site was 200 nM following a 1 min treatment, or 30 nM with 10-30 min treatment (Tran 04). Mass spectrometric analyses further confirmed a stoichiometry of phosphorylation of the β 2AR C-terminal fragment (residues 339-369) of 2 mol of phosphate / mol β 2AR in the presence of saturating levels of agonist (10 μ M isoproterenol (ISO)) and 1 mol of phosphate/ mol β 2AR in the absence of agonist (24). These findings along with their finding of 1 mol of phosphate / mol β 2AR in the third intracellular loop are consistent with our group's previous characterization of S355, 356, and 364 as the major GRK phosphorylation sites, and S262 as the major PKA phosphorylation site, although this group did not sequence the peptides in their mass spectrometry study.

Notably, GRK phosphorylation of the β 2AR causes little desensitization. Rather, the agonist-occupied and GRK-phosphorylated receptor recruits β -arrestin (arrestins 2 & 3), leading to the termination of the signal as it physically uncouples the receptor from Gs (25, 26). Further, the β 2AR-arrestin complex then interacts with clathrin-coated pits involving the adaptor protein AP-2 leading to receptor internalization or endocytosis (27). This process occurs with a rate of 0.22 / min (10). The EC₅₀ for internalization is very similar to that for

GRK-mediated phosphorylation (~ 100 nM) (28). Dephosphorylation of the GRK-phosphorylated receptor was proposed to occur only in endosomal vesicles following internalization (29). However, our group has demonstrated that dephosphorylation of both GRK and PKA sites in HEK293 cells can also occur at the plasma membrane (30), with a slow rate of ~ 0.04 / min. The specific phosphatase(s) involved remains an open question as phosphatase inhibitors are insufficiently specific enough to resolve this question, although both PP2A and PP1 blockade are possibilities (30, 31).

The fate of the internalized receptor is either recycling (0.091 / min) (10) to the cell surface in a fully sensitized state (32), or downregulation where receptor is targeted to lysosomes for degradation ($0.002 - 0.004$ / min) (33, 34). Our group has also shown that the rapid phase of resensitization of ISO-stimulated AC activity was much faster than GRK site dephosphorylation, occurring with a rate of ~ 0.44 / min. We have proposed that dissociation of these two events is attributable to the rapid dissociation of β -arrestin upon agonist removal (25), and that the persistent GRK phosphorylation on its own causes little desensitization (30). Additionally, kinetic modeling done by Sharat Vayttaden in our group shows that surface dephosphorylation as well as recycling of phosphorylated receptor are necessary to account for the measured dephosphorylation and resensitization rates (submitted for publication).

1.3 THE GRKs: STRUCTURE, FUNCTION, AND REGULATION

The serine/threonine G protein-coupled receptor kinase family includes seven members, GRK1-7, classified into three subfamilies on the basis of their sequence

homology, the rhodopsin kinase subfamily (GRK1 and 7) in the visual system, the β Adrenergic Receptor Kinase (β ARK) subfamily (GRK2, and 3), and the GRK4 subfamily (GRK4-6) (35-37). GRKs share common structural features. They all consist of a moderately conserved N-terminus RGS Homology (RH) domain (~ 185 amino acid residues), a highly conserved central kinase domain (~ 270 amino acid residues), and a poorly conserved C-terminal domain of variable length (100-230 residues) that includes a Plextrin Homology (PH) domain for only the β ARK (GRK2 and 3) subfamily (38). The C-terminus of the various GRKs is a key determinant for localization and/or translocation of the kinase to the membrane where their GPCR substrates are located (Figure 3). Among the GRKs only GRK2, 3, 5 and 6 are widely expressed in mammalian tissues; GRK1, 7 and 4 tissue distribution is limited (37).

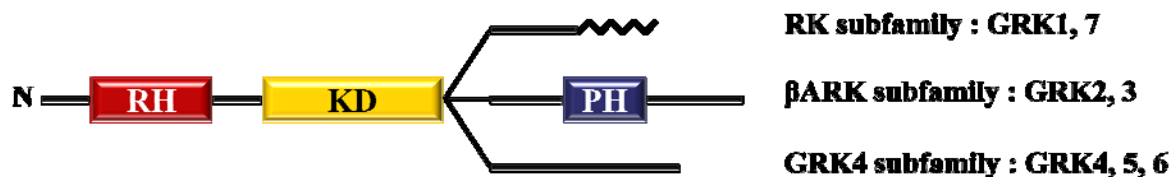


Figure 3. Structure of GRKs.

The PH domain of GRK2 and 3 has been shown to bind tightly to the G $\beta\gamma$ subunit which is presumably released in response to activation of the G protein by the stimulated GPCR, hence mediating GRK translocation to the plasma membrane (39). All other GRKs exhibit a constitutive association with the plasma membrane; the rhodopsin kinases contain a CAAX motif which undergoes an isoprenylation modification (40, 41), whereas splice variants of GRK4 and GRK6 are palmitoylated at cysteine residues which plays a role in anchoring them to the membrane (42-44). The non-palmitoylated variants may differ in their

regulation (45). GRK5 does not appear to undergo lipid modification, yet it is tightly bound to membrane phospholipids through a basic region (552-562) in its C-terminus (46, 47). All GRK4 subfamily members contain a phosphatidylinositol-4,5-bisphosphate (PIP₂) binding site that also contributes to membrane binding and activation (48, 49), and a nuclear localization sequence at their N-terminus, which confers a potential nuclear function (50), as it has been shown recently that GRK5 phosphorylates histone deacetylase in rat myocytes (51).

These kinases appear to play a role beyond the regulation of GPCRs; that is they are known to phosphorylate non-receptor substrates such as β -arrestin (52), tubulin (53), synuclein (54), and epithelial Na⁺ channel (55) to name a few although the physiological relevance is unknown. Furthermore, GRKs may modulate cellular functions in a phosphorylation-independent manner by interacting with a variety of proteins involved in signaling and trafficking; e.g., G α q (56), caveolin (57), G $\beta\gamma$, and PI3K (58); and may serve as scaffolds (59). Additionally, GRK isoforms undergo differential modifications which regulate their activity, such as phosphorylation by protein kinases PKA, PKC, and c-Src (58, 60-62), autophosphorylation (46, 63, 64), and association with calcium-sensing proteins (65, 66). These studies have been for the most part accomplished by the use of heterologous systems where rhodopsin phosphorylation has been assessed; however, there is a marked reduction in the apparent affinity of GRKs for rhodopsin relative to the rapid GRK phosphorylation of their cognate receptors in intact non-visual cells. In the light of these studies, GRK activity is not only regulated by GPCRs, but subcellular localization, expression levels in the different cells and tissues, alterations in intrinsic activity by protein

kinases and other proteins, and autophosphorylation also constitute important aspects of the mechanism of GRK regulation (67).

Importantly, crystal structures of GRK1, 2, and 6 representatives of the three subfamilies in the inactive state have been resolved by the Tesmer group. GRK2 was first crystallized in complex with the $\beta\gamma$ subunits of the G protein (68, 69), and later in complex with both $G\beta\gamma$ and the α subunit of Gq at two distinct sites of the RH domain (70), providing further support to earlier studies which reported the interaction of both GRK2 and 3 with G protein subunits (56, 71, 72). Subsequently, crystal structures of GRK6 complexed with AMPPNP as well as that of GRK1 in different ligand bound states were defined (73, 74). Although these structures revealed key elements in GRK regulation, the sites of GPCR interactions with the GRKs, and the transition to the active state conformation remain poorly defined.

1.4 SPECIFICITY OF GRKs IN β 2AR DESENSITIZATION

Since the cloning of the first member of the GRK family (GRK1), structure, function, activation and regulation of these kinases have been the subject of numerous studies. However, little is known about which GRKs in different cell types are involved in regulating their substrate receptors (75). Though, GRK1-6 have all been shown to phosphorylate the β 2AR (35, 36, 76-79), GRK2 has been considered the dominant activity in β 2AR desensitization (80), as it translocates to the plasma membrane through its binding to $G\beta\gamma$ (35, 80) and interference with $G\beta\gamma$ action impairs β 2AR desensitization. Alone this aspect does not contribute directly to the question of the relative role of GRK2 in β 2AR

desensitization relative to other GRKs. A number of other studies have attempted to identify the specific GRK(s) that mediate β 2AR phosphorylation. These include knockdown of different GRKs in HEK293 and U2-OS cell lines (81), use of inhibitors (82, 83), overexpression systems (84), transgenic mice (85), and knockouts approaches (37, 80). These findings and related studies of several other GPCRs were the basis of the proposal that different GRKs may phosphorylate unique sets of sites on GPCRs. In spite of all these research efforts the identity of the predominant GRK involved in physiological regulation of β 2AR remains under question, although the Lefkowitz group has implicated GRKs 2-6. This issue is compounded further by the expression level and localization of the GRKs in the different cell types and tissues.

Recent work from our group demonstrated that GRK5 plays a major role in β 2AR GRK site phosphorylation in HEK293 and COS7 cells. This was verified by a cell-free membrane assay, Bioluminescence Resonance Energy Transfer² (BRET²) analyses, and overexpression of GRKs 2, 5, and 6 (86); and is discussed in detail in the next chapter as we explore domains of GRK5 and 6 that may be involved in β 2AR activation of these kinases.

1.5 EVIDENCE FOR GPCR-GRK INTERACTION

In order to understand the mechanism underlying the activation of GRK by the agonist-activated β 2AR, it is essential to investigate the molecular details of the interaction between these two proteins, concerning which domains of the GRK and the receptor are required for their interaction, and as noted above, at present little is known. An original study by Palczewski et al., showed that an enzymatically truncated rhodopsin (Rho) that

lacks the C-terminal phosphorylation sites ($^{329}\text{G-Rho}^*$) was able to stimulate GRK1 phosphorylation of a peptide substrate indicating that the $^{329}\text{G-Rho}$ could bind an allosteric site of GRK1 removed from the catalytic domain (87). Moreover, studies based on site-directed mutagenesis and generation of deletion mutants of rhodopsin kinase and GRK2 further demonstrated the existence of an allosteric binding site of GPCRs to GRKs in addition to the obvious catalytic binding site (88, 89). Other studies have been reported on identification of GRK(s) sites responsible for interaction with GPCRs, many of which involved the N- and C-termini.

It was first shown that an antibody directed against residues (17-34) in the N-terminus of rhodopsin kinase inhibited phosphorylation of Rho^* , but not of a peptide substrate, suggesting the N-terminus is important in recognizing the active Rho (89). A GRK2 N-terminal fragment (residues 45-178) was shown to be sufficient to cause desensitization of the metabotropic glutamate receptor 1 (mGluR1) (90). Later this same group showed that a single residue, D527, localized to the C-terminus was essential for the GRK2-mGluR1 interaction (91). Moreover, mutations within the N-terminus of GRK5, namely L3Q-K113R and T10P as well as the deletion of the amino-terminal portion (residues 2-14), were shown to release the inhibition of the pheromone-activated growth in a yeast based bioassay and to significantly decrease both Rho^* phosphorylation and phospholipid-activated GRK5 autophosphorylation (92). This was attributed to loss of GRK5 binding to the phospholipids. A C-terminal amphipathic helix was also shown to mediate membrane localization of GRK5 through hydrophobic residues, as alanine and glutamine substitutions of L550, L551, L554, and F555 failed to localize to the plasma membrane and reduced GRK5 autophosphorylation and phosphorylation of Rho^* (93).

Another study involved a proline-rich motif within the C-terminus of GRKs 1, 2, and 5; this was shown to mediate kinase association with the light-activated rhodopsin (71, 72). Very recently, based on the crystal structure of GRK1 that includes the previously undetermined structures of the N- and C-termini, Singh et al., suggested that the site composite of the N-terminus, the C-terminal extension of the kinase domain and the small lobe of the kinase domain proximal to the hinge region, serves as the allosteric receptor docking site (74). Despite all these efforts, resolution of the allosteric interaction site on GRKs has not been forthcoming. These findings are summarized in Table 1.

Table 1. Summary of effects of GRKs 1, 2, and 5 mutations

GRK1	GRK2	GRK5	Results	ET rank	Ref
GRK1					
N-Ter (17-34)			Antibody inhibits Rho* phos.		(89)
S488A-T489A	x*	S484,T485	Autophos. (-) [#] ; Rho phos. (+) [#]	x	(94)
K491A	K494	K487	Peptide substrate phos. (-)	x	(94)
S21	K19	G18	PKA site; Rho phos. (-)	x	(62)
F3A, L6A, V9A, V10A, S13A, F15A	M1, L4, V7, L8, V11, Y13	x, L3, I6, V7, T10, L12	Recoverin binding (-) No effect on activity	x	(95, 96)
N-Ter (5-30), C-Ter extension of KD			Suggested receptor docking site		(74)
S5, T8	D3, A6	E2, N5	Autophos. No effect on Rho phos.	x	(74)
Helix 9			Dimer in crystal structure		(74)
R191A/K	R195A	R190A	Activity (-); Rho phos (-)	1	(97)
Δ N-Ter (1-19)			Activity (-)		(97)
GRK2					
Q107, x, Q117, A123, L125	R106A, F109I, D110A, E116A, L118A	L102, x, x, K113, P115	Gαq binding (-)	11.23, x, x, 9.85, 8.18	(72, 98, 99)
R31	S29	K28	PKC site; Rho phos. (+)	4.95	(100)
x	S685	x	PKA site, β2AR phos. (+)	x	(101)
	N-Ter (45-178)		mGluR1 binding (+); signaling (-)		(90)
G529	D527A	K522	mGluR1 binding (-)	x	(91)
x	K567A, W576A, R578E, R579A	N562 T571 F573 N574	β2AR phos. (-)	x	(102)

x	K663-, K665-, K667-, R669-E/Q	x	Gβγ response (-)	x	(69, 102)
	N-Ter (1-185) and (1-53)		Gβγ binding (+)		(69, 103)
F15, W89, Y95	Y13, Y86, Y92	L12, L84, Y90	c-Src sites; Gαq binding (+)	x, 3.59 , 3.8	(104)
K46, S49, x, E518	V42E, Y46A, P638D, E520A	Q41, L45, x, E514	Rho phos. (-); expression (-)	7.79, 1.66 , 2.35	(68)
V478	V477D	V472	Activity (-); Rho, β2AR phos. (-)	2.9	(105)
S5, L6, N12	D3K, L4A, D10A	E2, L3, N9	Activity (-); Rho, β2AR phos. (-)	x	(106)
GRK5					
S488, T489	x	S484A-T485A	Autophos. (-); Rho phos. (-)	x	(46, 79)
S27, P29, R31, K33, K34, Q28	T23, A25, R27, S29, K30, P24	K(22-24-26-28- 29)A + R23A	PIP ₂ binding (-); actin binding (-)	x, x, x, 4.95 , 4.19 , x	(49, 107)
		N-Ter (20-39)	Calmodulin binding (+)		(61)
L6, Q117, S13	L4, E117, V11	L3Q-K113R, T10P	Rho phos. (-); PIP ₂ binding (-)	x, 9.85, x	(92)
G558, M559, V562 S563	L555, G556, C559, I560	L550A-L551A- L554A-F555A (4A) or (AALF) or (LLAA)	PM localization (-); Rho phos. (-); autophos. (-)	x	(93)
P(467-468-471)A	P(467-468-469- 472)A	P(463-464-467)A	Rho phos. (-)	1.7 , 1.7 , 1.7	(108)
R394, G395, K397, E399, N400	H393, K394, K396, K398, H399	R388A-K389A- K391A-K393A- R394A	Nuclear exclusion	4.55, 2.24 , 1.69 , 4.09, 4	(50)
K46	V42	Q41L polymorphism	β2AR desensitization (+)		(109)

Residues corresponding to those examined (black) in either one of the GRKs are shown in blue

Ranks for important residues are given in red

** Unavailable ranks or residues in the corresponding GRKs are represented by “x”*

(-) and (+): negative and positive effects respectively

Phos. : phosphorylation; KD: Kinase Domain; Ter: Terminus

Another intriguing aspect of GRK structure, function, and regulation derives from increasing evidence that expression levels and mutations of the GRK family may lead to

disease states, mainly in the cardiovascular system where GRK2 and 5 are mostly expressed (110-115). Elevated GRK protein expression and or mRNA level or deficiency of specific GRKs in both animal models and humans, were associated with many diseases (Heart failure, myocardial ischemia, hypertension, rheumatoid arthritis, and hypothyroidism to cite a few) as reviewed by Metaye et al. (85). However, recently a GRK5 polymorphism (Q41L) that appears to have increased activity resulting in greater desensitization of the β 2AR was found to protect against congestive heart failure through blockade of the β AR signaling (109). We have also found a mutation in the RH domain that increases GRK5 activity and that we will discuss in chapter 2.

1.6 PEPTIDE MODULATORS OF GRK ACTIVITY

Disruption of protein-protein interaction is one of the most common approaches used in analyzing protein contact sites. This provides a unique perspective in understanding mechanisms regulating protein-protein interaction and ultimately developing tools to inhibit that interaction. Various kinds of inhibitors have been used to study GPCR regulation of GRK including pharmacological agents e.g. H7; or poly-anions and -cations e.g. dextran sulfate, heparin, polylysine (116). However these compounds are more likely to inhibit the catalytic activity rather than blocking the site of interaction with the GPCR, and further, they lack specificity. One way to circumvent this is through development of peptide disruptors mimicking interaction domains of GPCR-GRK. This is exemplified by the original work of Benovic et al., in which they synthesized peptides mimicking each of the intra- and extra-cellular loops as well as two portions of the C-terminus of the β 2AR and were able to show

in a reconstitution system that the intracellular loop 1 (il-1) (residues 56-74), and C-terminal portion (residues 219-243) peptidomimetics inhibited GRK2 phosphorylation of the receptor with IC_{50} s of 40 and 76 μ M respectively (117), suggesting that multiple β 2AR sites may be involved in its interaction with GRK as modeled in Figure 4. Subsequently, modification of the il-1 peptide sequence by either truncations or addition of charged residues led to a more potent peptide that inhibited GRK2, 3, and 5 activities with IC_{50} s of 0.6, 2.6, and 1.6 μ M respectively (83). This peptide was further shown by Xin et al. to inhibit the desensitization of the endogenous β 2AR in HEK293 cells (22). Moreover, inhibitors of the $G\beta\gamma$ interactions with various effectors were developed based on the identification of the $\beta\gamma$ “hotspot”, and they may serve as potential therapeutic agents (118). Importantly, recent complementary studies, one involving the isolation of a stable Rho*- Gt (transducin) complex (119), and the other the resolution of the crystal structure of the G α t C-terminus bound to opsin* (120), provided molecular insights on how GPCRs interact with their partner proteins (G protein, GRK, Arrestin). These studies provide evidence that peptide mimetics of interaction sites can modulate protein function/regulation. Similarly, Pao et al., showed that the amino-terminal peptide of GRK2 (residues 1-14) inhibited non-competitively β 2AR* and Rho* phosphorylation by GRK2 (106). Collectively, these pioneering studies lay groundwork for development of specific and effective inhibitors of GRKs.

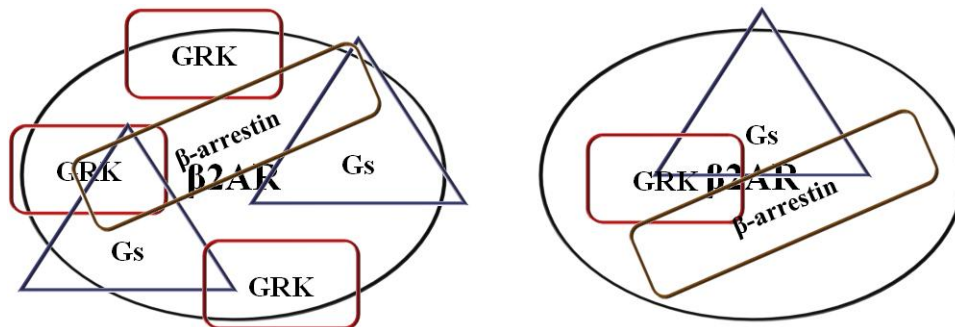


Figure 4. Venn diagram representing hypothetical contact sites between β 2AR and G protein, GRK, and β -arrestin. Interaction of these proteins with the receptor may involve multiple partially overlapping domains on each protein (left), e.g. the C-terminus, il-1, il-2, il-3 and helix 8 of the β 2AR. Another possibility is that the interaction domain involves one relatively discrete site on each protein (right).

Thus the goal of our study is to determine the structure and function of important domains in the GRKs in order to approach an understanding of the mechanism and specificity of the GPCR-GRK interactions, and eventually develop specific and effective inhibitors of GRKs.

CHAPTER 2

FUNCTIONAL STUDIES OF THE GRK RH DOMAIN

2.1 INTRODUCTION

At present we know very little about how GPCRs activate GRKs. Since this activation requires the activated state of GPCRs it is presumed that the mechanism will be analogous to GPCR binding to and activation of G proteins, and the binding of arrestins to the GRK-phosphorylated agonist-occupied receptors. From this analogy it seems likely that the surface of interaction will involve multiple interaction domains from the perspective of both the receptor (e.g., possible involvement of all the intracellular loops and helix 8), and from the matching sites on GRKs. While there have been many studies of possible interaction sites, at present little is known other than that it involves an allosteric interaction that may require contributions from both the RH and the kinase domains as well as sites required for docking to the membrane.

To approach this outstanding problem we first conducted an Evolutionary Trace of the GRK family in collaboration with Dr. Olivier Lichtarge's group at Baylor College of Medicine. As will be shown below this led to the identification of clusters in both the RH and kinase domain that indicated they could play important roles in GRK activation. From the following considerations we focused our studies on clusters in the RH domain: 1) that they had not previously been indicated as important or studied in detail; 2) that the allosteric interaction might involve sites other than those centered on the small and large lobes of the kinase domain; and 3) that mutations in and around the catalytic domain might simply disrupt this domain rather than blocking the putative allosteric site.

Following the ET study we selected highly ranked regions of the RH domain for focused mutagenesis and functional assays using: 1) intact cell assay of basal (constitutive)

β 2AR phosphorylation in HEK293 cells following transfection of GRK5 and GRK6, and 2) in vitro light-activated rhodopsin phosphorylation by 21K membrane preparations of GRKs from transiently transfected HEK293 cells. Our focus on the β 2AR and GRKs 5 & 6 derived from both our previous work and that of others demonstrating the importance of these GRKs in β 2AR phosphorylation as reviewed in Chapter 1.

2.2 MATERIALS AND METHODS

Materials: Human Embryonic Kidney (HEK293) cells were purchased from the American Type Culture Collection (Manassas, VA). Cell culture reagents are from Mediatech (Herdon, VA). Lipofectamine 2000 and TOP 10 competent cells are from Invitrogen (Carlsbad, CA). Peptide N-glycosidase F (PNGaseF) was from New England Biolabs (Beverly, MA). Polyclonal primary antibodies to pS-(355,356) C-Tail of the β 2AR, and to GRK2, GRK5, and GRK6 are from Santa Cruz Biotechnology (Santa Cruz, CA). N-terminal 6 His-tagged, recombinant, full length, human GRK5 was purchased from Millipore (Dundee, UK). The HRP-conjugated secondary antibody was from BioRad. Enhanced chemiluminescence SuperSignal reagent was purchased from Thermo Scientific (Rockford, IL), and hyperfilm was from Amersham Biosciences (Piscataway, NJ). QuickChange Site-Directed Mutagenesis Kit and XL1-Blue supercompetent cells were from Stratagene (La Jolla, CA). SP-Sepharose Fast Flow was purchased from GE Healthcare (Piscataway, NJ).

2.2.1 Cell culture

HEK 293 cells stably overexpressing Flag-tagged wild type (WT) β 2AR (WT- β 2AR) at 2-4 pmol/mg membrane were grown in 5 % CO₂ at 37 °C in Dulbecco's Modified Eagle's

Medium (DMEM) containing 10% fetal bovine serum, 100 units/ml penicillin, 100 µg/ml streptomycin, and 200 µg/ml G418. When seeding cells for experiments dishes were coated with poly-L-lysine to aid attachment.

2.2.2 Evolutionary trace analysis

Using ET analysis, protein-protein interaction sites can be predicted and be further characterized by experimental techniques. The trace is run by loading the single chain sequence of the protein of interest in the PDB format (121). Ranks and percent coverage are assigned to each alignment position correlating variance and evolutionary divergence. Residues corresponding to the top 30th percentile are evolutionarily important and deterministic of protein function. They typically form statistically significant clusters when mapped onto the representative 3-D protein structure (122, 123). As an extension to this technique, the Lichtarge group developed the Difference ET methodology that identifies ET residues within a subfamily of proteins of a phylogenetic tree as compared with the globally important residues within the encompassing superfamily (124).

Difference ET analyses were run by Drs. Yao and Morgan from the Lichtarge group to identify specific amino acids functionally determinants in the RH and kinase domains of the GRK subfamily. Since no crystal structure of GRK5 has been resolved yet, the crystal structure of GRK6 (PDB ID: 2ACX (73)) was used for visualization of ET residues on a 3D structure (GRK6 and GRK5 are > 70% homologous in their amino acid sequence (125)). To rank the important ET residues within the GRK subfamily as compared with the large Serine/Threonine kinases superfamily, Difference ET analysis was performed on the RH and kinase domains separately. For the RH domain, 56 aligned sequences of GRKs (GRK1-7)

from different species were included as part of a global alignment of 270 sequences of the RGS proteins superfamily. Likewise, for the kinase domain, 50 aligned sequences of GRKs were included as part of a global alignment of 463 sequences of the Serine/Threonine kinases superfamily. The superfamily ET residues were then subtracted from those of the subfamily to isolate GRK specific important sites. Residues in the 30th percentile rank produced evolutionarily important clusters. Ranks and percent coverage are given in Appendix 1.

2.2.3 Mutagenesis of top ranked residues

The WT hGRK5 (NM_005308), hGRK6 (NM_001004106), and hGRK2 (NM_001619) cDNA plasmids were cloned into pcDNA3.1 +. The cDNA plasmid of membrane tethered GRK2-PP was also cloned into pcDNA3.1 +. It was constructed by adding a cDNA sequence to its C-terminus that encodes a GFP² tag and an extra 17 amino acids k-ras sequence (KDGKKKKKKSKTKCVIM). This peptide contains a polybasic region and a prenylation site to ensure its plasma membrane localization. These plasmids were all gifts from Dr. Rasmus Jorgensen (7TM Pharma, and NovoNordisk, Denmark). All clones were verified by DNA sequencing.

Another hGRK5 cDNA plasmid cloned in pcDNA3.1 + used in our first mutagenesis studies was a gift from Dr. Jeffrey Benovic (Thomas Jefferson University, PA). When sequenced this GRK revealed three non-synonymous substitutions in the coding region as compared with the WT GRK5 (NM_005308); namely, sequences at positions 310 (G to A), 911 (A to G), and 1313 (G to A). These three base changes alter the amino acid sequence

such that E104→K, R304→H, and G439→E. This GRK5 mutant will be referred to as **KHE-GRK5**.

For WT & KHE-GRK5 and GRK6 plasmids, single and double alanine substitutions of ET residues were generated as listed in Table 2 and shown in Appendix 2, using the QuickChange Site directed mutagenesis kit. Mutagenic oligonucleotide primers were designed to convert the above residues to alanine as listed in Appendix 3. The template pcDNA 3.1 + - GRK5/6 (10 ng) and the two complementary oligonucleotide primers containing the desired mutation (125 ng each) were extended by Pfu Turbo DNA polymerase using the Px2 Thermal Cycler. The plasmid was then treated with Dpn I endonuclease to select for the mutated plasmid and then was transformed into XL1-Blue supercompetent or One Shot TOP10 competent cells. The transformation reaction was then plated onto LB-agar plates containing ampicillin. Plasmids were purified using the QIAprep Spin Miniprep Kit and direct DNA sequencing of the entire GRK5 coding region was performed on all plasmids to confirm the predicted sequence.

Table 2. List of mutations

mutations #	location	mutations #	location
GRK5		KHE-GRK5	
F36, P37, H38	loop $\alpha 0$ - $\alpha 1$	P61, L66, R68	$\alpha 3$
C42	$\alpha 1$	D85	$\alpha 4$
P61, I62, L66, R68, Q69	$\alpha 3$	F166	$\alpha 9$
F166, R169, Q172, W173, L176	$\alpha 9$	P510, E514, E517, T518	$\alpha 10$
E514	$\alpha 10$		
P61-Q69	$\alpha 3$	GRK6	
F166-Q69, F166-P61, F166-L66	$\alpha 3$ - $\alpha 9$	L66, R69	$\alpha 3$
L66-H38, L66-P37	$\alpha 3$ -loop	Y166, L176	$\alpha 9$
F166-E514	$\alpha 9$ - $\alpha 10$	L66-R69	$\alpha 3$
L66-E514	$\alpha 3$ - $\alpha 10$	Y166-L66, L66-Q172	$\alpha 3$ - $\alpha 9$
F166-Q172, F166-W173, Q172-L176	$\alpha 9$	Y166-Q172, Y166-L176, Q172-W173	$\alpha 9$
E104K, R304H, G439E	$\alpha 5$, KD, KD*	# Residues mutated to Ala except where mentioned	
S484-T485	KD	* KD: Kinase domain	

2.2.4 Intact-cell phosphorylation of the β 2AR by WT or mutant GRK5/6

WT- β 2AR cells (2.5×10^5) were grown in 35 mm plates to reach 70-80 % confluence after 24 hours. Using Lipofectamine 2000 transfection reagent, cells were transiently transfected with 150 ng of WT or mutant GRK5 or 6 and 1.35 μ g of empty vector (pcDNA3.1+) cDNA plasmids (1.5 μ g total cDNA / plate), with a DNA (μ g) to Lipofectamine 2000 (μ l) ratio of 1:3 (1.5 μ g: 4.5 μ l). Controls were transfected with empty vector only. After 48 hours, cells were treated either with the β 2AR agonist isoproterenol (ISO) (100 nM), dissolved in the carrier, 0.1 mM ascorbate / 1 mM thiourea pH 7 (AT), or AT alone for 2 min at 37 °C. The medium was removed and cells washed twice with 1 ml of ice-cold phosphate-buffered saline (PBS). To solubilize the β 2AR, the contents of each well were scraped into 500 μ l of ice-cold solubilization buffer (20 mM Hepes, pH 7.4, 150 mM NaCl, 0.9% dodecyl- β -maltoside, 20 mM Na_4PPi , 10 mM NaF, 20 μ M Na_3VO_4 , 10 μ g/ml benzamidine, 10 μ g/ml leupeptin and 100 ng/ml okadaic acid). The samples were rocked for 30 min and centrifuged at $21,000\times g$ for 15 min at 4 °C to remove cell debris. The supernates were treated with 150 U PNGaseF for 2 hrs at 37 °C to allow deglycosylation of the receptor, and then heated to 65 °C for 15 min in SDS-sample buffer (2% SDS, 10% glycerol, 100 mM Tris, pH 6.8, bromophenol blue, and 1mM dithioreitol (DTT)) (10). Samples were resolved on 12% SDS-PAGE, transferred to nitrocellulose membrane and immunoblotted first with anti-pS-355,356 antibody, then stripped and reprobed with anti-C-Tail antibody, and stripped again and reprobed with the anti-GRK5/6 antibodies. Western blots were visualized on film using SuperSignal, and band densities quantified using the Syngene software. Results were normalized first to the β 2AR levels (anti-C-Tail) then to GRK5/6 levels (anti-GRK5/6).

2.2.5 Preparation of GRK5/6 from 21K membrane fractions

WT- β 2AR cells were grown to ~ 60-80% confluence in 100 mm dishes. Cells were transfected with 8-10 μ g of cDNA plasmid (vector, WT or mutant GRK as described above). After 48 hours cells were washed twice with ice-cold PBS and scraped into 1 ml of ice-cold lysis buffer (20 mM Tris-HCl, pH 7.5, 1 mM EDTA, 1mM phenylmethylsulfonyl fluoride (PMSF), 20 μ g/ml leupeptin, and 3 mM benzamidine), followed by homogenization with 7 strokes of a Dounce homogenizer. Lysates were centrifuged at $600 \times g$ for 5 min at 4 °C to remove all intact cells and nuclei. The supernate was centrifuged at $21,000 \times g$ for 10 min at 4 °C. Pellets were resuspended and washed twice with 1ml of lysis buffer, spun at $21,000 \times g$ for 10 min at 4 °C to make 21K membrane fractions, then suspended in 1 ml of lysis buffer supplemented with 50 mM NaCl, 0.02 % TritonX-100, 1 mM DTT (86). Samples were frozen at -80 °C and either used directly after dilution, or partially purified on SP-sepharose columns as described below.

2.2.6 Purification of GRK5 on SP-sepharose

Cell lysates were diluted 10 times in lysis buffer supplemented with 50 mM NaCl, 0.02 % TritonX-100, 1 mM DTT, and applied to SP-sepharose column. The resin (250 μ l) was washed six times with 2 ml of lysis buffer before eluting GRK5 with 20 mM Tris-HCl, 1 mM EDTA, 450 mM NaCl, and 0.02% Triton X-100. The partially purified GRK5 was then diluted to a final salt concentration of 50 mM and assayed for rhodopsin phosphorylation (all steps at 4 °C). Purification of GRKs was assessed by westerns and the levels quantitated by reference to standard curves generated with purified GST-GRKs (10-200 ng) or 6His-GRK5 obtained from Millipore. The GST-GRK fusion proteins were

generated by cloning the full length GRK cDNA plasmid into the pGEX-4T-1-GST vector at the 3' end with BamH I and EcoR I restrictions sites. Plasmids were transformed in *E. coli*, and grown to produce fusion proteins. Bacterial lysates were purified by affinity chromatography on glutathione-sepharose resin as described in the Amersham Biosciences GST Gene Fusion System handbook (86). No GRK other than GRK5 was detectable in this fraction.

2.2.7 In-vitro phosphorylation of light-activated rhodopsin by WT or mutant GRK5/6

Urea-stripped Rod Outer Segments (ROS) were a generous gift from Dr. Kevin Ridge (The University of Texas Health Science Center in Houston, TX) and prepared as described by Wilden and Kuhn (126). WT and mutant GRK, solubilized as described above from WT- β 2AR 21K membrane fractions or following purification with SP-sepharose chromatography, were diluted in lysis buffer (5-10 nM of GRK5 and GRK6) and incubated with 4 μ M of rhodopsin in 20 mM Tris-HCl, pH 7.5, 1 mM EDTA, 10 mM MgCl₂, and 100 μ M [γ ³²P]ATP at 30°C in a final volume of 32 μ l (61). Rhodopsin was activated by illumination (475 nm) for 30 sec (127). Reactions were stopped after 10 min by addition of 4X SDS-sample buffer (8% SDS, 60% glycerol, 0.4 M Tris-HCl, pH 6.8, bromophenol blue, and 0.4 M DTT). Samples were then resolved on 12% SDS-PAGE, transferred to nitrocellulose membrane, and ³²P-labeled proteins were visualized by autoradiograms. Of note, samples were not heated after adding the SDS buffer to prevent rhodopsin precipitation in the stacking gel. With these levels of GRK5 or 6, rhodopsin phosphorylation was linear for 0 to 30 min. ³²P-Rhodopsin bands were quantified by densitometry directly from autoradiograms, by using a Storm Molecular Dynamics Phosphorimager (GE Healthcare),

and by direct counting of excised bands; comparable results were obtained from these measurements.

2.3 RESULTS

2.3.1 Evolutionary Trace Analyses

As discussed, functionally important residues in proteins can be identified based on specific evolutionary patterns using the ET method. Highly ranked residues for the GRK subfamily were generated by running two separate traces for both the RH (Figure 5) and the kinase domains (Figure 6). Analysis of the RGS proteins superfamily included the alignment of 270 protein sequences and the Ser/Thr kinase superfamily 463 sequences (Figures 5C and 6C respectively) (Appendix 1-Tables A and C). Typically the top 30 % ranked residues form clusters that are thought to be key determinants of protein function. Additionally, a different set of rank scores for each residue was generated for only the GRK subfamily, this included 56 or 50 sequences for the RH and the kinase domains respectively (Appendix 1-Tables B and D). Difference ET was then applied to isolate GRK-specific determinants from global determinants. Our study focuses on both GRK5 and 6, and since these two kinases are more than 70 % homologous in their amino acid sequence, and show near identical homology in the RH domain (125), ET results were mapped onto the GRK6 crystal structure (73) since no crystal structure has been yet resolved for GRK5.

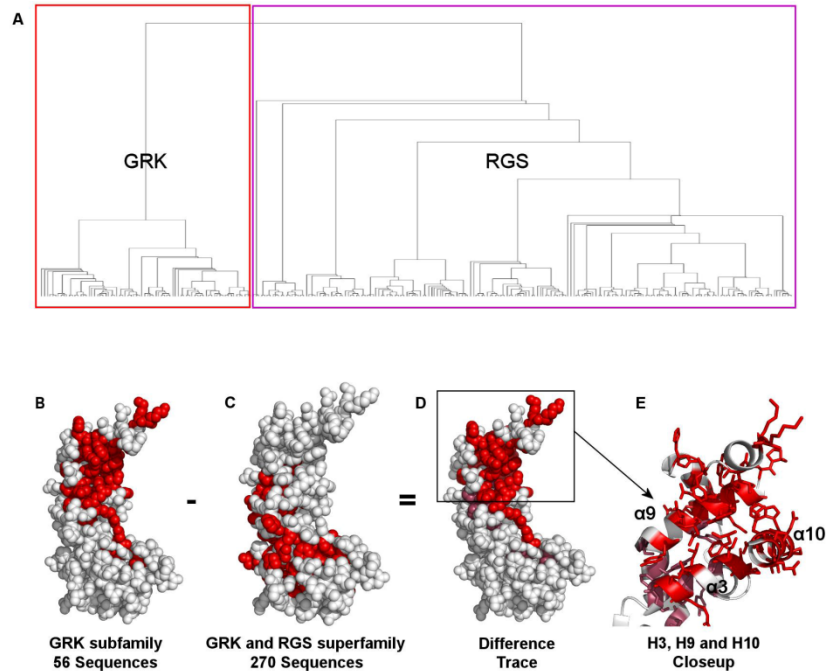


Figure 5. ET of the RH domain. Evolutionary trace results shows strong clustering of the highly ranked residues mapped onto GRK6 crystal structure (73). **A.** The phylogenetic tree of 270 analyzed sequences consisting of the RGS proteins superfamily including 56 GRK proteins with GRK1-7 from different species represented. **B-E.** ET results showing the top 30% ranked residues in the RH domain of GRK6 with helix 11 and the kinase domain removed. **B.** Results of the GRK subfamily alone with a large cluster in terminal subdomain. **C.** Results of the superfamily showing global conservation in the bundle subdomain. **D.** The Difference ET results for the RH domain. **E.** Close up of conserved residues clustering in helices 3, 9, and 10. Red residues are subfamily specific while pink residues are conserved in both the GRK/RGS superfamily and GRK subfamily. Figure generated by Dan Morgan.

ET analysis for the RGS proteins superfamily revealed a cluster of important residues centering on helices 4, 5, and 7 (Figure 5C). A number of these residues in GRK2

helix 5 are known to form a binding interface with the Gαq subunit of the G protein both from mutagenesis and the crystal structure (R106, D110, L118, and Q133 (α6)) (98, 99). Similar analysis for the GRK subfamily revealed a distinct cluster of important residues (Figure 5B). Difference trace analysis uncovered a conserved cluster including helices 0, 1, 3, 9, 10 and 11 (Figure 5D-E), presumably domains functionally important in the GRK subfamily. Residues within helices 0, 1 have been shown to be involved in membrane and PIP₂ binding (48, 49). Likewise, Difference ET analyses for the kinase domain of the AGC kinase superfamily and the GRK subfamily were performed as represented in Figure 6.

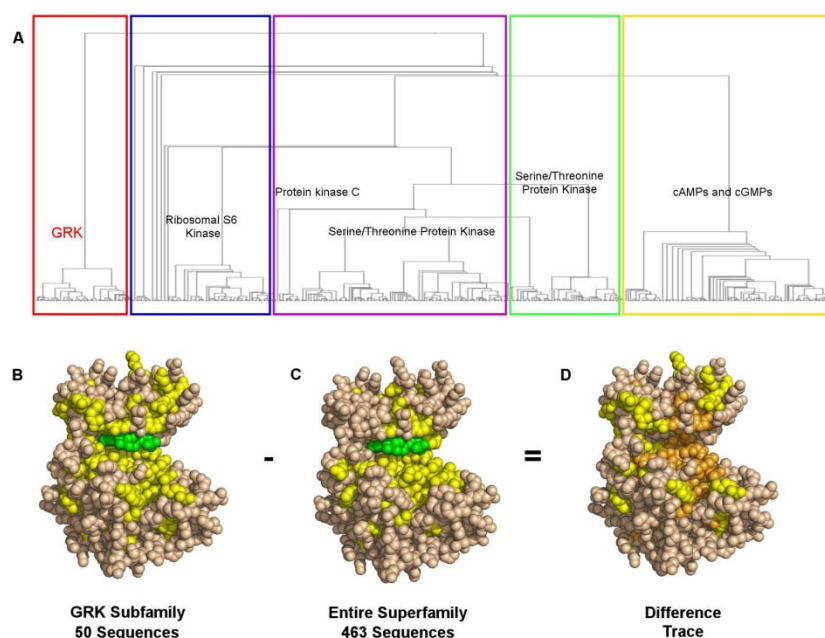


Figure 6. ET of the Kinase domain. **A.** The phylogenetic tree of 463 analyzed sequences of the AGC kinases superfamily including 50 GRK proteins (GRK1-7). **B-D.** ET results mapping the top 30% ranked residues onto the kinase domain of GRK6. **B.** Results of the GRK subfamily alone. **C.** Results of the kinase superfamily. **D.** The Difference trace results for the kinase domain. Yellow residues are subfamily specific while orange residues are

conserved in both the superfamily and subfamily; the green molecule represents AMPPNP. Figure generated by Dan Morgan.

Trace analyses for both the RH and the kinase domains were combined for better visualization using the GRK6 structure (73) as shown in Figure 7. The domains unique to the GRK subfamily for the RH domain are colored in red and the kinase domain in yellow, and those residues shared by the GRK subfamily with the superfamilies are colored in pink and orange respectively. To test the potential importance of the conserved cluster in the RH domain, residues within helices 0, 3, 9, and 10, were targeted for mutagenesis and analyzed for functional effects. Of note, part of this site is buried under the C-terminus (helix 11), however, we reasoned that this site was still close enough to the surface to be accessible to GPCRs, and that the C-terminal tail as well as the N-terminus might possibly undergo conformational rearrangements that may expose it further.

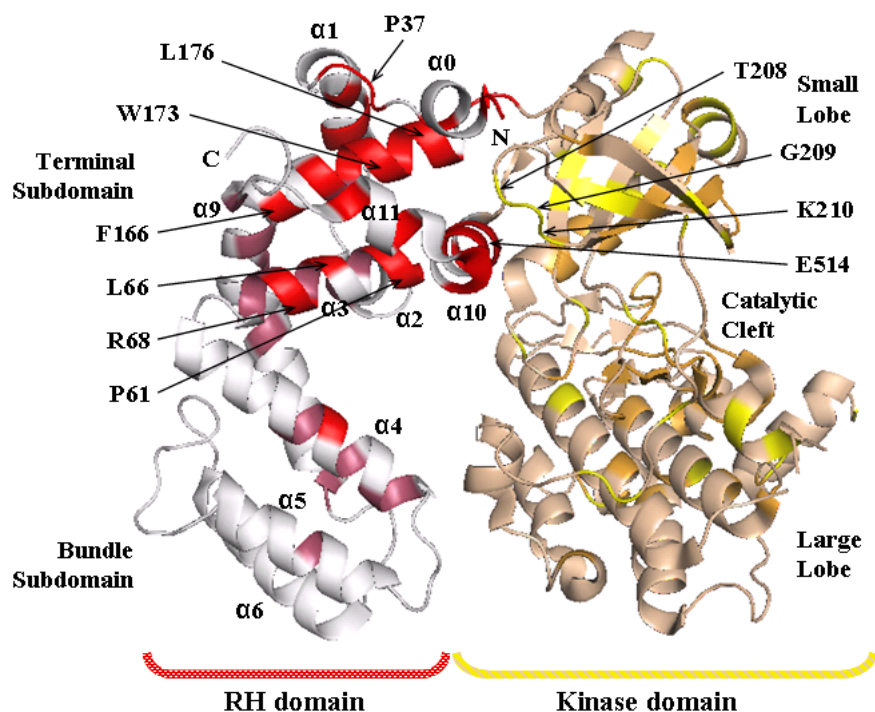


Figure 7. ET analysis mapped onto GRK6. GRK6 x-ray structure PDB code 2ACX (73) is shown in cartoon using PyMol Molecular Graphics System. The structure shows the Difference ET analysis of the RH domain (white and red), and the kinase domain (brown and yellow). Red and yellow colored residues represent the evolutionarily important residues unique to GRK subfamily.

ET revealed other interesting features such as a clustering of lysine residues on an exposed surface proximal to the conserved cluster in the RH domain, which likely contributes to membrane binding (Figure 8). Of interest recent mutagenesis studies showed the importance of kinase domain residues (R191 in GRK1, and V477 in GRK2) in GPCR phosphorylation (105, 128), consistent with our ET analysis. However, for reasons discussed in 2.1, we did not further examine these residues for functional effects, but rather focused the present studies on the RH domain.

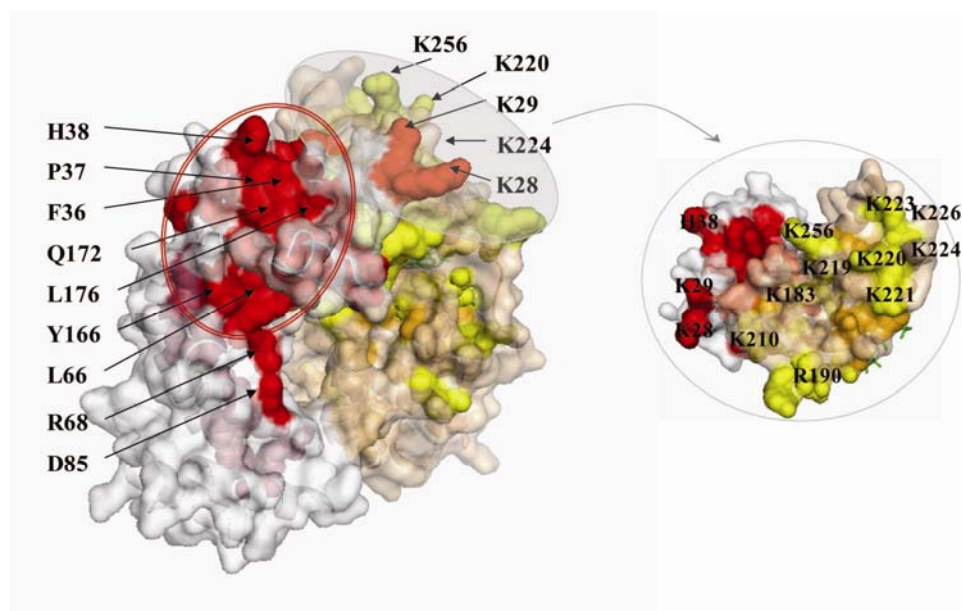


Figure 8. Surface representation of ET residues mapped onto GRK6. Helices 3, 9 and 10 are circled in red. On the right: a flat surface cluster shows basic residues identified by difference ET: K28, K29, R190, K210, K219, K220, R221, K223, and K256 (putative plasma membrane binding site).

2.3.2 Mutagenesis of top-ranked residues in GRK RH domain

To test whether the top-ranked residues in the RH domain are involved in activation of GRKs by GPCRs, mutations of over 30 key trace residues in the RH terminal subdomain were generated by both single and double alanine substitutions to avoid introducing any charged amino acids. Alanine mutations of these residues are allowed since variability at these positions does not include alanine, or rarely in a distant branch. Following the site-directed mutagenesis, constitutive phosphorylation of the β 2AR was used to screen for WT and mutant GRKs activity (10, 86). Following screening we employed in-vitro GRK phosphorylation of light-activated rhodopsin using urea washed ROS.

2.3.3 Constitutive phosphorylation of the β 2AR

As already mentioned, our group had previously shown the important role GRK5 plays in phosphorylating the β 2AR GRK site (S355,S356) in intact cell and cell-free assays using both HEK 293 and COS7 cells (10, 30). Transient overexpression of either GRK5 or 6 causes a strong constitutive phosphorylation of S-(355,356) of the β 2AR in WT- β 2AR cells, unlike GRK2 unless membrane tethered (10, 86, 129) as shown below in Figure 9. We feel that this constitutive phosphorylation of the β 2AR likely reflects GRK phosphorylation of the R* or activated conformation of the receptor. This is based on our earlier studies and that of the Lefkowitz group that demonstrated increasing levels of basal AC activity correlated strongly with the level of transfected β 2AR (130, 131). Thus given the 30-50 fold transient overexpression of GRK we observe in cells coupled with the high, stable expression of the β 2AR it seems likely that the constitutive phosphorylation we observe is in fact a reasonable facsimile of agonist-activated β 2AR phosphorylation. This is no doubt aided by the slow rate of dephosphorylation of the β 2AR we have documented in these HEK293 cells (30). Irrespective of the validity of this argument, this approach allows us to assess GRK mutant activity in an intact cell setting, and it correlates well with our in vitro rhodopsin assay discussed below.

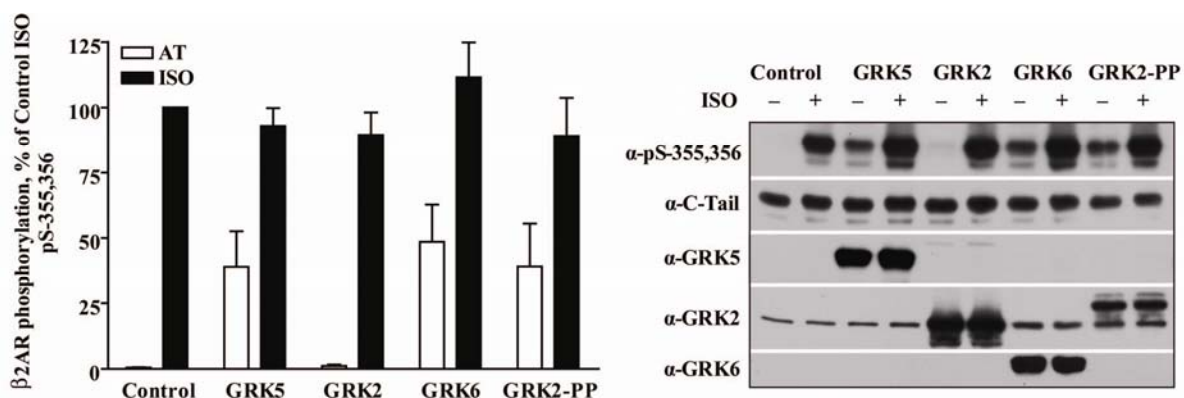


Figure 9. β 2AR constitutive phosphorylation by overexpression of GRKs. WT- β 2AR cells were transiently transfected with either pcDNA 3.1+ (Control), GRK5, GRK2, GRK6, or GRK2-PP. After 48 hours, cells were treated with 100 nM ISO (filled bars) or the carrier AT (open bars) for 2 min, solubilized and processed for western blotting (Methods). The data were normalized to the total receptor levels (α -C-Tail) and are means \pm SEM of three experiments. Representative western blots are shown next to the graph.

To optimize the constitutive assay, GRK was transiently expressed over a range of cDNA plasmid levels in WT- β 2AR cells. The level of 150 ng / 35 mm well was found to be optimal to achieve half the β 2AR phosphorylation relative to 100 nM isoproterenol (ISO) activation (Figure 9). Measurement of receptor phosphorylation was assessed by western blotting with the anti pS-(355,356), followed by normalization to the receptor level with the anti C-tail antibody, and to the level of GRK expressed with the anti-GRK5 or -GRK6.

2.3.3.1 Effects of mutant KHE-GRK5

As described in methods, the mutagenesis were begun using the KHE-GRK5 prior to our belated discovery that it was altered relative to the consensus hWT GRK5 (G104K,

R304H, and G439E) (Figure 10C). Fortunately the activity of KHE-GRK5 is identical to that of the WT GRK5, and as it turned out, observations we made on this altered GRK5 have been of interest. The reason for this is that our first screen of a series of mutants of the RH domain revealed four residues in which substitution to an alanine caused a significant reduction in β 2AR constitutive phosphorylation as compared to KHE-GRK5 (72 – 95 % inhibition); namely mutants P61A, L66A, F166A, and E514A (see Table 2 above summarizing these single alanine substitution mutations). Based on the X-ray structure it appears that the side chains of the four residues mutated are facing in different directions (Figure 10C). Importantly, the mutants' expression levels were not significantly altered. Further discussion of these mutations of GRK5 will follow in the next section.

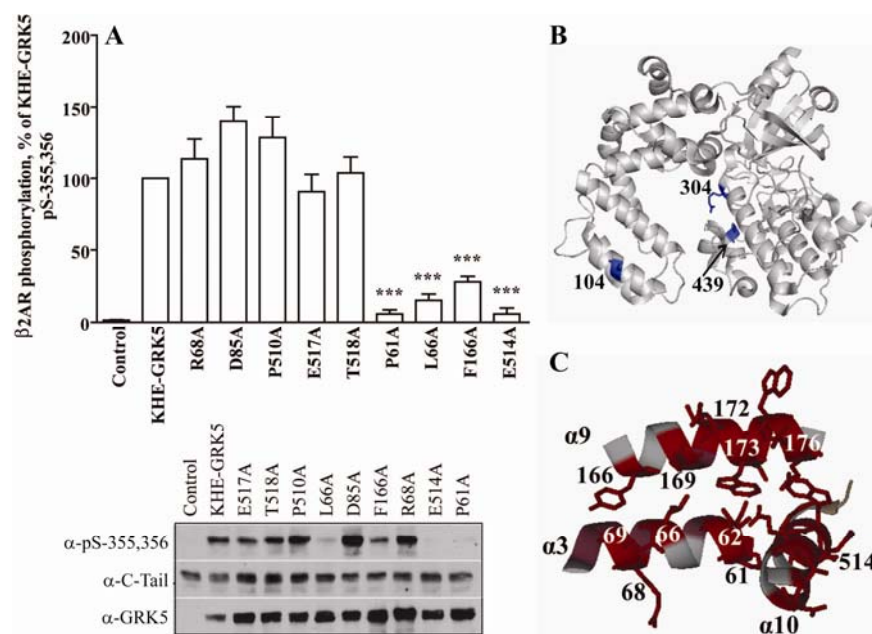


Figure 10. Effect of KHE-GRK5 mutations on constitutive β 2AR GRK site phosphorylation. **A.** WT- β 2AR cells were transiently transfected with either pcDNA3.1+ (Control) or mutant KHE-GRK5. After 48 hours, cells were solubilized; lysates were run on SDS-PAGE, probed with anti-pS-355,356, then stripped and reprobed with anti-C-Tail, and

with anti-GRK5. The data were normalized to the total receptor levels and GRK5 levels. Several point mutations showed significant decrease in GRK site phosphorylation (*** $p < 0.001$ by One-way ANOVA). The data are means \pm SEM of at least five experiments. Representative Western blots of the constitutive phosphorylation of S-355,356, receptor and GRK5 levels are shown below the graph. **B.** Relative positions of residues 104, 304, and 439 are shown in blue in the GRK6 crystal structure cartoon. **C.** Cartoon representation of helices 3, 9, and 10 showing side chains of ET residues (red) mapped onto GRK6 using PyMol Molecular Graphics system.

2.3.3.2 Effects of WT and mutant GRK5

After realizing the “extra” mutations in KHE-GRK5, we quickly performed similar point mutations in the WT GRK5. Surprisingly, none of these single mutations altered constitutive GRK phosphorylation of the β 2AR as compared to the WT. To sort out this interesting observation, E104K, R304H, and G439E mutations were introduced into WT GRK5 either individually or as a pair along with any of the four mutants P61A, L66A, F166A, and E514A. We found that both R304H and G439E were required to reproduce the same effect seen with the KHE-GRK5 point mutants. Neither E104K-R304H nor E104K-G439E mutants had a significant effect when combined with any single defective mutant. Of importance, neither one of these three residues is evolutionarily important, but they are positioned in the bundle – large lobe interface.

Double mutations of the WT GRK5 result in defective phosphorylation

Next, we generated more single and double mutations of only ET residues in the WT GRK5 (see Table 2 for a summary). No new single mutations produced any significant

reduction in GRK5 phosphorylation in the constitutive assay. One mutation (R68A) actually showed double the activity relative to WT. However, several double alanine substitution mutants in various combinations from helices 3, 9, and 10 and the N-terminus significantly reduced the activity by 50 – 95 % as compared to WT GRK5; namely L66A-H38A, F166A-E514A, P61A-F166A, L66A-F166A, L66A-E514A, F166A-Q172A, F166A-W173A, Q172A-L176A, and L66A-P37A (Figure 11). Of note, some of these mutations are within helix 9 alone; *e.g.*, F166A-Q172A. Most of these residues side chains are on the same face of helices 3 and 9, and would be exposed if helix 11 was lifted away. In contrast, mutants P61A-Q69A and F166A-Q69A showed no significant effect on GRK5 activity, this is consistent with the fact that Q69 side chain is directed away from helices 3, 9, and 11 interfaces. These results demonstrated that multiple hits were required to sufficiently affect activity.

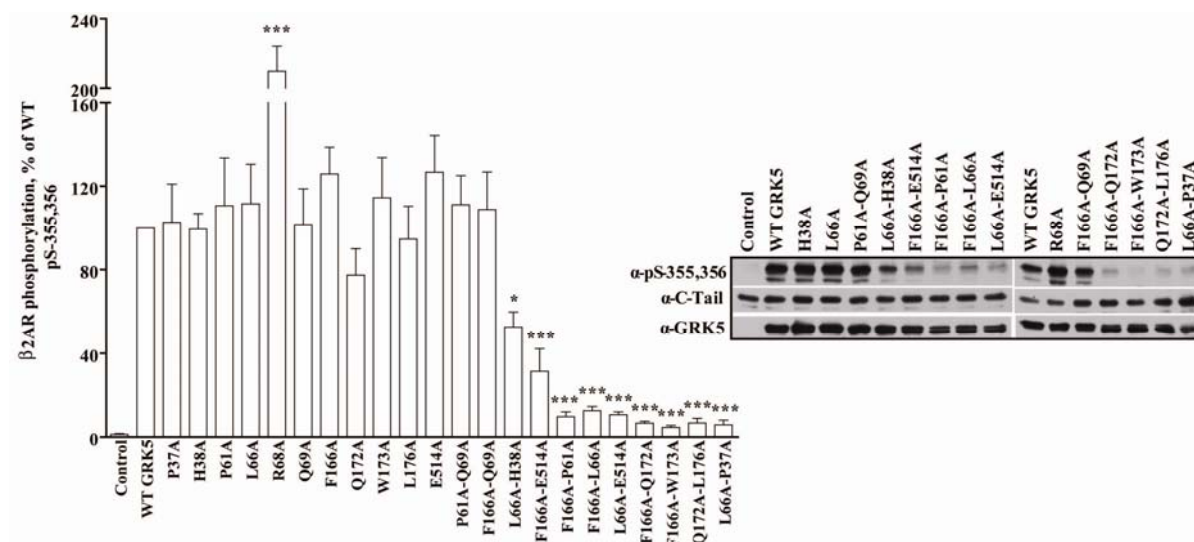


Figure 11. Effect of GRK5 mutations on constitutive β 2AR GRK site phosphorylation.

WT- β 2AR cells were transiently transfected with WT or mutant GRK5. After 48 hours, cells were solubilized, and constitutive phosphorylation of the β 2AR measured as described in the

legend to Figure 10. Several double mutations showed significant decrease in GRK site phosphorylation (*** $p < 0.001$ or * $p < 0.05$ by One-way ANOVA). The data are means \pm SEM of at least four experiments performed in duplicate. Representative Western blots are shown next to the graph.

As important controls, we showed that neither expression levels (Figure 12A) nor membrane localization of the defective GRK5 mutants were significantly altered (Figure 12B).

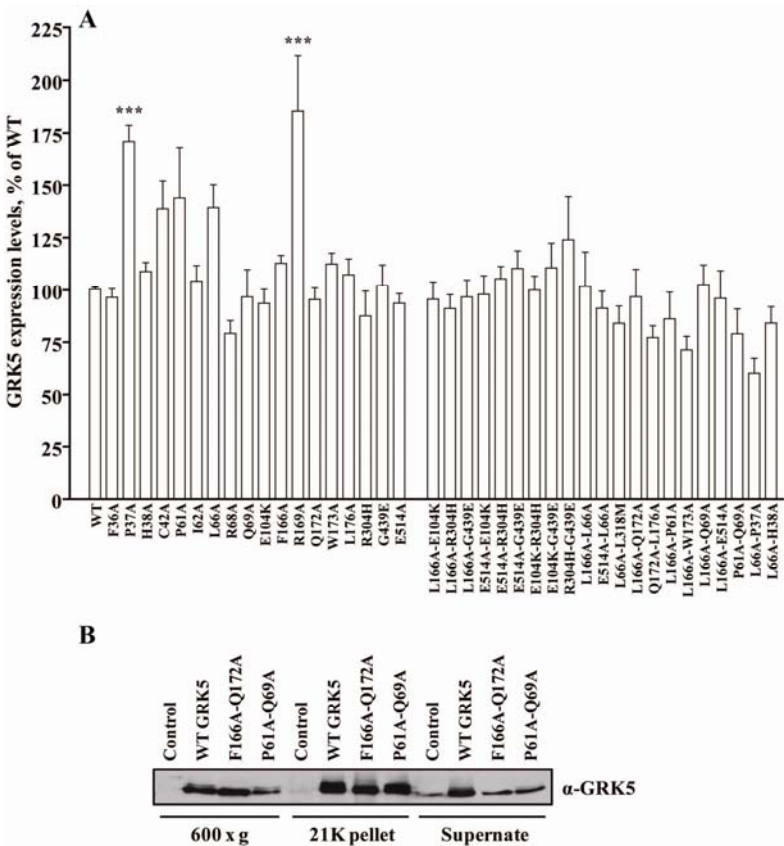


Figure 12. Expression levels and locale of mutant GRK5. **A.** GRK5 mutant expression levels. WT- β 2AR cells transiently overexpressing WT or mutant GRK5 (150 ng cDNA plasmid / 35 mm well) were processed as described in the legend to Figure 10. Data shown

represent WT and mutant GRK5 expression levels as quantified from western blots using anti-GRK5 antibody, and are given as percent of WT GRK5. Data are means \pm SEM of at least four experiments (** $p < 0.001$ by One-Way ANOVA). **B.** Distribution of WT and mutant GRK5 in membrane versus cytosol fractions. WT- β 2AR cells were transiently transfected with either pcDNA3.1+ (Control), GRK5-WT or mutants (8 μ g cDNA plasmid / 100 mm plate). After 48 hours cell lysates were centrifuged at $600 \times g$ for 5 min and supernatant fraction centrifuged at $21K \times g$ for 10 min. The 21K pellet was washed twice and solubilized. Equivalent fractions of the lysate, supernate and 21K pellet were run on the SDS-PAGE and western blots performed with GRK5 antibody.

Furthermore, we found that overexpression of these mutants did not inhibit ISO stimulation of β 2AR GRK site phosphorylation by endogenous GRKs, implying they lack dominant negative activity (Figure 13). Moreover, as a further test of dominant negative activity, we performed transient cotransfection of the β 2AR with WT or mutant GRK5 in COS7 cells. This was followed by treatment of HEK293 cells with carrier or by stimulation at low ISO concentration (10 nM) for 2 min. While the mutant GRKs showed much reduced constitutive phosphorylation without stimulation as expected, we surprisingly observed a significant increase over the background in ISO-stimulated β 2AR phosphorylation with the mutants similar to WT GRK5 (Figure 13A). As a control, the dominant negative GRK5-K215R (49) did not show any increase in constitutive phosphorylation; however, it also showed no dominant negative activity against ISO stimulation. Interestingly, all of these mutants with the exception of L66A-P37A showed a slow moving GRK5 band which was previously suggested by Benovic's group to be caused by autophosphorylation of GRK5

(61) (Figure 11). This result suggests that autophosphorylation was not altered by mutants other than L66A-P37A. However, we also found in a further control that the mutation (S484A-T485A) that should eliminate activity according to Benovic's study (46, 79) also caused constitutive phosphorylation of the β 2AR as well as phosphorylation of Rho* (Figure 14). These controls, in particular the result with the co-transfection with the β 2AR and GRKs, were critical as they argue against any major conformational change due to the mutations.

Ideally mutant activity should have been measured in WT- β 2AR cells with agonist-stimulation of the receptor. But because of the rapid and complete agonist-stimulated phosphorylation by endogenous GRKs, any additional activity of overexpressed GRK would be masked. Remarkably, levels of endogenous GRK2, 5, and 6 in WT- β 2AR cells are \sim 200 fold over that of the receptor (86), consistent with the rapid phosphorylation observed upon ISO stimulation.

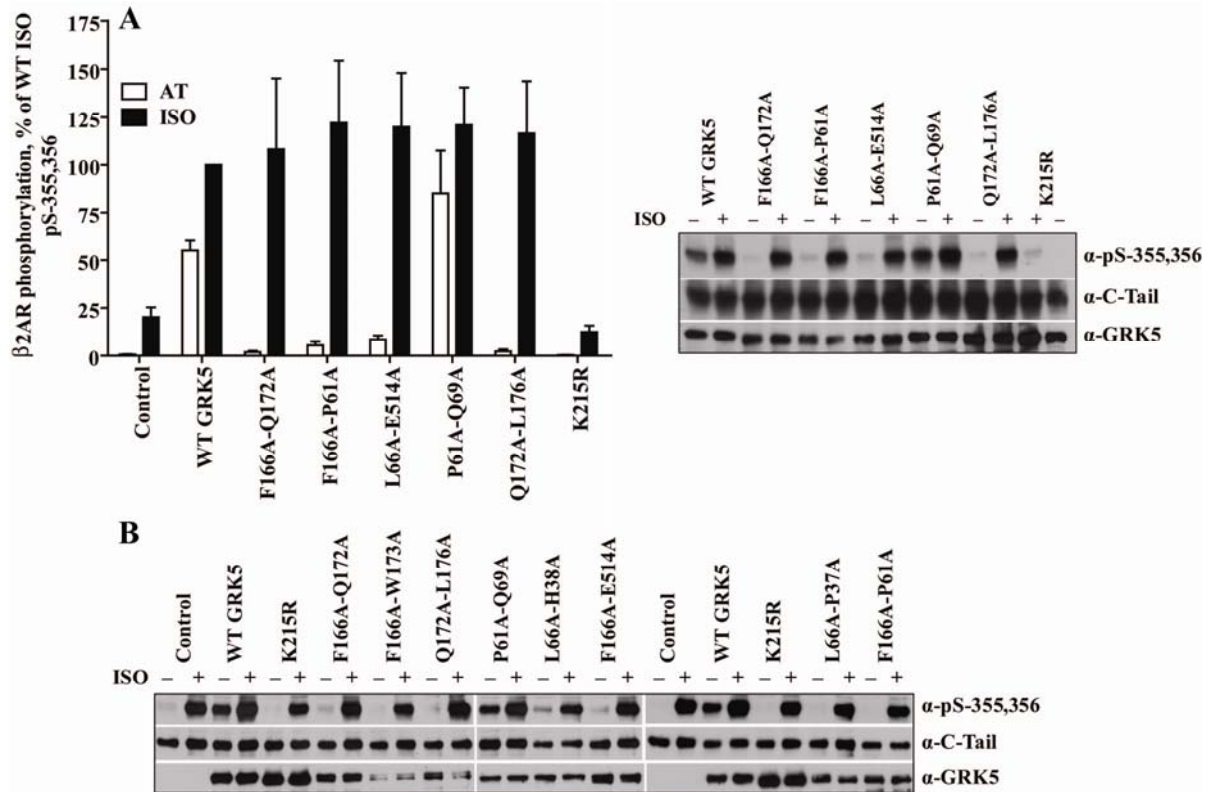


Figure 13. Effect of GRK5 mutations on ISO-stimulated β 2AR GRK site phosphorylation. **A.** COS7 cells were transiently transfected with either Flag- β 2AR (500 ng / 35 mm well) alone (Control) or Flag- β 2AR and WT or mutant GRK5 (150 ng). After 48 hours, cells were treated with 10 nM ISO (filled bars) or the carrier AT (open bars) for 5 min, solubilized, lysates were run on SDS-PAGE, probed with anti-pS355, 356, and then stripped and reprobed with anti-C-Tail, and with anti-GRK5. The data were normalized to the total receptor levels and GRK5 levels (except for the Control) and are means \pm SEM of 2 experiments. Representative Western blots are shown next to the graph. **B.** WT- β 2AR cells were transiently transfected with WT or mutant GRK5 (150 ng / 35 mm well). After 48 hours, cells were treated with 100 nM ISO for 2 min, and processed as described above. Representative western blots are shown. Mutations did not affect ISO-stimulated phosphorylation of S-(355,356)

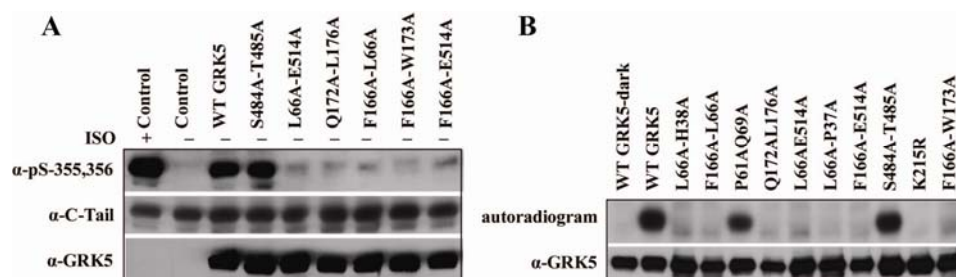


Figure 14. Effect of mutant GRK5 (S484A-T485A) on β 2AR and Rho* phosphorylation. **A.** Constitutive phosphorylation of the β 2AR. WT- β 2AR cells transiently overexpressing WT or mutant GRK5 (150 ng cDNA plasmid / 35 mm well) were processed as described in the legend to Figure 10. Western blots using anti-pS-(355,356), anti-C-Tail, and anti-GRK5 antibodies are shown. **B.** Phosphorylation of Rho*. WT or mutant GRK5 solubilized from 21K fractions (5-10 nM) was incubated with Rho (4 μ M), all samples are with light-activated with the exception of the WT GRK5 labeled dark. The control represents solubilized 21K membranes from cells transfected with only the empty vector (pcDNA3.1+). The autoradiogram and GRK5 levels are shown. Mutation of the autophosphorylation sites (S484, T485) did not alter β 2AR constitutive phosphorylation or Rho* phosphorylation.

2.3.3.3 Effects of WT and mutant GRK6

Since we and others have shown that GRK6 also plays a role in β 2AR phosphorylation, we examined the effects of equivalent mutations in GRK6. The evolutionarily important cluster we identified in the RH terminal subdomain is shared by all the GRKs; therefore we expected that the results obtained with mutant GRK5 would carry over to the other members of the family. Single and double mutations similar to those in GRK5, as well as some novel combinations, were generated in GRK6, and their activity

assessed in the constitutive assay. Expectedly, key double mutations within helices 3 and 9 significantly reduced (75-90%) the constitutive phosphorylation of the β 2AR; namely Y166A-L66A, L66A-Q172A, Y166A-Q172A, Y166A-L176A, and Q172A-W173A (Figure 15). Expression of most of the GRK6 mutants was reduced by \sim 20-40% relative to WT GRK6, and two mutants, Q172A and Q172A-L176A failed to be expressed and could not be assayed. Mutant L66A-R69A did not affect significantly β 2AR constitutive phosphorylation.

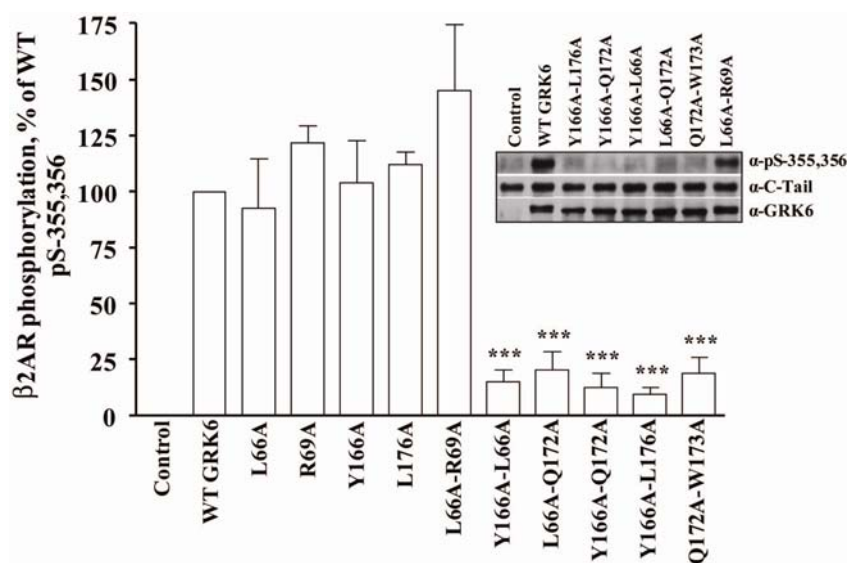


Figure 15. Effect of GRK6 mutations on constitutive β 2AR GRK site phosphorylation.

WT and mutant GRK6 were expressed in WT- β 2AR cells and constitutive phosphorylation of the β 2AR measured as described in the legend to Figure 10. The data were normalized to the total receptor levels and GRK6 levels. The data are means \pm SEM of four experiments performed in duplicate (***) $p < 0.001$ by One-Way ANOVA). Inset: Representative Western blots.

2.3.4 Phosphorylation of light-activated rhodopsin

To further explore the activity of GRK5 and 6 mutants, we examined the effects of WT and mutant GRK5 and 6 on phosphorylation of light-activated rhodopsin (Rho*). This *in vitro* assay (89) has the important advantage that it allows observation of agonist-stimulation of a GPCR (in this case the agonist is light activated trans-retinal). While this assay is not of physiological relevance it has been the standard in the field for its convenience. Rhodopsin is present at extremely high levels in ROS, and relatively large amounts of ROS membranes can be isolated from bovine retina. This assay would provide further support for the effects of mutations on agonist-induced GPCR activation of phosphorylation.

2.3.4.1 Effects of WT and mutant GRK5

For the rhodopsin assay, we transiently overexpressed WT and mutant GRK5 in WT- β 2AR cells (30-50 fold). We then either isolated the 21K membrane fraction from which GRKs were solubilized, or directly solubilized the intact cells followed by partial purification by step elution from a SP-sepharose column (79, 132). Expression of the mutants in 100 mm plates was generally lower than that of WT GRK5 in the 21K membrane fraction, and most of the mutants showed low recovery in the purification process. To circumvent this problem we used the 21K solubilized GRKs for most assays. Levels of GRK5 expression were estimated by westerns by comparison to a standard curves generated using GST-GRK5 run on the same gels (86). Levels so measured were adjusted such that approximately equivalent amounts of WT and mutant GRK were used in the rhodopsin assay.

Our findings demonstrate that all of the key double mutants that showed no constitutive phosphorylation of the β 2AR, showed even more reduced activity (92-98 %) in inducing light-activated rhodopsin phosphorylation relative to WT GRK5. Mutants such as P61A-Q69A that were active in the constitutive assay showed robust activity (Figure 16). Important controls were also performed demonstrating that no activity was detected with endogenous GRKs isolated from cells that were transfected with only the empty vector. Moreover, no constitutive phosphorylation of dark-adapted rhodopsin was observed with either increased Rho up to 32 μ M, or increased levels of GRK5 up to 40 fold higher (Figure 17), consistent with 11 *cis*-retinal acting as an inverse agonist (133).

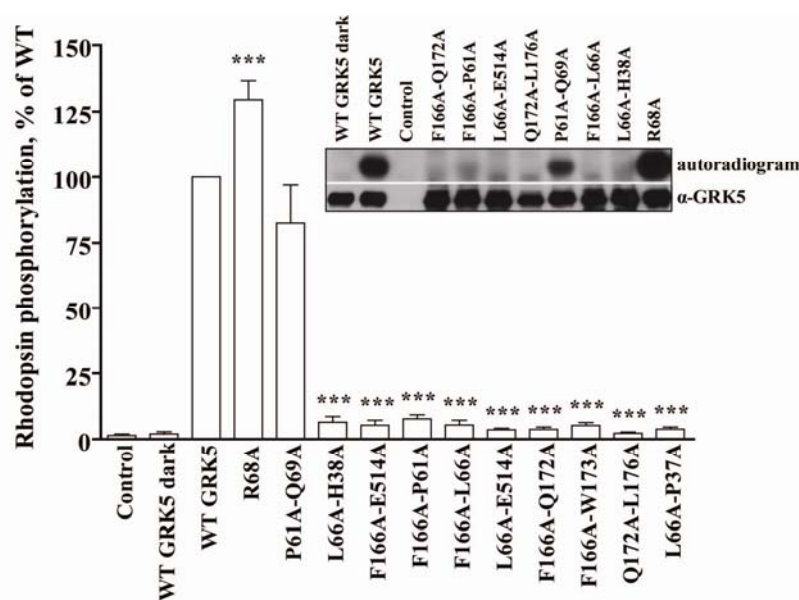


Figure 16. Effect of GRK5 mutations on Rho* phosphorylation. WT and mutant GRK5 were expressed in WT- β 2AR cells, solubilized from the 21K membrane fractions (5-10 nM GRK5) and assayed as described in Methods. All the data shown are with light-activated rhodopsin with the exception of the WT GRK5 labeled dark. The control represents solubilized 21K membranes from cells transfected with only the empty vector

(pcDNA3.1+). The reaction mix was run on SDS-PAGE and the autoradiogram was developed. Data show the percent activity of mutant GRK5 as compared to WT GRK5 and normalized to GRK5 expression levels. Quantitation was performed by use of Molecular Dynamics Storm Phosphorimager. The data are means \pm SEM of at least three experiments performed in duplicate. One-Way ANOVA statistical analyses were determined (***) $p < 0.001$). Inset: Representative autoradiogram and GRK5 expression levels.

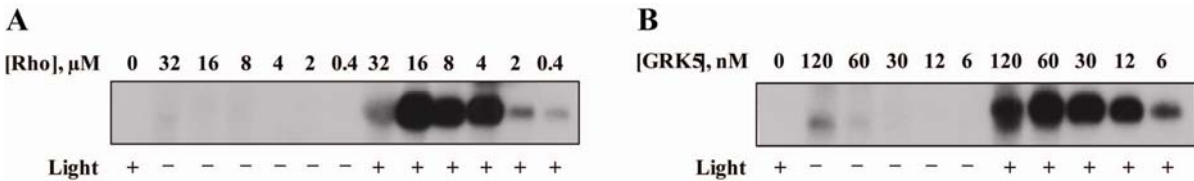


Figure 17. Effect of increased Rho and GRK5 concentrations on Rho phosphorylation. **A.** WT GRK5 solubilized from 21K fractions (~ 6 nM) was assayed for its phosphorylation of Rho in the absence (–) or presence (+) of light with increasing concentrations of Rho (0 – 32 μM). **B.** WT GRK5 (0 – 120 nM) was incubated with Rho (4 μM), and Rho phosphorylation was assessed in the absence or presence of light. Autoradiograms are shown; no constitutive phosphorylation was detected with either increasing Rho or GRK5 concentrations.

2.3.4.2 Effects of WT and mutant GRK6

Similarly to GRK5, WT and mutant GRK6 were transiently overexpressed in WT-β2AR cells, and 21K membranes fractions prepared and assayed for their activity in vitro with light-activated rhodopsin. The results shown in Figure 18 further support our findings in the constitutive assay, as all the double mutants that were inactive in the constitutive

assay, failed to phosphorylate Rho* by > 95%. Interestingly, the full activity of mutant L66A-R69A in the constitutive assay was not retained in the rhodopsin assay, as it showed ~ 75% diminution in Rho* phosphorylation. Our mutagenesis of GRK6 was not as extensive as of GRK5, but overall both sets of results are in agreement providing further evidence for the importance of these helices in GPCR activation of GRKs.

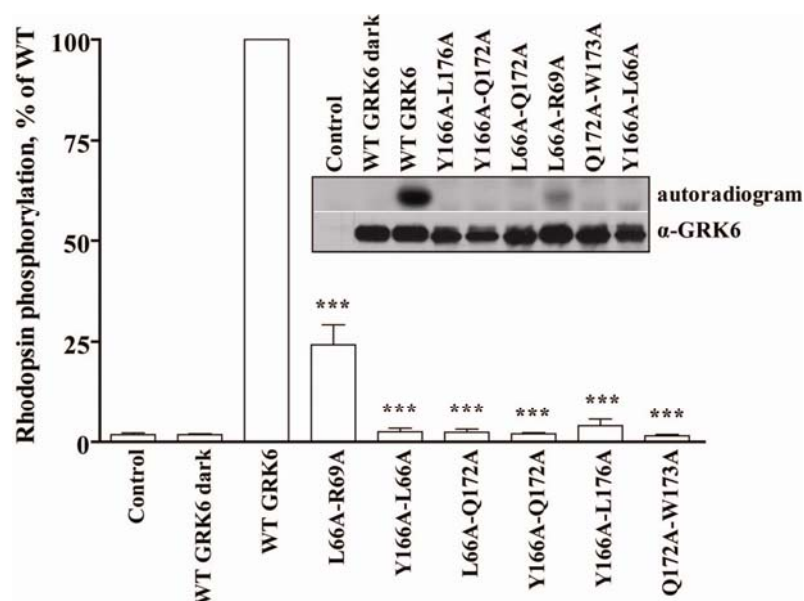


Figure 18. Effect of GRK6 mutations on Rho* phosphorylation. WT and mutant GRK6 were expressed in WT- β 2AR cells, solubilized from the 21K membrane fractions (~ 5 nM GRK6) and assayed as described in the legend to Figure 17. The percent activity of mutant GRK6 as compared to WT GRK6 was calculated, and normalized to GRK6 expression levels. The data are means \pm SEM of three experiments performed in duplicate (***) $p < 0.001$ by One-Way ANOVA). Inset: Representative autoradiogram and GRK6 expression levels.

2.4 DISCUSSION

As discussed in the first chapter, previous studies have identified many GRK residues and clusters responsible for interaction with GPCRs. These studies showed the importance of both the N- and C-termini in localization of the kinase to the plasma membrane and subsequently receptor phosphorylation (49, 92, 93, 107). Moreover, it was shown very recently that point mutations (GRK2 (V477D), and GRK1 (R191A/K)) within the kinase domain severely diminished receptor phosphorylation in vitro (97, 105). Further, Tesmer's group has recently achieved a crystal structure of GRK1 in the active state (personal communication) showing that the N-terminus forms an intramolecular interaction with the small lobe of the kinase domain. Based on these collective results, Dr. Tesmer has proposed that the allosteric site for GPCR interactions may involve both the N-terminus and the small lobe of the kinase. However, as yet no direct evidence for this interaction has been demonstrated. Further kinetic studies of N-terminal mutations and small lobe kinase domain mutations show non-competitive interactions in the rhodopsin assays (97, 106), suggesting that this site is unlikely involved in the allosteric activation of GRK by GPCR. It was also suggested that the dimer interface observed in the crystal structures of GRK1 and 6 is a likely area of protein-protein interactions (73, 74). Thus, although these studies provide molecular insights on how GRKs are activated by GPCRs, it is still not clear which sites are directly involved in the allosteric activation of GRK and what role the RH domain may play in the conformational change to the active state induced by GPCR activation. As discussed in the introduction to this chapter it is likely that the interaction sites are complex.

In our studies we aimed at determining regulatory domains of GRKs involved in allosteric activation of GPCRs, we sought to first identify important residues within the GRKs using a computational technique based on evolutionary conservation of proteins.

To test the importance of the sites identified by ET in activation of GRK, ET residues in the RH domain were targeted for site-directed mutagenesis and examined for their effects on β 2AR and Rho phosphorylation. Through serendipitous study of the KHE-GRK5, we found four single mutations of this GRK (P61A, L66A, F166A, and E514A) that showed marked defects in constitutive phosphorylation of the β 2AR. The results obtained with the KHE-GRK5 constructs did not carry over when only these single mutations were later introduced in the WT GRK5. To further explore this, we pursued multiple double mutations of the WT GRK5 in the ET defined clusters and found six double mutations that severely reduced GRK5 and 6 activities. These mutations involved residues in helix 9 alone, as well as combinations of residues from helices 3 and 9, 3 and 10, and 9 and 10. Further mutations involving residues in loop α 0- α 1 in combination with helix 3 (L66A-P37A and L66A-H38A) also significantly reduced GRK5 activity by 50 and 95 % respectively in β 2AR constitutive phosphorylation and by > 95 % in Rho phosphorylation. To determine which preexisting mutant in KHE-GRK5 caused the observed reduction in activity when combined with any of the four defective mutants, we found that both R304H and G439E in the kinase domain large lobe were required to obtain the reduced activity. While our findings demonstrate that the catalytic activity of several double mutants is inhibited in the β 2AR constitutive assay in intact cell and in the agonist-dependent assay with rhodopsin phosphorylation in vitro, we have not yet resolved how the mutants affect kinase activation. Possibilities include: 1) disruption of the allosteric binding to the receptor; 2) indirect

impairment of the catalytic activity through delocalized effects propagated from the close apposition of the RH domain ET clusters to the small lobe of the kinase domain and the N-terminus; 3) loss of intramolecular interactions such as $\alpha 3$ - $\alpha 9$ interaction leading to destabilization of the GRK; 4) loss of plasma membrane binding. We have shown that mutants expression was not altered in the 21K crude membrane fractions ruling out the 4th possibility. However to better characterize the mechanism of action of the mutants; we generated peptides mimicking helices 3, 9, and 10 of GRK with the aim of determining their ability to inhibit GRK-GPCR interaction. This hypothesis is the main focus of the next chapter in this study.

Interestingly, the single mutant R68A showed a doubling in activity as compared to WT GRK5 in the $\beta 2$ AR assay and to a lesser extent in the rhodopsin assay. In the GRK6 crystal structure R68 appears to form a salt bridge with the ET residue D85 in helix 4 (Figure 19). Importantly, mutants R68A and D85A in the KHE-GRK5 both caused an increase in activity although not significant relative to KHE-GRK5; activity of mutant D85A was not further tested in WT GRK5. However we would expect a similar increase activity as that observed with R68A. These results suggest that disruption of the salt bridge might cause the release of a constraint on the catalytic cleft facilitating its closure, hence an increase in activity. Recently, a GRK5 polymorphism Q41L was shown to cause an increase in the kinase activity (109). Together, these findings indicate that there may be residues in GRKs that when mutated increase the activity.

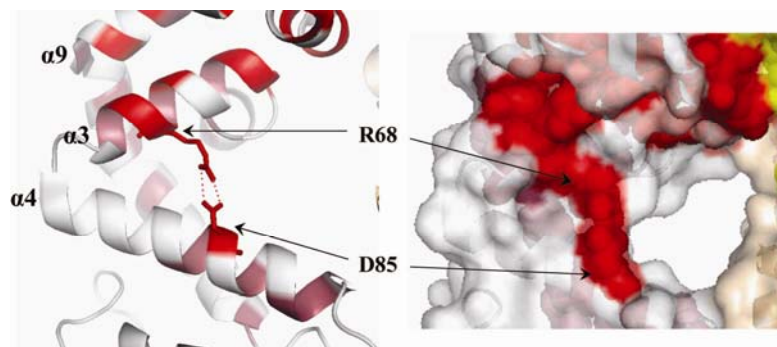


Figure 19. Representation of the interaction between residues R68 and D85 on helices 3 and 4 (cartoon diagram (left) and surface representation (right)).

Furthermore, our results showed unexpectedly that GRK5 autophosphorylation site double mutant (S484A-T485A) had no effect on either the constitutive phosphorylation or rhodopsin phosphorylation; this site was previously shown by Benovic's group to be required for both rhodopsin and β 2AR phosphorylation. From a personal communication with Dr Benovic we found that he had 1) not followed up on this study, and 2) likely used a mutant similar if not identical to the KHE mutant we characterized (obtained indirectly from his group). Thus at present we feel that the autophosphorylation of GRK5 may not be a requirement for activity. Our results will be pursued in future studies.

CHAPTER 3

DEVELOPMENT OF PEPTIDE INHIBITORS OF THE GPCR-GRK

INTERACTION

3.1 INTRODUCTION

One of the goals of our group is to develop novel inhibitors of GRK-mediated desensitization of the β 2AR. Our identification of new sites within the GRK RH domain that are important for kinase activity provided us with several possible approaches for generation of a peptidomimetic inhibitor (22, 83, 106, 117). Also demonstration that a peptide mimicking the ET clusters of the RH domain inhibits GRK phosphorylation of GPCRs, would further support the relevance of our structure/function findings. Toward these ends, we generated a library of peptide mimetics of GRK5 helix 9 based on either straightforward mimicry of the helix coupled with alanine scanning, computational design aimed at preserving highly ranked ET residues, or chemical modifications that lock the peptide in a helix. For screening of the peptides we utilized the rhodopsin phosphorylation assay. A number of peptides were found to profoundly inhibit GRK phosphorylation of Rho* with IC_{50} s in the range of 10-40 μ M. While we have not yet defined the physical site of interactions of the peptides, our findings appear to confirm the importance of these sites.

3.2 METHODS

3.2.1 *Computational design of peptides*

Daniel Morgan from the Lichtarge group used the peptide builder AGADIR algorithm (134) to model peptides on an alpha helix structure based on helix 9 native sequence **FFDRFLQWKWLE** with ET residues shown in red. Analysis of the isolated α 9 sequence by AGADIR predicted less than 5% helical propensity when it is in solution as a

monomer, as opposed to the stabilized helical conformation in the crystal structure. This suggests that this fragment might fold differently than in the native protein, thus it would be less active alone than as a part of the whole structure. As an alternative, we sought to generate peptides that were more likely to fold into helices, and with increased solubility. To build such peptides, an algorithm was created by Drs Morgan and Lichtarge such that the non-ET residues were substituted randomly until helicity was maximized. Peptides including 14-16 residues were generated following the sequence x-x-x-F166-x-x-R169-x-x-Q172-W173-x-x-L176-x, the free residues ‘x’ were replaced over 500 iterations under the condition that a replacement was accepted only if helicity increased, or until a helicity of 85% was reached. Peptide Builder generated a list of peptides to which scores for helicity, hydrophobicity or charge are assigned. From this list three peptides (1, 2, and 3) were selected (Table 3). Models of these peptides were created using PyMol (DeLano 2002), and energy was minimized using MESHI (135). The relative positions of the residues in the modeled peptides were similar to those of the native helix 9 (Figure 20). Peptides 1-5 were purchased from Genemed Synthesis, Inc. (San Antonio, TX). All of the other peptides were synthesized by Dr. John McMurray’s group at the UT M.D.Anderson Cancer Center.

Table 3. Sequences and modifications of the helix 9, GRK5/6 N-Ter, and il-1 β 2AR peptides

Peptide	Sequence	Modification	Result
Designed by Peptide Builder			
1	E F DR R WR Q WRE L WLR	Modified sequence except for ET residues	***
1AA	Ac-E F DR R WR Q WRE L WLR-NH ₂	(AA) Acetylated and amidated peptide 1	***
2	D F E E RRR Q W L I L YR	Modified sequence except for ET residues	*
2AA	Ac-D F E E RRR Q W L I L YR-NH ₂	(AA) Acetylated and amidated peptide 2	—
3	EEY F K R RWE Q WY K LY	Modified sequence except for ET residues	*

Native sequence of Helix 9

4	YFNRFLQWKLE	Unmodified GRK6 α 9 (166-177)	***
5	Ac- FFDRFLQWKLE -NH ₂	Acetylated and amidated GRK5 α 9 (166-177)	***
6	Ac-SNle FFDRFLQWKLE LER-NH ₂	Acetylated and amidated GRK5 α 9 (164-M165Nle-178)	***

Constrained peptides

7	Ac-SNle FFDRFLQWKLE LER-NH ₂	E170 side chain – K174 side chain bridge (underlined)	***
8	Ac-SNle FFDRFLQWKLE LER-NH ₂	E167 side chain – K171 side chain bridge (underlined)	**

Mutant peptides

F166A	Ac-SNle <u>AFDRFLQWKLE</u> LER-NH ₂	Mutation F166A in peptide 6	*
R169A	Ac-SNle FFDRFLQWKLE LER-NH ₂	Mutation R169A in peptide 6	****
Q172A	Ac-SNle FFDRFLQWKLE LER-NH ₂	Mutation Q172A in peptide 6	***
W173A	Ac-SNle FFDRFLQWKLE LER-NH ₂	Mutation W173A in peptide 6	*
L176A	Ac-SNle FFDRFLQWKLE LER-NH ₂	Mutation L176A in peptide 6	***

Truncated peptides

A	Ac-Nle FFDRFLQWKLE LER-NH ₂	GRK5 α 9 (M165Nle-178)	***
B	Ac- FFDRFLQWKLE LER-NH ₂	GRK5 α 9 (F166-178)	***
C	Ac-SNle FFDRFLQWKLE -NH ₂	GRK5 α 9 (164-M165Nle -177)	*
D	Ac-SNle FFDRFLQKWL -NH ₂	GRK5 α 9 (164-M165Nle-176)	***
E	Ac-SNle FFDRFLQKW -NH ₂	GRK5 α 9 (164-M165Nle-175)	***
F	Ac-SNle FFDRFLQWK -NH ₂	GRK5 α 9 (164-M165Nle-174)	—
G	Ac-SNle FFDRFLQW -NH ₂	GRK5 α 9 (164-M165Nle-173)	*

Additional peptides

N-Ter	MELENIVANTVLLKAR-NH ₂	Unmodified GRK5/6 N-terminus (1-16)	***
il-1 β 2AR	AKFERLQTVTNYFITSE	Truncated and modified β 2AR il-1 (59-74E) (83)	***

ET residues are shown in bold and red.

Mutated residues are shown in bold and underlined.

The linked residues are shown in blue.

Peptides 6, 7, and 8: Nle was substituted for M165 to avoid sulfur oxidation.

***: > 65 % inhibition, **: 45-65 % inhibition, *: 25-45 % inhibition, —: no effect

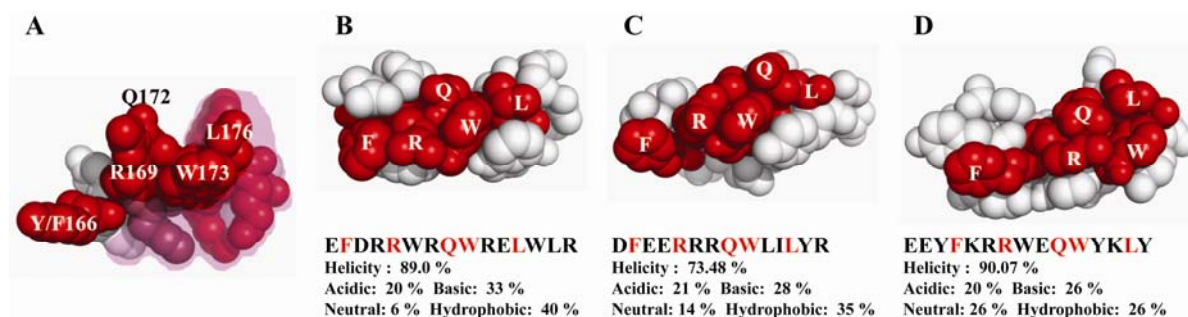


Figure 20. Model of the Peptide Builder designed peptides. **A.** Structure of the native helix 9 of GRK5/6, shading shows the buried residues in the native structure. **B-D.** Peptides 1, 2, and 3 were modeled using PyMol, the relative positions of ET residues (red) were similar to those of the native helix. White residues were randomly selected using Peptide Builder (136-138) to enhance helicity and solubility.

3.2.2 Synthesis of chemically modified peptides

In order to generate peptides with higher helical propensity, and near native sequence that would mimic the bioactive conformation, Subir Sabui and Dr. McMurray designed and synthesized constrained analogues of GRK5 helix 9 by introducing side chain to side chain bridges (139, 140) as shown in Figure 21 and listed in Table 3 (peptides 7 and 8). Also in order to develop peptides with higher affinity, Dr. Richard Hammitt (the McMurray group) did a partial alanine scan of GRK5 helix 9 peptide (mutant peptides in Table 3). For controls Dr. Hammitt also synthesized a peptide that mimics the N-terminus of GRK5/6 (residues 1-16) (97), and one that mimics the intracellular loop 1 (il-1) of the β 2AR (83). Finally he systematically synthesized truncated peptides based on helix 9 sequences to enhance cell penetration as listed in Table 3.

Peptides 6, 7, and 8 were acetylated on the N-terminus and were synthesized as C-terminal amides. Polydimethylacrylamide-based PL-DMA resin (Varian, Inc) was treated overnight with neat ethylenediamine (141). After thoroughly washing the resin with DMF/CH₂Cl₂, Fmoc-Rink amide linker was added in three-fold excess, as calculated from the nominal loading of 1 mmol/g. Coupling was mediated with 3-fold excesses of PyBOP, HOBt, and a 6-fold excess of DIEA. On completion of the coupling as judged by negative ninhydrin tests, the resin was drained, washed with DMF/CH₂Cl₂ and CH₂Cl₂ then dried under vacuum and stored. By weight gain, the loading was 0.65 mmol/g. Peptides 6, 7, and 8 were synthesized in parallel on aliquots of 0.20 g of this resin (0.65 mmol/g, 0.13 mmol) on an AAPPTEC 348 multiple synthesizer employing a 16-well reactor block. Fmoc-amino acids were added in 6-fold excess and coupling was mediated by DIPCDI/HOBt in 7 ml of DMF/CH₂Cl₂ (1:1). Methionine 165 was replaced by Nle to avoid oxidation of the sulfur group. Resins were washed 5× with 7 ml of DMF/CH₂Cl₂ (1:1) after coupling and deprotection steps. Fmoc deprotection was mediated by treatment of the resins for 5 and 15 minutes with 7 ml of 20% piperidine in DMF. For peptide 7, Fmoc-Glu(OPip)-OH was used at position 170 and Fmoc-Lys(Mtt)-OH was used at position 174. For Peptide 8, Fmoc-Glu(OPip)-OH was used at position 167 and Fmoc-Lys(Mtt)-OH was used at position 171. Peptides were acetylated at their N-termini by addition of acetic anhydride on the automated synthesizer. On completion of the amino acid chains, these two resins were treated with 1% trifluoroacetic acid (TFA) in CH₂Cl₂ (5×7 ml, 5 min each). After washing, cyclization was achieved by treatment of the resins with 3 equivalents each of diisopropylcarbodiimide and 1-hydroxybenzotriazole for 20 hr. All three peptides were cleaved from their resins with TFA:triethylsilane:H₂O (95:2.5:2.5) (142) for 2 hr, the volumes were reduced, the products

were precipitated in Et₂O and collected by centrifugation and dried. Peptides were purified by Sephadex G-25 chromatography (2.5×100 cm) in 0.1 M AcOH followed by reverse phase HPLC using gradients of acetonitrile in H₂O (both solvents containing 0.1% TFA). All peptides were greater than 95% pure and gave the correct mass by ESI TOF mass spectrometry.

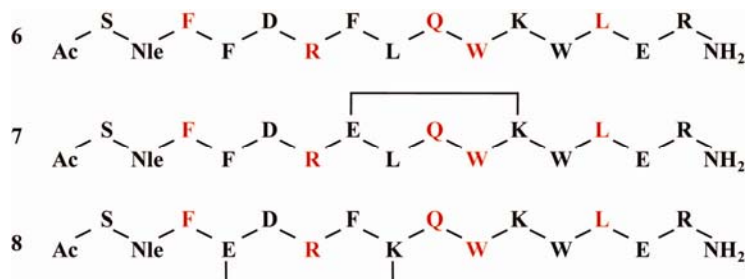


Figure 21. Sequence of chemically modified GRK5 helix 9 peptidomimetics. Peptides 7 and 8 analogous to peptide 6 (native sequence of GRK5 α 9) were built with side chain to side chain bridges to constrain the peptide into a helical conformation. The Bridges are located to the back side of the helix relative to ET residues (red).

3.2.3 *In-vitro* peptide assay

Peptide mimetics of GRK5 helix 9 and the N-terminus (residues 1-16) as well as a peptide mimetic of the β 2AR il-1 (83) were designed as described above, and tested for their inhibition of GRK5 phosphorylation of light-activated rhodopsin (Rho*). Peptide concentrations were calculated based on absorbance at 280 nm. The assay was performed as follows: 2 μ l peptides dissolved in DMSO (Dimethyl Sulfoxide) were added first to the reaction tube on ice such that the final concentration would be 10, 30, or 100 μ M. Rhodopsin (4 μ M or as indicated) was incubated in 20 mM Tris-HCl, pH 7.5, 1 mM EDTA, 10 mM MgCl₂, and 100 μ M [γ ³²P]ATP in a final volume of 32 μ l, activated by illumination

(475 nm) for 30 sec, and 12 μ l was added to each tube. Lastly, SP-sepharose-purified GRK5 (5-10 nM) or purified 6His-GRK5 (4.6 nM) was added to the tubes in the absence or presence of peptides, and incubated at 30 °C for 10 min to induce the phosphorylation. To stop the reaction, 4X SDS-sample buffer was added and samples were processed as described above. 32 P-Rhodopsin bands were quantified by use of a Storm Molecular Dynamics Phosphorimager and by direct counting of excised bands.

3.3 RESULTS

3.3.1 Peptide inhibition of GRK5 phosphorylation of light-activated rhodopsin

We have shown in the previous chapter that key sites in GRK5 and 6 were required for both β 2AR and Rho* phosphorylation. We identified three helices in the RH terminal subdomain that were crucial for GRK5 and 6 activities. Based on these results, we aimed to develop peptide inhibitors of GRK activity. Since double mutations in helix 9 consistently resulted in a dramatic reduction of GRK phosphorylation of both receptors, this helix was selected first for peptide design. Notably, the crystal structure of GRK6 shows that most of what appear to be key residues for activity are displayed as a continuous surface on one side of helix 9 (Figure 10D). A library of peptides (Table 3), were synthesized and tested for their ability to block GRK5 phosphorylation of Rho*. These included first and foremost those based on the native sequence of GRK5; peptides 5 (residues 166-177) and 6 (164-M165Nle-178) and GRK6 peptide 4. Of note, Met165 in peptides 6, 7, and 8 was replaced by Nle to avoid oxidation of the sulfur group. Peptides 1, 1AA, 2, 2AA, and 3 were designed using a peptide builder algorithm such that ET residues were fixed while the others were

selected to increase helicity and solubility. Peptides 7 and 8 were chemically modified such that the native sequence of helix 9 was locked into a helical conformation by building side chain to side chain bridges.

Results from assay of 100 μ M peptide inhibition of Rho* phosphorylation by partially purified GRK5 are shown in Figure 22A. Of the three computationally-designed peptides, only 1 and 1AA (acetylated and amidated) showed significant inhibition of ~ 73 and $\sim 86\%$ respectively, indicating that ET residues are sufficient for activity. Peptides 2 and 3 had much reduced inhibitory activity. The chemically locked peptides 7 and 8 inhibited GRK5 phosphorylation of Rho* by ~ 85 and 51% respectively, implying helicity is important. Importantly, the native helix 9 peptides 5 and 6 were both active and showed significant inhibition of ~ 66 and 82% respectively. Likewise peptide 4 derived from GRK6 and which differs in only two residues from that of GRK5 (Y166 and N168 in GRK6 vs. F166 and D168 in GRK5), showed similar inhibition as with peptide 6. We then tested the inhibitory activity of peptides 1AA, 4, 6, and 7 at concentrations of 10 and 30 μ M. No significant inhibition was observed at 10 μ M with any of the peptides; however at 30 μ M peptides 1AA, 4, and 6 showed significant inhibition of ~ 45 , 40, and 63 % respectively (Figure 22B).

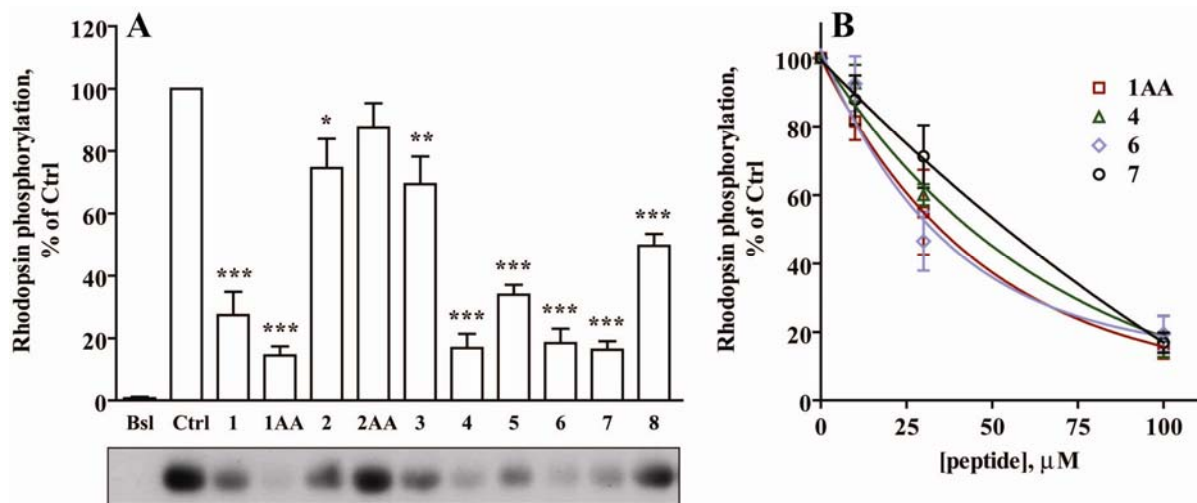


Figure 22. Peptide inhibition of GRK5 phosphorylation of Rho*. Illuminated rhodopsin was incubated with SP-sepharose-purified GRK5 in the absence (Ctrl) or presence of the peptides listed in Table 3. Bsl (basal phosphorylation) refers to samples incubated with non-illuminated rhodopsin and in the absence of peptide. **A.** Peptides were used at 100 μ M. Data shown are means \pm SEM for at least three experiments performed in duplicate (*** $p < 0.001$, ** $p < 0.01$, * $p < 0.05$ by One-Way ANOVA). A representative autoradiogram is shown below the graph. **B.** Peptides 1AA, 4, 6, and 7 were used at 10, 30, and 100 μ M. Data shown are means \pm SEM for three experiments performed in duplicate, except for peptide 4 (two experiments in duplicate at 10 and 30 μ M). P values for peptides 1AA, 4, 6, and 7 at 30 μ M were < 0.01 , < 0.01 , < 0.001 , and > 0.05 respectively by One-Way ANOVA.

3.3.2 Kinetic analysis of peptide 6 inhibition

To further investigate the mechanism of peptide inhibition, we examined GRK5 activity with varied concentrations of Rho* (0-25 μ M) in the presence of 100 μ M peptide 6. The nature of inhibition of this peptide appeared mixed competitive/non-competitive (Figure 23), since we observed a consistent decrease in the V_{max} and an increase in the K_m .

However, confirmation of this result will require more refined kinetics since the data showed non-hyperbolic, possibly positively cooperative kinetics at low rhodopsin concentration in the absence and presence of the peptide confounding interpretation. Further confounding this issue is the inherent nature and complexity of the GPCR-GRK5 interaction. That is, GPCRs both activate GRKs and are substrates for the enzyme and it is not resolved whether the GPCR activating the kinase is in turn phosphorylated only by its “private” kinase or must phosphorylate another in the vicinity. While highly purified GRK5 was used for these experiments, the possibility of further complexity from either autophosphorylation or other contaminating kinases is unresolved. Finally phosphorylation of rhodopsin by GRK5 is not the native situation, and it is not known whether GRK5 binding to the ROS discs reflects its *in vivo* binding to membranes.

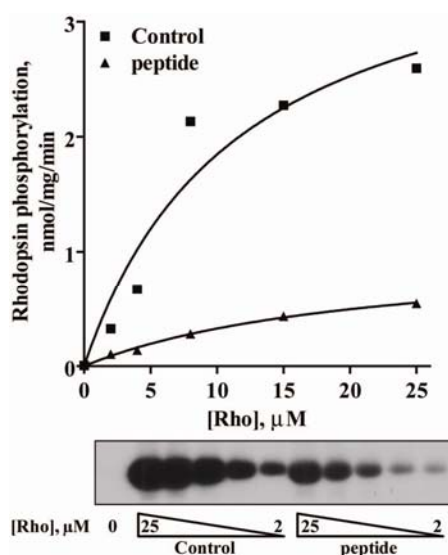


Figure 23. Kinetic analysis of peptide 6 inhibition of GRK5 phosphorylation of Rho*.

Increasing concentrations of Rho* (0 – 25 μM) were incubated with purified 6His-GRK5 (4.6 nM) in the absence (Ctrl) or presence of peptide 6 (100 μM) for 10 min at 30 °C. The experiment shown is representative of four similar experiments each performed in duplicate.

Kinetic parameters for the control and peptide treated were as follows: $V_{\max} = 4.0 \pm 1.1$ and 1.0 ± 0.1 nmol/mg/min; and $K_m = 11.7 \pm 6.9$ and 21.1 ± 4.0 μ M respectively. An autoradiogram is shown below the graph.

3.3.3 Specificity of peptide inhibition

Furthermore, since both peptides 4 and 6 inhibited GRK5, we tested their effects on GRK6 activity. Surprisingly, we found that peptide 6 (based on GRK5) did not inhibit GRK6 phosphorylation of Rho*, whereas peptide 4 which is derived from GRK6 was active (Figure 24). This indicates specificity for GRKs and suggests that the site of action is on GRK rather than on rhodopsin, since if it interacts with the Rho* one would expect similar inhibition of both GRKs.

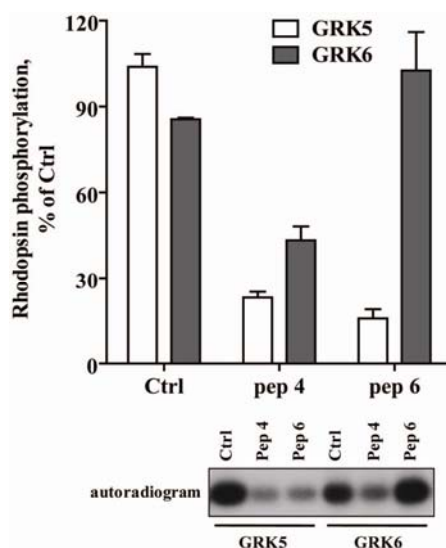


Figure 24. Peptides 4 and 6 inhibition of GRK phosphorylation of Rho*. Peptides 4 and 6 (100 μ M) were incubated with Rho* (4 μ M) and either GRK5 (open bars) or GRK 6 (filled bars) for 10 min at 30 °C. Data shown are the means \pm SEM for three experiments

performed in duplicate and normalized to % of control. A representative autoradiogram is shown below the graph.

3.3.4 Effects of mutant peptide 6 on GRK5 phosphorylation of Rho*

Because the native sequence peptide 6 (100 μ M) showed > 80 % inhibition of Rho* phosphorylation by GRK5, and to further explore the importance of ET residues, we designed another set of peptides by replacing each ET residue in peptide 6 by an alanine as shown in Table 3. The test of these peptides' activity revealed interesting features as shown in Figure 25A. We found that mutant peptides F166A and W173A showed much reduced activity relative to peptide 6, however their inhibition of phosphorylation was still significant as compared to the Control (~ 42 and ~26 % respectively), this suggest these hydrophobic residues are important for inhibition. Peptides R169A, Q172A, and L176A showed inhibitions of ~ 98, 95, and 74 % respectively; interestingly alanine substitution of the charged residue R169 showed a somewhat greater inhibition relative to peptide 6, and inhibited with an IC_{50} of ~ 10 μ M (Figure 25B). This result was exciting and was a considerable improvement over the WT peptide 6 (IC_{50} of ~ 30 μ M).

In recent studies the N-terminal domain of GRK1 and 2 was shown to play an important role in the phosphorylation of rhodopsin (97), so we tested the inhibitory activity of the GRK5 N-terminus peptide (residues 1-16) as well as a peptide derived from the il-1 of the β 2AR (residues 59-74E) which was previously shown to inhibit GRK2, 3, and 5 phosphorylation of Rho* (83). These peptides showed inhibitions of ~ 85 and 97 % respectively, indicating these sites are also important in GPCR phosphorylation. These peptides will be useful in the future for comparative studies with the helix 9 peptides.

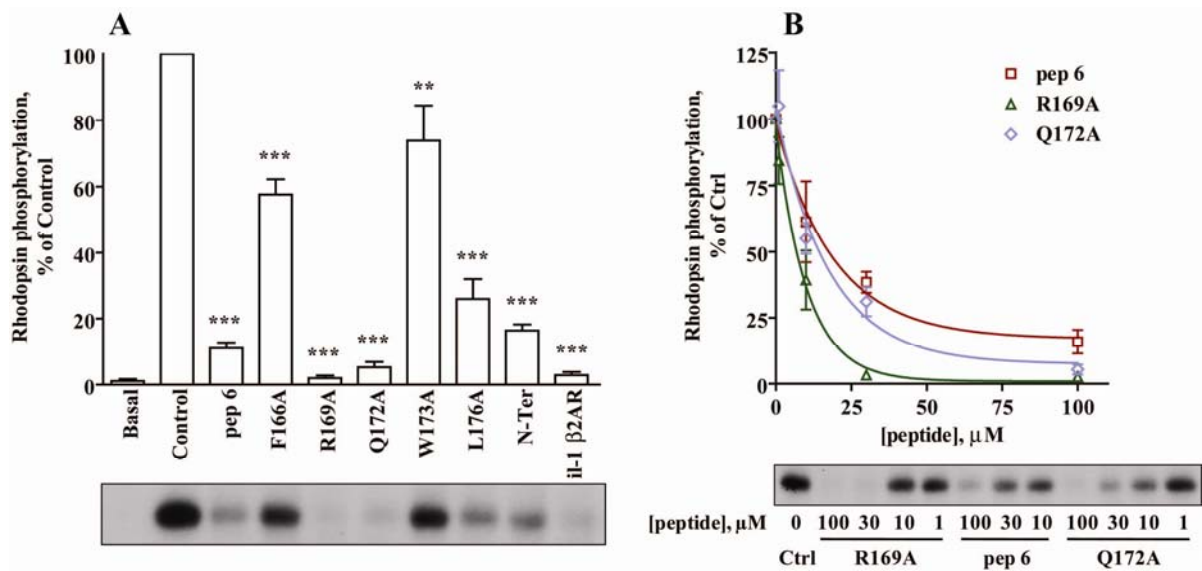


Figure 25. Mutant peptide inhibition of GRK5 phosphorylation of Rho*. Illuminated rhodopsin was incubated with SP-sepharose-purified GRK5 as described in the legend to Figure 22. **A.** Peptides were used at 100 μ M. Data shown are means \pm SEM for at least three experiments performed in duplicate, except for the N-Ter peptide (two experiments in duplicate) (***) $p < 0.001$, ** $p < 0.01$ by One-Way ANOVA). **B.** Peptides 6, R169A, and Q172A were used at 10, 30, and 100 μ M. Data shown are means \pm SEM for three experiments performed in duplicate. P values for all three peptides at 30 μ M were < 0.001 , and at 10 μ M $P < 0.01$ for R169A by One-Way ANOVA. Representative autoradiograms are shown below the graph.

3.3.5 Preliminary results of truncated peptide effects

Ideally, peptide activity should be assessed in an intact cell assay for their inhibition of β 2AR phosphorylation by GRK5 or 6. However, this mode of assay necessitates permeable peptides, hence why we opted for the cell-free rhodopsin assay. In the early stages of peptide studies, we found a small inhibition by peptide 6 of β 2AR phosphorylation

in the 21K membrane fractions by endogenous GRKs (86). Unfortunately results were variable, perhaps due to the inability of peptides to penetrate the membrane vesicles. For future studies we are planning to reinvestigate this assay. Also, to circumvent the permeability problem, one could use cell penetrating systems to deliver peptides into the cell e.g. Chariot, PULSin (143) or peptide transduction domains; e.g., TAT (YGRKKRRQRRR), poly-arginine (144, 145). Another approach is to work on making the peptide shorter since it is well established the shorter peptides generally have enhanced permeability. Preliminary results with several shortened peptides based on peptide 6 (peptides A-G listed in Table 3) are shown in Figure 26. Additional modifications of the peptides might be required to further confirm these results.

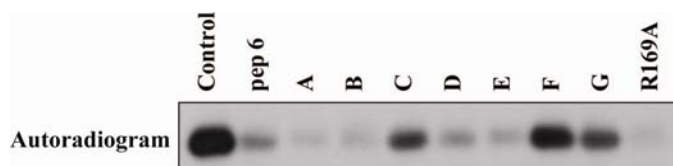


Figure 26. Truncated peptide inhibition of GRK5 phosphorylation of Rho*. Illuminated rhodopsin was incubated with SP-sepharose-purified GRK5 as described in the legend to Figure 22. The autoradiogram is from for one experiment.. Peptides were used at 100 μ M.

3.4 DISCUSSION

We aimed to develop a specific peptide inhibitor of GPCR activation of GRKs based on mimicking sites in GRK that are important for interaction with and or phosphorylation of GPCRs. Thus we reasoned that we should first search for residues in GRKs that were

required for GPCR phosphorylation. In chapter 2, we showed that helices 3, 9, and 10 in the RH terminal subdomain formed an evolutionarily conserved cluster; and that double mutations of numerous residues within this cluster impaired GRK5 and 6 phosphorylation of both β 2AR and Rho* in intact and cell-free assays respectively. Based on these results we designed peptide mimetics of GRK5 helix 9 that would potentially disrupt GRK-GPCR interaction. These peptides included: 1) unmodified helix 9 sequence; 2) modified sequences where only ET residues were kept unchanged; 3) peptides chemically locked into helical conformation; and 4) truncated peptides.

Results from assays of peptide inhibition of GRK5 phosphorylation of Rho* showed that the native helix 9 peptides 5 and 6 derived from GRK5, as well as peptide 4 derived from GRK6, inhibited ~ 66-83 % at 100 μ M and displayed IC_{50} s around 30 μ M. We have not yet performed circular dichroism to determine the helicity of these peptides; however, the peptides that were locked into a helical conformation, peptides 7 and 8, also showed significant inhibitions of GRK5 activity, suggesting that helicity is important. We also found that the peptide builder-designed peptide 1 whether acetylated and amidated at the N- and C-termini, significantly reduced GRK5 phosphorylation of Rho*, indicating that the top-ranked ET residues retained on one face of the helix may be critical. The other peptide builder-designed peptides 2 and 3 showed much reduced activity as compared to peptide 1, perhaps due to the introduction of several charged residues such as Glu which likely interfere with the binding of the peptide.

Results from the alanine screen of ET residues in peptide 6 demonstrated that substitution of the two hydrophobic residues F166 and W173 markedly reduced peptide activities as compared to the WT peptide. Whereas substitution of the charged residue R169

resulted in a peptide with the highest affinity yet, showing an IC_{50} of $\sim 10 \mu M$ and near complete inhibition at $100 \mu M$. This experiment indicates that hydrophobic residues are necessary for peptide binding, and is congruent with results obtained with peptides 2 and 3 into which charged residues were introduced. On the other hand it possibly increases the probability of the peptide binding hydrophobic pockets in either rhodopsin or GRK that may not be involved in the allosteric activation.

The findings of kinetic studies of peptide 6 inhibition of GRK5 phosphorylation of Rho* were ambiguous since it appeared that the peptide altered both the K_m and the V_{max} for Rho*, suggestive of a mixed competitive/non-competitive inhibition. One problem with the kinetic study is that the increase in activity with increasing rhodopsin concentrations was clearly not hyperbolic. This is not a straightforward system for kinetic studies, not the least of which is that GRK5 is not the physiological regulator of rhodopsin. To further explore the site of action of peptide inhibition, we tested whether these peptides would inhibit GRK6 activity. We found that peptide 6 derived from GRK5 inhibited GRK5, but not GRK6, while the peptide derived from GRK6 inhibited both GRKs, demonstrating some specificity for the GRK5 based peptide. These data coupled with the apparent mixed nature of inhibition by peptide 6, suggest that the peptides may act on GRK rather than the receptor, possibly by altering the interaction between helices 3 and 9. Further investigations will be required to determine the site or sites of peptide binding.

As already shown and discussed, helix 9 based peptides obviously block the catalytic activity of GRK, and although this helix is away from the catalytic site, the effect might propagate through the small lobe of the kinase. Potential role for helices 3 and 10 and other conserved sites within the RH domain need to be examined. Furthermore, we showed that

GRK5 N-terminus (residues 1-16) based peptide inhibited GRK5 phosphorylation of Rho* confirming and extending a very recent report of GRK2 inhibition by its N-terminal peptide. Clearly the N-terminus plays a role in activation by GPCR (89, 97, 106); however kinetic studies to date suggest that its action is non-competitive. This appears to be incompatible with it acting at the allosteric site in competition with receptor. The crystal structure of GRK6 in the active state shows that the N-terminus folds over the small lobe of the kinase domain (a key residue being R190). This domain lies between the two kinase domain lobes, and is in apposition to the active site tether (Dr. John Tesmer, personal communication). This supports the idea that the GRK N-terminus likely stabilizes the active state through intramolecular interactions, but does not resolve its role in the allosteric binding to the GPCRs.

Complementing these findings our results suggest that the RH domain contributes to stabilizing the active state of the kinase. Possible mechanisms of helix 9 peptide inhibition include: 1) peptide binding to the GRK allosteric site preventing GRK association with the receptor; 2) peptide binding to the receptor perhaps in a hydrophobic pocket similar to what has been shown for transducin C-terminal peptide binding to rhodopsin; 3) peptide interactions with helix 3 and 10 that prevent the transition to the active state by delocalized effects; and 4) peptide alteration of GRK localization to the plasma membrane. Whatever the mechanism of helix 9 peptide inhibition proves to be, we believe that the peptides developed thus far will serve as lead agents for future development of a GRK inhibitor with higher potency and specificity. Hopefully these will be suitable for use as probes of the roles of GRK phosphorylation in β 2AR desensitization in cells.

CHAPTER 4
GENERAL SUMMARY

4.1 CONCLUSIONS

One of the most critical aspects of GPCR regulation is that immediately following agonist-activation, the GPCRs are desensitized. This process is crucial for maintenance of homeostasis and cell function. Our group's long term goal is to establish the basic mechanisms of desensitization of the β 2AR and the development of pharmacological means of intervening in the desensitization events. GRKs play a central role in regulating β 2AR signaling by phosphorylating the agonist-stimulated receptor which then promotes profound desensitization. As such, understanding both the mechanisms of GRK activation and phosphorylation of GPCRs and the varied roles in physiology are important. Therefore, the development of inhibitors of the GPCR-GRK interaction is of considerable interest, both as a tool for the study of their actions, as well as ultimately for their use in the treatment of disease states; such asthma where the loss of β 2AR response by desensitization is limiting for drug efficacy.

The goals of this study were to probe the nature of the allosteric GRK activation by GPCRs, and to develop peptide inhibitors based on knowledge of and mimicry of the GRK-GPCR interaction domains. Towards this endeavor, we merged computational, biochemical, and pharmacological approaches made possible by our collaborations with both the Lichtarge (ET study) and the McMurray (peptide chemistry) groups. We first identified key functional residues within GRK's RH and kinase domains employing the evolutionary trace methodology. Top-ranked residues were generated by using Difference trace such that traces of both the RGS and AGC kinase superfamilies were subtracted from those of the GRK subfamily to isolate GRK-specific key residues. By mapping Difference trace results onto

the 3-dimensional structure of GRK6, clusters of important residues were revealed in both domains presumably important for protein-protein interfaces. We focused this study on the RH domain cluster around helices 3, 9, and 10. An alanine scan of the key residues was performed involving over 50 single and double mutations. Biochemical assays were then performed to determine effects of these mutations on GRK5 and 6 activities. We assessed both the constitutive phosphorylation of the β 2AR GRK site in an intact cell setting using HEK293 cells stably overexpressing the receptor, and the phosphorylation of light-activated rhodopsin in vitro by GRK constructs. Consistent with the ET results, our mutagenesis strategy demonstrated that the structural integrity of helix 3, 9, and 10 cluster was crucial; and numerous double alanine substitutions within helix 9 alone, helix 3 and 9, helix 3 and N-Terminus, and helix 3 or 9 and 10 severely reduced GRK activity. No point mutations altered GRK activity with the exception of R68A which exhibited a doubling in activity in the constitutive assay. Importantly, these mutations did not alter membrane binding. For reasons not understood, they did not exhibit dominant negative activity against ISO-stimulated β 2AR phosphorylation by endogenous GRKs. In summary, while our mutagenesis study identifies a novel domain required for activity, we have not yet resolved the role it plays in GRK activation. Possibilities include 1) disrupting direct contact points with the receptor, thus altering the allosteric binding site; 2) blocking signal propagation from GPCR binding to kinase activation, such that this domain bridges the binding and catalytic domains; and 3) disruption of contacts with neighboring helices leading to a destabilization of the tertiary structure of the kinase. The latter requires a major conformational change leading to a catalytically dead or mostly dead kinase. Based on several recent studies it has been proposed that the receptor interacts with the N-terminus of

GRKs and the small lobe of the kinase domain; however kinetic studies of mutant GRK characteristics at present are unresolved. Since this region lies close to the ET cluster we identified, it remains difficult to make any strong conclusions on the specific residues involved in the GPCR-GRK interaction.

In the second phase of this work we used our findings on the role of the RH cluster to develop peptide mimetics that would potentially disrupt the β 2AR-GRK5 interaction. Based on these findings that a number of helix 9 mutations alone or in combinations with close regions reduced GRK activity, peptide mimetics of helix 9 were designed and assayed for their ability to inhibit GRK phosphorylation of light-activated rhodopsin. Peptides were synthesized as follows: 1) the native sequence of both GRK5 and 6; 2) peptides designed by Peptide Builder such that ET residues were preserved while others modified to optimize helicity and solubility, 3) chemically locked peptides into helical conformation; 4) alanine scan of ET residues sequences, and 5) shortened peptides. Using these approaches we found the following: 1) the native helix 9 sequence of GRK5 and 6 inhibited GRK5 phosphorylation of Rho* by 65-98 % at 100 μ M with IC_{50} s of 30-40 μ M; 2) a computationally designed peptide preserving several key ET residues was effective; 3) a peptide locked into a helix inhibited GRK5; 4) based on alanine scanning that the native peptide of GRK5 with Arg169 converted to alanine gave us our most potent inhibitor ($IC_{50} \sim 10 \mu$ M); 5) the hydrophobicity of the peptide was important; 6) the kinetics of peptide inhibition was complex and not clearly competitive or non-competitive; 7) there may be some specificity in inhibitor action as the GRK5 peptide did not block GRK6 phosphorylation; and 8) truncation of the LER from the C-Terminus did not appear to diminish activity suggesting we can reduce peptide size. Thus we have successfully

generated a unique inhibitor fulfilling one of our goals. This work appears to confirm the mutagenesis findings on the importance of the RH domain cluster. However, we are unsure as to the mechanism; that is, do the peptides bind the receptor or the GRK. The kinetics and specificity (points 6 and 7 above) seem to indicate binding to the GRKs. If as we propose, the peptides bind to the GRK, it seems unlikely energetically that the peptides can bind and displace the $\alpha 3$ - $\alpha 9$ interaction. The hydrophobicity of our most potent peptide (R169A) raises the possibility that it binds to a matching hydrophobic site on the GRK. In order to tease out how the peptide inhibitor binds GRK and to further pursue the possibility that receptor binding is directly affected, we propose the following experiments.

4.2 FUTURE DIRECTIONS

As discussed above, though we have discovered a novel role for the RH terminal subdomain domain of GRK critical for activation by GPCRs through mutagenesis of evolutionarily important sites and functional assays; both mechanisms of inhibition of receptors phosphorylation by RH domain key mutants and helix 9 peptidomimetics effects have not been resolved. To address the potential mechanisms for mutant actions, the following experiments are being considered: 1) examine whether GRK mutations affect direct binding to the receptor by FRET or BRET methodologies. We have previously shown the tight association of the $\beta 2$ AR with GRK5 using BRET (86). If the mutations affect the allosteric binding then FRET/BRET signals should be reduced as compared to WT GRK5. However the mutations could alter the structure through delocalized effects that indirectly alter binding of GPCRs; 2) determine the association of the $\beta 2$ AR with mutant GRK5/6

through immunoprecipitation. This has not been previously accomplished because of the tight membrane localization of both proteins of interest. Thus it would require finding conditions that would preserve the association with mild detergent solubilization. Recently it was reported that the serotonin receptor 5HT4-R was able to bind GRK5 through the use of a procedure involving binding of the receptor to an affinity column (52); 3) analyze mutant activities against increased concentrations of Rho* to determine K_m vs. V_{max} effects. Pure competitive kinetic i.e. an increase in K_m would imply disruption of the activation binding site. A decrease in V_{max} would imply a reduction in catalytic activity; 4) measure the “basal” activity of the mutants through assays of non-receptor substrates phosphorylation, autophosphorylation, and ATP binding to the active site to sort out direct effects on catalytic activity. This will help resolve delocalized effects which would result in reduced activities; 5) extend the mutagenesis/functional assays to the other clusters identified by ET (N-Terminus and the kinase domain small lobe), as well as to GRK1 and 2 representatives of the two other subfamilies. These studies should help refine the possibility as proposed by Tesmer that the N-terminus directly interacts with the receptor; 6) develop in vitro assays of reconstituted highly purified $\beta 2AR$ and GRK5 constructs to assess the activity of the mutants for phosphorylation of the agonist-stimulated $\beta 2AR$.

To further explore the nature of helix 9 peptides inhibition, we propose to: 1) improve their affinity/potency through alanine scanning of ET residues, chemical modifications, truncations, and permeability modifiers; 2) establish the binding sites of peptide inhibitors by generating photolabeled peptides; 3) compare and contrast kinetics of inhibition of helices 3, 9, and 10, N-Terminus, il-1 $\beta 2AR$ based peptides to determine whether their effects are additive, competitive or mixed; 4) optimize conditions for the use

of the cell-free 21K membrane fraction and/or the intact cell assay to test for the inhibition of ISO-stimulated β 2AR phosphorylation by endogenous GRKs. This would require peptides with enhanced permeability through truncations, introduction of transduction domains, or use of peptide delivery agents; 6) determine “basal” phosphorylation of non-receptor substrates. If the peptides are acting on GRK, one would expect an inhibition of the substrate phosphorylation; 7) characterize specificity of the peptides for the other GRKs; 8) encourage Dr Tesmer to resolve the structure of the GPCR-GRK complex.

APPENDIX

APPENDIX 1

Tables below (A-D) display ET results generated by Dr. Daniel Morgan from the Lichtarge group (Baylor College of Medicine)

Top ranked residues of the RH and kinase domain are shown in red and yellow respectively.

Table A. ET analysis of the RGS superfamily

Alignment #	Residue #	Type	Variability	Rank	Coverage
317	28	K	KR.ASQDNTELHMP	62.66	0.7
318	29	K	MK.RPHETAGCNQ	62.66	0.7
307	30	W	CRWLIYES.DKTPFMGHANV	57.19	0.7
315	31	R	RPQVLK.SETNDAWIGHMF	62.58	1.3
316	32	Q	DPLERKHA.FSMQGYNTV	62.62	0.7
314	33	M	ESNIPQMGK.LDVARFHTCW	62.44	0.7
294	34	L	SENPLDK.VMRGQTYFCH	48.81	1.3
310	35	Q	KETPNS.DGAQMVRHLIFY	59.68	0.7
308	36	F	RSFKLM.VEATCIDGPHY	57.57	1.3
302	37	P	PVMIAQ.GLSEKCDTYHNW	51.35	0.7
304	38	H	PLDRHK.SGAEYNTVCFQ	53.65	0.7
309	39	I	SNIVGA.LWPEKTCYFDRM	59.45	1.3
301	40	S	NAP.SVETQRGCFKMLDI	51.11	0.7
306	41	Q	LQT.MCPKSHNEAGDVRYW	55.77	0.7
287	42	C	TDE.CQHPAKGRVILSYN	46.71	1.3
297	43	E	LNK.SERDAHPCTQVWIYG	49.51	0.7
305	44	E	ER.YDHNQSGVTKPAL	55.63	0.7
266	45	L	EQV.LDPGCKYIHWARMTS	41.29	0.7
275	46	R	VK.RELAPDGCQHMI	44.31	1.3
320	47	L	LRKEHDA.SWQMTYVNPIC	62.66	0.7
303	48	S	QKRSTNDG.VAHWLIEM	52.34	0.7
264	49	L	WIGHL.RNFMVDTAQS	40.49	1.3
291	50	E	AEDVRKGS.TQP	48.21	0.7
300	51	R	QTIFKVRLEG.DMAHSPC	50.99	0.7
222	52	D	SNDTE.YGALRHQIV	32.56	1.3
155	53	Y	FLIY.MSHAW	23.67	0.7
285	54	H	ESYDVHN.TRCQGMPKA	45.82	0.7
263	55	S	NSEKHLRF.VTDAPMIYGQ	40.28	0.7
168	56	L	LSIVM.ANT	27.40	0.7
139	57	C	MLVICFK.YHGA	20.87	0.7
295	58	E	ADSRNQLGEKHV.TYI	49.14	0.7

321	59	R	.KEDQRS	62.66	0.7
158	60	N	TDQNS.HCAEF	24.71	1.3
201	61	P	KPRASDH.QNEVT	29.13	0.7
243	62	I	YKTILVNA.CDESPRGM	34.12	1.3
1	63	G	G.L	5.75	0.7
166	64	R	PVLRYPKAM.IHQS	27.00	0.7
271	65	L	VAQLRKNE.DISYTGMH	43.96	1.3
163	66	L	VESLYTAQ.NHRMFCD	25.62	1.3
17	67	F	YF.L	8.70	1.3
200	68	R	AITQRKHSL.MG	29.08	0.7
250	69	E	ADGYQELSR.IKTMHN	37.42	0.7
41	70	F	YF.S	11.61	1.3
9	71	C	LC.IYSA	8.36	0.7
235	72	A	KEDLNRQPA.MGH	33.65	0.7
323	73	T	.TNSVQDAK	62.66	0.7
245	74	R	MKHRG.SEAVFLTQDCNY	34.82	0.7
141	75	P	EPMSYFL.LDVGKNCTQA	21.45	0.7
249	76	E	HFYTEGDLNKNVAP.RQ	37.18	0.7
144	77	L	SLEVKHCQY.FND	21.68	1.3
252	78	S	DEHGKIS.AVLQRTN	38.06	0.7
140	79	R	ERPCLAGD.SKQVH	21.23	0.7
87	80	C	NHLYECQAT.PV	15.78	0.7
212	81	V	ILVM.STANCR	31.24	0.7
240	82	A	QLRGENTKDYS.AH	33.85	0.7
2	83	F	FL.IY	7.08	0.7
8	84	L	WLYL.F	7.50	1.3
167	85	D	MLIEDKQFTVG.N	27.27	0.7
136	86	G	AELDV.SHGQT	19.54	0.7
22	87	V	CVI.EAL	9.12	0.7
172	-	.	.V	62.66	0.7
135	88	A	ENAKGQ.STV	18.22	0.7
214	89	E	TDREKYGN.SALQ	31.71	1.3
52	90	Y	YFLI.WMGH	13.84	1.3
47	91	E	KREQDNHS.	12.35	0.7
234	92	V	KRYVIGHQTLFAMWC.	33.03	0.7
230	93	T	ITSGALMEQVRNC.D	32.93	0.7
258	94	P	SDAPKHNTL.IEFGCQM	38.69	1.3
254	95	D	RKHQDEPANLGTISYV.	38.51	1.3
280	96	D	WDELTKAIHRQPNVF.	45.78	1.3
267	97	K	SQKDENALVTRGIMH.	41.94	1.3
203	98	R	RMVLSQIKTW.	29.71	1.3

299	99	K	ILAKSTGHRPEVNQDFM.	49.60	0.7
288	100	A	SKREDVAQTCYHPLMGIN.	46.94	1.3
171	101	C	RKCQLYEMFTVAHNS.	28.82	1.3
45	102	G	AVGSLIRM.	11.80	0.7
248	103	R	KHNELRTQ.DSCFA	37.07	0.7
292	104	N	KDESQRHTLA.IMNGVIFY	48.40	0.7
34	105	L	LIV.MA	11.20	0.7
160	106	T	YLFMW.VITARHG	25.00	1.3
261	107	Q	KTEDYNASQ.RMLVHG	39.67	0.7
257	108	N	ITELRKQD.ASVWNMH	38.66	0.7
76	109	F	YFH.CM	14.11	1.3
120	110	L	ILF.AVMC	17.97	0.7
229	111	S	QSKANMTRCDE.VLHW	32.83	0.7
324	112	H	P.NKRVEADHTMS	62.66	0.7
236	113	T	QSPKE.TINGVADMFR	33.82	0.7
219	114	G	SKGLVEQANDRMH	32.32	1.3
142	115	P	PALGKSEDTCMQ	21.46	0.7
244	116	D	RSPAVKLTIQGCH.DNYY	34.50	1.3
255	117	L	ETCRPFQSKVHDA.YLN	38.52	0.7
148	118	I	IQEWLSCPAVTG	22.54	0.7
157	119	P	.VIPHASKECRTNQYDG	24.47	0.7
137	120	E	NELQDPFSTR.IAY	20.07	0.7
143	121	V	IVFLYDT.M	21.62	0.7
70	122	P	DEPSGTKLNF	13.93	0.7
159	123	R	SGPKQHREDFAYWC	24.89	1.3
269	124	Q	SQKDTHFREGACPVYNI	42.22	1.3
150	125	L	T.VALESIGMRD	23.17	1.3
152	126	V	R.MVTKLIQFYHNAP	23.42	0.7
251	127	T	ESDTNKRWA.GVFHQI	37.67	0.7
274	128	N	TKSIEHQNLVFARYGM.W	44.16	1.3
147	129	C	IVTCGFL.KQAPM	22.41	0.7
262	130	T	ISLVRQEWKANMCHTGP.	40.04	0.7
268	131	Q	REKLSDTQWMHGNCAY	42.16	0.7
247	132	R	NKGRAFVHDESPCYT	36.15	0.7
169	133	L	IMLPVAHSTFC	27.92	0.7
276	134	E	QLKTVASERGMPNFDIC	44.75	0.7
259	135	Q	ENHKQGDA SRTMICPV	38.82	0.7
325	136	G	.ENQSRDAGKTILFV	62.66	0.7
145	137	P	PVKALIGECSFHD.	21.77	0.7
256	138	C	THSPCEDRQAGNVF.Y	38.57	1.3
277	139	K	EPRKTSADQLIVNHFY.	44.90	0.7

286	140	D	TLFYKDESVGQHARNPCIW.M	46.03	1.3
162	141	L	CMTVLISGAF.	25.25	0.7
23	142	F	FLYVSAM.	9.63	0.7
199	143	Q	EQDSNYRKAHTLGV.C	28.85	0.7
226	144	E	EKSAPDLVQMTH.	32.78	0.7
97	145	L	AHCYIQLTSKV.P	15.89	0.7
113	146	T	QSTIAKLMVEG.R	17.77	0.7
241	147	R	KDETRQS.WLGMAVHNCI	33.97	0.7
156	148	L	IQHVESNR.KALTMW	24.23	0.7
165	149	T	VIAL.TEPC	26.30	1.3
149	150	H	YFMHCRL.QGVDK	22.96	1.3
289	151	E	MNLQDRT.AEKSCGHYIV	47.15	0.7
146	152	Y	HLRKT.SAFNVMCDQ	22.13	0.7
7	153	L	MLF.IR	7.30	0.7
138	154	S	EKRNSGHQADT.L	20.51	0.7
206	155	V	RYKGDEFQMSNAHTV.	30.77	1.3
153	156	A	DEKSANTQVI.GH	23.64	0.7
81	157	P	SCPVIETA.L	15.63	1.3
25	158	F	YFL.H	11.05	1.3
253	159	A	PSAEQHGTN.RKV	38.12	0.7
127	160	D	REKP.MFSLDVAQ	18.16	0.7
27	161	Y	FY.	11.07	0.7
164	162	L	LIQVM.K	26.19	0.7
170	163	D	KREDLG.TNVSQA	28.55	0.7
11	164	S	S.TA	8.65	1.3
290	165	I	EPSMDLQ.NARTKIGYHF	47.66	0.7
227	166	Y	MTHIYKRQAL.FVSE	32.81	0.7
102	167	F	YF.QLC	17.54	1.3
246	168	N	QLKSTD.RNMGHFEYA	35.80	0.7
260	169	R	KRDQ.ECSNGATHVL	38.96	0.7
154	170	F	LMFY.CHVI	23.66	0.7
202	171	L	L.CAIVTSRMF	29.59	0.7
326	172	Q	.AQRENPKMS	62.66	0.7
327	173	W	.WTQAKRLSFG	62.66	0.7
329	174	K	K.ASERGP	62.66	0.7
330	175	W	TDAWN.LCVESRGKIQ	62.66	1.3
335	176	L	MKTILV.AFSEYP	62.66	0.7
336	177	E	QEG.VNSKFDCRMLA	62.66	0.7
270	178	R	SEIPRL.TAVMKDGQHC	43.12	1.3
265	179	Q	NQ.ETRSVGDKHIA	41.08	0.7

Table B. ET analysis of the RH domain of the GRK subfamily

Alignment #	Residue #	Type	Variability	Rank	Coverage
1	28	K	QKRL	4.95	21.6
2	29	K	RK	4.19	17.0
3	30	W	RYFHWLI.VP	7.68	40.5
4	31	R	RHLKN.VP	9.37	50.3
5	32	Q	RKASEQNLD	8	41.8
6	33	M	SKRLIMYP	8.24	45.1
7	34	L	LDEG	4.43	20.3
8	35	Q	MASKRTQPH.	10.41	62.7
9	36	F	LFSC	5.38	24.2
10	37	P	PVI	2.97	9.2
11	38	H	GKHPR	4.97	22.2
12	39	I	PLIVYS	6.26	32.0
19	40	S	QDETSNVI	6.95	34.6
20	41	Q	SCGQVKME	7.79	41.2
21	42	C	CYQH	3.94	15.7
22	43	E	ETAGVSILKR	9.18	49.0
23	44	E	QEAGSDNPYHF	12.56	79.1
24	45	L	LV	1.66	1.3
25	46	R	RKEALQ	6.16	29.4
26	47	L	QESDAWHLTK	13.14	85.0
27	48	S	ASKTNREM	12.73	80.4
28	49	L	MLIVGHN	10.93	66.7
65	50	E	PASEDV	10.37	61.4
66	51	R	ATQLPKRIVM	12.91	82.4
67	52	D	DNHQGAESTK	10.12	58.2
68	53	Y	FY	3.41	11.8
69	54	H	NHETKQDRSGYCA	17.88	98.7
70	55	S	SNLTGWYFKH	10.35	60.8
71	56	L	LIVMQN	7.67	39.2
72	57	C	CIVF	2.28	5.9
73	58	E	EVSLDN	8.93	47.7
74	59	R	QRKE.	18.44	100.0
75	60	N	QNHE	3.35	10.5
76	61	P	PAVKR	5.65	26.8

77	62	I	IVL	4.29	18.3
78	63	G	G	1	0.7
79	64	R	RKHYF	7.12	35.3
80	65	L	RKLEMV	6.43	34.0
81	66	L	LF	2.4	7.8
82	67	F	FYL	2.34	6.5
83	68	R	RQHK	5.35	23.5
84	69	E	DQEL	6.16	29.4
85	70	F	FY	3.86	15.0
86	71	C	LCYSA	4.38	19.6
87	72	A	AEDKQRNL	13.04	83.7
88	73	T	TNQSAK	8.19	44.4
89	74	R	VTGINDAHKRYE	14.95	90.2
90	75	P	PGNQERSLMIC	10.23	59.5
91	76	E	APTKERQGDSN	15.18	92.2
92	77	L	YFNEHLVQDS	9.49	52.3
94	78	S	QRSLKNHVGAEFIC	18.44	100.0
95	79	R	EGKQVLAPRCSH	14.22	87.6
96	80	C	APCHYQLE	8.96	48.4
97	81	V	MRVACSLGIT	13.24	86.3
98	82	A	GATDERQKN	12.91	82.4
99	83	F	FL	1.88	2.6
100	84	L	LWFY	3.59	12.4
101	85	D	EDKT	4.37	19.0
102	86	G	EDALSGKQ	10.27	60.1
103	87	V	VLIA	4.48	20.9
131	88	A	QSYNEAVK	7.36	36.6
132	89	E	SNDTEAKL	11.67	71.2
133	90	Y	WYF	3.8	13.7
134	91	E	EDNQ	5.16	22.9
135	92	V	LTMCVIKGA	10.51	64.1
172	93	T	ASCTLIM	8.01	42.5
174	94	P	EDIPTCSNK	10.13	58.8
175	95	D	GDANEQYKP	9.32	49.7
176	96	D	PNAKESDG	9.62	52.9
177	97	K	AVTIDELKNG	12.55	78.4
178	98	R	KRQL	6.34	32.7
179	99	K	GDT SAPRKLVI	15.32	93.5
195	100	A	SKQAEDHRVCT	13.94	86.9
196	101	C	TAMKFCHRVQ	12.94	83.0
199	102	G	LMRAGNS	6.14	28.1

200	103	R	QETASLKRCNF	11.23	68.0
201	104	N	AGQNKTSRED	15.11	91.5
202	105	L	LITVM	6.26	32.0
203	106	T	VAILRFYMT	12.81	81.0
204	107	Q	ATNQSKD	9.84	54.9
205	108	N	TNKREQAILSH	15.76	96.7
206	109	F	CFYLH	7.38	37.3
221	110	L	AVLCMFIH	7.65	38.6
222	111	S	VASRKEDTNM	12.26	76.5
223	112	H	ADTPENHKRV	11.87	73.2
234	113	T	PGDSQKNT	9.85	55.6
235	114	G	NVAGSLKQM	11.3	69.9
236	115	P	PKTQAEL	8.18	43.8
294	116	D	GQNTSHLEVADF	11.92	73.9
295	117	L	QRHN.YFSPLVWC	16.69	98.0
296	118	I	P.LCITSA	8.89	47.1
297	119	P	HQSTPNADY	11.25	69.3
298	120	E	SPFEQVLADN	12.57	79.7
299	121	V	FLMIVY	8.12	43.1
300	122	P	LFSTPDGN	10.4	62.1
301	123	R	SQGREAPDK	10.78	65.4
302	124	Q	PQDENGHAHST	15.55	95.4
303	125	L	ALPVDGIMTS	13.23	85.6
304	126	V	LVAIT	10.05	57.5
305	127	T	VATSEKHQN	15.58	96.1
306	128	N	TKRPEQNSHF	10.81	66.0
307	129	C	KCVFAPT	7.68	40.5
312	130	T	CRQKAESTD	10.54	64.7
313	131	Q	QASEDWCLKNGY	15	90.8
316	132	R	ADVRKNGSYH	12.13	75.2
317	133	L	ATSHLPG	8.32	46.4
318	134	E	TEDKVGALNHS	15.43	94.8
319	135	Q	TDKFEVGPQS	10	56.9
321	136	G	ED.SNKGQR	11.25	69.3
322	137	P	EDVASI.PGK	10.46	63.4
323	138	C	RQYMFAG.SCPT	12.11	74.5
324	139	K	ARVKED.QSPT	14.82	89.5
325	140	D	SVATNEDGKQ	14.41	88.2
326	141	L	LAVKDI	6.43	34.0
331	142	F	VMF	2.79	8.5
332	143	Q	EATQGVSKNH	14.44	88.9

333	144	E	QLDEAPKR	12.5	77.1
334	145	L	AGVITLCPY	8.32	46.4
335	146	T	KRVQMLATSYI	13.14	85.0
336	147	R	ADREQGNL	11.78	72.5
337	148	L	E.ASKIVL	9.43	51.6
338	149	T	AVT.LI	12.24	75.8
339	150	H	MK.FLCYHR	11.72	71.9
340	151	E	ATSVEDKNQR	15.4	94.1
341	152	Y	FYHQNRSK	9.4	51.0
342	153	L	LF	1.75	2.0
343	154	S	QKRSGETAN	12.52	77.8
344	155	V	DEGQMVTK	11.02	67.3
345	156	A	QKVAGTEIDNS	15.96	97.4
346	157	P	PAVILE	6.25	30.7
347	158	F	FYWL	4.18	16.3
348	159	A	RQKTVAEGHNS	15.25	92.8
349	160	D	EDFPKR	7.57	37.9
350	161	Y	FY	5.4	24.8
351	162	L	LVQEAIM	9.75	53.6
352	163	D	VATGEDS	9.82	54.2
353	164	S	ST.	3.22	9.8
354	165	I	PAQEMLTSID.	11.49	70.6
355	166	Y	FYK.R	6.08	27.5
356	167	F	YFL.	7.3	35.9
357	168	N	DEKLGNSHT.	9.98	56.2
358	169	R	KRQ.	4.29	18.3
359	170	F	FY.	3.37	11.1
360	171	L	LTC.	3.8	13.7
361	172	Q	Q.	2.01	4.6
362	173	W	WF.	2.39	7.2
363	174	K	K.	2.01	4.6
364	175	W	VLEWN.	5.54	26.1
365	176	L	FYLV.	5.43	25.5
366	177	E	E.	2.01	4.6
367	178	R	MKAGRL.	6.17	30.1
368	179	Q	QRN	3.81	14.4
369	180	P	PIM	2.19	5.2

Table C. ET analysis of the AGC kinases superfamily

Alignment #	Residue #	Type	Variability	Rank	Coverage
6	180	P	KSRNQP.GVTYIELHDMAF	62.06	84.6
7	181	V	YITWEL.HFMASVCKPNR	50.07	75.2
8	182	T	SVTAGKQRH.NCEPFD	63.19	85.5
9	183	K	LYIP.VSFMTAKQRDE	35.77	57.6
10	184	N	QKSYNHTGDAI.RELP	66.59	88.1
11	185	T	DNFE.QHVASCRTYW	37.77	61.1
12	186	F	FLP.YWV	11.79	18.3
13	187	R	QSDETALNHK.IRVYM	64.55	86.8
14	188	Q	ILVFMQ.TRKHGYPEACD	42.38	68.5
15	189	Y	LMQERKGYVIH.CF	41.01	67.2
16	190	R	RQNDE.KAICTSGMVHY	34.34	55.6
17	191	V	TSVNILKM.	19.64	34.1
18	192	L	LVRIS.	17.39	30.5
19	193	G	G.D	1.9	2.6
20	194	K	T.KSMNREVIGQA	24.31	41.8
21	195	G	GHDC	2.9	5.5
22	196	G	STPLAQGNHM	15.81	28.0
23	197	F	FLMYV	8.18	12.5
24	198	G	GSALR	3.72	6.8
25	199	E	RPKTIVNQE	12.47	19.3
26	200	V	VSAGI	3.93	7.4
27	201	C	HRPLYCNEWIMQKTSFV	32.43	52.4
28	202	A	LISFQMVKEGA	14.28	23.5
29	203	C	IVTACSRG	20.01	35.0
30	204	Q	RQHKLTDCEVPIMS	39.26	63.3
31	205	V	SLRHQNDEPFYTIVA.KMG	85.07	100.0
32	206	R	RNIVKTASMHQGELFYD	56.58	81.4
33	207	A	HSGDK.NRQIVEATMFL	37.14	59.2
34	208	T	.RPEDASLGTKNHQV	33.95	55.0
35	209	G	.DAQTESKRNCGPIHV	34.29	55.3
36	210	K	.VENIQKSRDGATLPF	85.07	100.0
47	211	M	.PVIFYLWTM	22.64	38.6
48	212	Y	.MVYFSLC	13.71	21.9
49	213	A	ASVT	3.37	5.8
50	214	C	MLIVHASQCN	25.39	43.4
51	215	K	KR	1.28	1.3
52	216	K	VTCIKRMQASYLE	29.15	47.6
53	217	L	LMFYVI	14.69	23.8

54	218	E	KNREASDPQHGTC	29.57	47.9
55	219	K	KMIWRF	5.06	8.7
56	220	K	EHQAKRSTPVCFLDIGN	37.67	60.8
58	221	R	ITVRQKEDYSNHALMF	39.96	64.6
59	222	I	VILMF	21.7	37.9
60	223	K	VILRKMNHTFQAS	33.19	53.7
61	224	K	RKQDSYANELIMGTC.V	40.54	65.9
88	225	R	LMHQTNCKRDEF.AVS	28.23	45.7
89	226	K	KRNSQPCDEHGT	24.5	42.4
90	227	G	QMTL.EDAHSNGR	13.36	20.6
91	228	E	VIQEGTL.MARSYF	30.6	49.2
92	229	A	EQDSANRKTVM	38.1	61.7
93	230	M	HNCASLWYRQTMG	16.52	29.3
94	231	A	TVILMAPS	18.09	32.2
95	232	L	NCLASMKQHRFTYIVE	38.28	62.4
96	233	N	DSNQAHLCGTIVME	32.6	52.7
97	234	E	EVK	2.26	3.5
98	235	K	RKACQSNHIL	15.91	28.6
99	236	Q	LRKSEAYGQICNHTDV	46.96	73.6
100	237	I	MILVAF	13.78	22.2
101	238	L	LMTQF	10.05	14.8
102	239	E	SKGQNVEMTRLAIY	41.7	67.8
103	240	K	IVLEDQRQSKAYGNT.CH	50.72	76.8
104	241	V	VAILMNTSC.QPRGEF	36.11	58.2
105	242	N	TSQEKRDCHNAGVFWP.LY	52.14	77.5
106	243	S	.GNSATMLKERHQDIC	85.07	100.0
107	244	R	.PKADLGVMITENRQ	85.07	100.0
116	245	F	FNWSY.L	7.85	12.2
117	246	V	ILVCT.M	20.28	35.7
118	247	V	IVTMC.LA	18.05	31.8
119	248	S	RTNIASEKGYCPQLH.D	46.17	73.3
120	249	L	MLCQFV.	12.93	19.6
121	250	A	WHMLIYREFTQKADVNC.S	43.09	69.8
122	251	Y	GSKRAQWTFYNDI.VH	27.14	44.4
123	252	A	TSGANHC.	23.63	41.2
124	253	Y	FWYSTGEL.ID	15.51	26.7
125	254	E	QKMHWASRTE.FD	19.53	33.8
126	255	T	DECSTNAF.H	12.16	18.6
127	256	K	ASCWVEDKQNHTFRPMG.	56.35	81.0
128	257	D	QHRKNTAICSYDEMG.	47.97	74.3
129	258	A	QNFKRCHSYDEP.A	32.92	53.4

130	259	L	IVLCFA.	14.72	24.1
131	260	C	FYCVR.HIGS	14.78	24.8
132	261	L	MIFL.	17.43	31.2
133	262	V	IVLMFCA.S	19.69	34.4
134	263	L	MILFTV.	15.71	27.3
135	264	T	DLEFSRPAQ.T	19.72	34.7
136	265	L	YKFLAVSTHC.I	28.26	46.0
137	266	M	IVALCRMKS.F	31.31	49.8
138	267	N	EAPTMVNSCILQGKRH.	32.26	51.8
139	268	G	GR.	2.52	4.8
140	269	G	G.KM	4.36	7.7
141	270	D	E.DHQ	8.35	12.9
142	271	L	LMIVFS.	15.08	26.0
143	272	K	FYWMSILH.KR	14	23.2
144	273	F	STHYDFWILMRAV.	36.07	57.9
145	274	H	LYHFRAVITMQ.W	17.23	30.2
146	275	I	LHICVMA.	12.19	19.0
147	276	Y	RQVKDSNLHYAE.CG	17.86	31.5
148	277	H	KRTSNAHEDGL.QPM	39.26	63.7
149	278	M	SCARYNIVKLE.DQTMFH	35.65	57.2
150	279	G	QKGHMNRVDATE.LS	85.07	100.0
174	280	Q	.LEDCKQNPT	85.07	100.0
175	281	A	.QGRKEHDNIAP	85.07	100.0
176	282	G	RDKHCSTLNQYFGEVIMAP.	40.63	66.2
177	283	F	FILMSW.	9.38	13.8
178	284	P	PSDTNAGQELKRM.	55.99	80.4
179	285	E	NTHEASLRKDMVQP	21.11	37.3
180	286	A	PSKNDAQVTYLGREH	64.38	86.5
181	287	R	VTQAMHNWELRPDYI	28.18	45.3
182	288	A	ASTGCVLMI	27.31	44.7
183	289	V	KQRNVLCTAGIMS	37.22	59.5
184	290	F	FILYAVSH	14.77	24.4
185	291	Y	YFCIV	5.2	9.0
186	292	A	AHCLISGTVPM	32.3	52.1
189	293	A	ASCTVG	19.11	33.4
190	294	E	ESTQCN	11.25	16.7
191	295	I	VALIMNT	23.14	40.8
192	296	C	CFITAVLHRSM	44.38	70.1
193	297	C	LSCMNEQTVIAF	31.36	50.2
194	298	G	AIVTSCGR	18.57	32.5
195	299	L	LIFVPTM	18.84	32.8

196	300	E	EDQGASHRIKLFMVN	34.58	56.3
197	301	D	YFKNTSCVHAQD	23.12	40.2
198	302	L	LIMSQFV	9.81	14.1
199	303	H	HQNR	5.03	8.4
200	304	R	SAKTQHNEDYMGR.LV	49.11	74.9
204	305	E	KLHRQNMEDCFYISG	54.21	78.8
205	306	R	DNQTKHSEG.RFYC	40.07	65.3
206	307	I	IVLMT	20.62	36.0
207	308	V	ITVLAM	28.45	46.3
208	309	Y	YHLFI	2.84	5.1
209	310	R	RK	2.44	4.2
210	311	D	DKN	1.44	1.9
211	312	L	LMFVIC	13.29	20.3
212	313	K	KC	1.31	1.6
214	314	P	PL	3.73	7.1
215	315	E	EDNA	6.21	10.9
216	316	N	NSD	2.25	3.2
217	317	I	ILVFCT	16.55	29.6
218	318	L	LMIF.V	14.8	25.4
219	319	L	LIMV.	11.34	17.0
220	320	D	DGSNQMATEC	15.85	28.3
227	321	D	.EDSN	85.07	100.0
228	322	H	.HFYNSRLQEDA	85.07	100.0
229	323	G	GA	1.76	2.3
230	324	H	HNYFSQ	14.79	25.1
231	325	I	ILVTMCAGS	37.27	59.8
232	326	R	KRAQYVICEML	13.87	22.8
233	327	I	ILVMQ	20.95	36.7
234	328	S	TVAIGCS	10.83	16.1
235	329	D	DN	2.2	2.9
236	330	L	FLMY	5.73	10.0
237	331	G	G	1	0.3
238	332	L	FCTLMV	6.16	10.6
239	333	A	ADTCSR	10.62	15.8
240	334	V	KRVCLMTI	7.79	11.9
241	335	H	.PLAEKQDTMYIVRH	20.87	36.3
242	336	V	.VLGDQENHSFACIMK	85.07	100.0
243	337	P	YERKHVQIL.FNDGCMSAPT	45.59	72.3
244	338	E	VLI.KMSTFWYNCARGDQEP	45.31	72.0
245	339	G	PQDSTEKRVIGNAYFLHCM	52.05	77.2
246	340	Q	.TDNGEMVIRKFSHAYPQL	52.77	78.1

258	341	T	VKINR.EHLATGQMCSP	36.81	58.5
259	342	I	TCASMP.NLGIV	22.93	39.5
260	343	K	YWCFSMDNRTQGKAHLV	35.13	56.9
261	344	G	TSPAGQE	7	11.6
262	345	R	LIMFYQ.SRKT	13.66	21.5
263	346	V	CVAIT.S	8.97	13.5
264	347	G	GI.	1.17	1.0
265	348	T	TS.	1.17	1.0
266	349	V	PHTSLIVEQ.NG	16.72	29.9
267	350	G	DEQHGNSA	10.07	15.1
268	351	Y	Y.F	5.71	9.6
269	352	M	ILTMV.SCF	13.87	22.8
270	353	A	APS.D	6.65	11.3
271	354	P	P.G	2.47	4.5
272	355	E	EK.GD	4.46	8.0
273	356	V	VISMNL.TFQK	20.22	35.4
274	357	V	VIL.P	85.07	100.0
275	358	K	SATQLGHRKM.NIVCEDF	48.65	74.6
277	359	N	.GNDEKARLQSCMTH	85.07	100.0
278	360	E	TNSLCRAG.EDYQKPH	30.7	49.5
279	361	R	KRQSTVAHLC.ENIMDP	52.68	77.8
281	362	Y	YH.QCD	5.83	10.3
282	363	T	NGDTAS.R	38.11	62.1
283	364	F	KRSLTMCFIHQYN.PAGVE	41.08	67.5
284	365	S	SAPGQTVMH.ECND	32.21	51.4
285	366	P	IVAWCT.SP	21.06	37.0
286	367	D	DT.	3.64	6.4
287	368	W	WTIALYF.MVC	15.6	27.0
289	369	W	WYSG.RF	10.35	15.4
290	370	A	SATGC.	23.14	40.8
291	371	L	FLMYI.TVA	29.13	47.3
292	372	G	G.	3.5	6.1
293	373	C	IVTA.SC	24.38	42.1
294	374	L	LFCYV.MIST	15.38	26.4
295	375	L	ILTGVM.CA	31.67	50.5
296	376	Y	YFCH.	24.63	42.8
297	377	E	EV.RQDK	9.93	14.5
298	378	M	MFIL.	13.45	21.2
299	379	I	LIFMANVCT.	27.72	45.0
300	380	A	ATCVGSINLY.HFEMRKQD	34.36	55.9
301	381	G	GRD.CQA	11.16	16.4

302	382	Q	YFHLKIQCRSPEGTNW.VAD	44.79	70.7
303	383	S	TPSAVLQ.CGR	24.8	43.1
304	384	P	P.	5.6	9.3
305	385	F	.PF	85.07	100.0
306	386	Q	.PFRQK	85.07	100.0
310	387	Q	.QGKAMDSTVR	85.07	100.0
311	388	R	FIAVYL.QRK	16.2	28.9
312	389	K	YWFVRDHNGASTQEP.KLI	37.95	61.4
313	390	K	DNTSGHA.CILVYKE	29.8	48.6
314	391	K	SQPTVNEDKR.CIAG	40.97	66.9
315	392	I	.GDQVNEKYTHSRI	85.07	100.0
316	393	K	.AEQLTDSGKN	85.07	100.0
325	394	R	TPHLVQINED.SRKAW	29.13	47.3
326	395	E	MILVFSDYPNQAEGT.CKRH	39.96	65.0
327	396	E	KGRLAEQSVMITDYF.	37.47	60.1
328	397	V	TILMV.K	23.9	41.5
329	398	E	YFCEM.VIDSAQLKTR	22.72	39.2
330	399	R	EQNRDKSTAMHW.	42.44	68.8
331	400	L	KNAQLRDEISV.CTM	31.73	50.8
332	401	V	IVT.M	11.68	18.0
333	402	K	LIVCMATQRK.EP	33.56	54.0
334	403	E	NQAKRESVLTYIGDFHM.	56.22	80.7
335	404	V	AGCHK.EQNDSRMTIV	45.03	71.1
336	405	P	.IVNAPETQS	85.07	100.0
337	406	E	.GSTDEYVP	85.07	100.0
338	407	E	ESKRDNPIQMHA VT.	42.97	69.5
339	408	Y	LVIFPYMA.KQW	29.75	48.2
340	409	S	RKTVHNQLAEDSYIMFPW.G	50.28	75.9
341	410	E	FYWMIL.CVPADESHT	34.71	56.6
342	411	R	PSETAKRL.GVQD	21.44	37.6
354	412	F	FLIVMTNKDER.W	33.88	54.7
355	413	S	NHPQDESGTKA.LF	40.89	66.6
356	414	P	EPATVGSYFLNKQRD.	73.96	91.0
357	415	Q	DKLGARFYITHNEQSWP.V	50.49	76.2
358	416	A	VAISCLTPG.M	32.77	53.1
359	417	R	KQRLVICGAHSTEWM.	47.41	74.0
360	418	S	DNESHKVAQTGR.LC	42.29	68.2
361	419	L	LMFIVAC.Y	31.75	51.1
362	420	C	LIVMC.FA	25.44	43.7
363	421	S	SKQGTERDHIMAV.LNC	42.82	69.1
364	422	Q	RKQNHGSCELPAVWM	45.07	71.4

365	423	L	LFICVM	13.45	21.2
366	424	L	ILCQMFP	14.84	25.7
367	425	C	TVIQSEKNCRHMADG	45.99	73.0
368	426	K	RKADSGTLHNVPQE	23.12	40.2
369	427	D	DNLVTQKAEHCSR	39.81	64.3
370	428	P	LIHPRVTKAQYSE.	28.92	46.6
371	429	A	STLEQCMAGKNRDVHFIYP.	68.06	89.1
372	430	E	QEKRCHVGLTNDMIAS.F	50.11	75.6
373	431	R	R.S	2.33	3.9
374	432	L	LIY.FKMWP	17.42	30.9
375	433	G	G.LAKQTNDM	8.78	13.2
376	434	C	NT.ACHEGYSMVFDL	39.36	64.0
377	435	R	.SVITQHKRGLNDACYMP	85.07	100.0
378	436	G	L.MQISRGNDAEKPTVH	55.63	79.7
379	437	G	.TSAPYFEDRGKNV	85.07	100.0
401	438	S	G.QREDAIKNST	85.07	100.0
402	439	A	TSPA.VRNCYFIGELM	85.07	100.0
403	440	R	EQDRANSKM.TLGVPHIC	71.66	90.7
404	441	E	DG.RNSEALQTMPKCV	37.04	58.8
405	442	V	VI.ELPMFY	33.83	54.3
406	443	K	KRFLMSQVCLNAT	37.56	60.5
407	444	E	NASTGM.KRHDELQVIYC	79.13	91.3
408	445	H	H.QVNMARELS	22.37	38.3
409	446	P	PQGLK.RVEAIMSFDTCNH	57.96	83.0
410	447	L	WY.FRPLGIV	18.94	33.1
411	448	F	F.GLYSW	11.56	17.4
412	449	K	KNSQARH.YETGDMLVC	69.44	89.7
413	450	K	EDG.HSKNTRQALPYFW	57.48	82.3
423	451	L	VILA.TFMW	38.82	63.0
424	452	N	VITDSNEQYHA.GKP	44.4	70.4
425	453	F	WFC.	11.64	17.7
426	454	K	EDTNRKVIFHYSLWQA.GP	67.81	88.7
427	455	R	KRMVSADNGPWELQH.TY	60.65	83.9
428	456	L	LIVCTQF.AMPW	26.19	44.1
429	457	G	LAYFEQIPRKMWCTGSNVD.	57.5	82.6
430	458	A	SACRKTNEQHYPMGDL.I	64.75	87.1
431	459	G	RKGLMQSFC.NAVWH	38.46	62.7
432	460	M	NYDEKQRAHTVSGL.MIP	62.38	84.9
433	461	L	.WYLNVIP	85.07	100.0
434	462	E	IYDLVFMERG.ATHPQ	60.16	83.6
435	463	P	EDPGLNRKTSVMIQA.H	67.76	88.4

436	464	P	TAVPGSLH.RQKI	22.71	38.9
437	465	F	PL.TAHSEFW	13.11	19.9
438	466	K	YIFS.WALRGTVKC	30.58	48.9
439	467	P	ETVLPKIF.QHAYMRNC	54.75	79.4
440	468	D	PVS.HRLIGDK	15.73	27.7
441	469	P	PKTRYND.FSAEIHQVMCLG	58.25	83.3
442	470	Q	IVNAQLTYCG.FRSPEMHK	53.66	78.5
443	471	A	QHTKRDAGVSYE.NLMCIF	71.12	90.4
444	472	I	QASGE.FHYNRDTKPVI	50.63	76.5
445	473	Y	GASTKRHDPNI.VMELQCY	54.24	79.1
446	474	C	QVIATSEDMPGF.YLNRKHC	61.72	84.2
474	492	E	GSPVQRKAIED.YHTNMWCL	68.86	89.4
475	493	P	VIAS.GKRPTLHYEDNMF	65.69	87.5
476	494	T	QLSIMVTCAFY.NHKEWPGD	56.99	81.7
477	495	D	GSTQADFYPNEV.CKIMLHR	40.12	65.6
478	496	Q	.VGNLEDFYASIRCPTQK	45.14	71.7
479	497	D	.YGRSMLVDKQCEHTAIPFN	85.07	100.0
480	498	F	EDHSP.VAYNKFITRQML	85.07	100.0
481	499	Y	DGPSAKQE.VRNCYL TIF	45.78	72.7
482	500	Q	PQEVSATIRKHD.LNGWFY	70.11	90.0
483	501	K	YHLFQTDEMC.AGPWSNVKRI	64.35	86.2
484	502	F	AMQRGDTYSLKNV.PEIFH	66.1	87.8
485	503	A	DAESHNQGK.RLYFMPIVT	62.61	85.2
486	504	T	LQYMFIECT.KPRVAGNSDH	63.69	85.9
487	505	G	FMLSHWYP.VNTAQEDGICKR	57.39	82.0
488	506	S	RKSQVLTPENIAHDYF.CGM	85.07	100.0
489	507	V	DEGNHA.RSKVTLPMCQIFY	55.98	80.1

Table D. ET analysis of the kinase domain of the GRK subfamily

Alignment #	Residue #	Type	Variability	Rank	Coverage
1	180	P	QNHTP	4.52	63.7
2	181	V	LVIM	5.37	71.7
3	182	T	TSDAG	5.92	75.2
4	183	K	MKYDEA	4.88	68.2
5	184	N	NKHD	2.96	46.0
6	185	T	DETYWA	4.25	62.1
7	186	F	F	1	19.0
8	187	R	SRETYLA	5.12	69.5
9	188	Q	VQHMLED	4.55	64.6

10	189	Y	HYF	2.61	40.2
11	190	R	R	1	19.0
12	191	V	IVT	2.22	34.4
13	192	L	IL	1.69	27.7
14	193	G	G	1	19.0
15	194	K	RK	2.68	41.5
16	195	G	G	1	19.0
17	196	G	G	1	19.0
18	197	F	F	1	19.0
19	198	G	G	1	19.0
20	199	E	EK	1.6	21.2
21	200	V	V	1	19.0
22	201	C	YCSF	3.59	53.4
23	202	A	GA	1.69	27.7
24	203	C	CV	1.82	29.6
25	204	Q	RQ	1.69	27.7
26	205	V	KVMR	2.77	43.1
27	206	R	ARK	6.15	76.8
28	207	A	DAN	2.43	37.3
29	208	T	TS	1.34	19.6
30	209	G	G	1	19.0
31	210	K	KQ	1.56	20.3
32	211	M	ML	2.74	42.8
33	212	Y	Y	1	19.0
34	213	A	A	1	19.0
35	214	C	MCLN	2.61	40.2
36	215	K	K	1	19.0
37	216	K	CKR	3	47.3
38	217	L	L	1	19.0
39	218	E	DEQCN	4.04	57.9
40	219	K	K	1	19.0
41	220	K	K	1	19.0
42	221	R	R	1	19.0
43	222	I	IVL	3.45	52.1
44	223	K	K	1	19.0
45	224	K	MLK	2.68	41.5
46	225	R	KR	3.23	49.5
47	226	K	QGTKHNS	8.24	90.0
48	227	G	GA	1.34	19.6
49	228	E	EY	1.63	22.5
50	229	A	MTASKEQ	6.22	77.5

51	230	M	LMGA	3.01	47.6
52	231	A	AVS	1.76	28.9
53	232	L	LMI	2.8	43.4
54	233	N	NILSV	4.1	59.2
55	234	E	E	1	19.0
56	235	K	RK	1.69	27.7
57	236	Q	NIQREK	7.06	82.6
58	237	I	MI	1.69	27.7
59	238	L	L	1	19.0
60	239	E	QSEATM	5.59	73.0
61	240	K	ALKR	5.27	71.1
62	241	V	VLI	2.69	41.8
63	242	N	SNHQ	4.94	68.8
64	243	S	TS	1.69	27.7
65	244	R	GVRQPL	5.66	73.3
70	245	F	F	1	19.0
71	246	V	IVL	5.83	74.6
72	247	V	V	1	19.0
73	248	S	CSN	4.17	60.8
74	249	L	ML	1.69	27.7
75	250	A	TSA	3.7	54.3
76	251	Y	YC	1.6	21.2
77	252	A	AT	2.06	29.9
78	253	Y	FY	2.3	35.7
79	254	E	HQRED	5.19	70.4
80	255	T	TS	3.04	47.9
81	256	K	PK	1.69	27.7
82	257	D	DESTA	5.8	74.3
83	258	A	KNAHED	4.72	65.6
84	259	L	L	1	19.0
85	260	C	CS	3.23	49.5
86	261	L	FL	1.69	27.7
87	262	V	ISV	2.47	38.3
88	263	L	LM	2.09	31.5
89	264	T	DTS	3.37	51.4
90	265	L	LI	3.27	50.2
91	266	M	M	1	19.0
92	267	N	N	1	19.0
93	268	G	G	1	19.0
94	269	G	G	1	19.0
95	270	D	D	1	19.0

96	271	L	LMVI	4.43	63.0
97	272	K	HKR	2.24	35.4
98	273	F	YF	2.96	46.0
99	274	H	H	1	19.0
100	275	I	LIV	2.52	39.2
101	276	Y	SY	1.69	27.7
102	277	H	QHNS	4.55	64.6
103	278	M	HMLVI	4.09	58.8
104	279	G	GMDN	3.14	48.9
111	280	Q	.QNDEPT	13.02	100.0
112	281	A	.APGRK	13.02	100.0
113	282	G	IVG	2.44	37.9
114	283	F	FLI	2.18	32.8
115	284	P	SNPEDAQ	9.31	92.0
116	285	E	ELM	2.23	34.7
117	286	A	DQASKPEN	12.96	97.7
118	287	R	EDR	3.79	55.9
119	288	A	MVAI	3.89	56.3
120	289	V	KRVLQIC	8.41	90.4
121	290	F	FYSH	5.76	74.0
122	291	Y	Y	1	19.0
123	292	A	AST	4.18	61.1
124	293	A	ATS	3.12	48.2
125	294	E	EQ	2.09	31.5
126	295	I	VILM	5.85	74.9
127	296	C	ICLATV	6.77	79.4
128	297	C	LCTQS	5.2	70.7
129	298	G	G	1	19.0
130	299	L	LVMI	4.16	60.5
131	300	E	EQL	2.44	37.9
132	301	D	HDQ	3.62	53.7
133	302	L	MVL	2.48	38.6
134	303	H	HQ	2.15	31.8
135	304	R	KVNSTRHEGDQ	11.41	96.8
136	305	E	RCEKQLMH	7.05	82.0
137	306	R	CGFYRND	7.3	84.6
138	307	I	IVT	4.33	62.7
139	308	V	VLI	4.12	59.5
140	309	Y	Y	1	19.0
141	310	R	R	1	19.0
142	311	D	D	1	19.0

143	312	L	LCM	3.43	51.8
144	313	K	K	1	19.0
145	314	P	P	1	19.0
146	315	E	AE	1.69	27.7
147	316	N	ND	2.17	32.5
148	317	I	IV	2.09	31.5
149	318	L	L	1	19.0
150	319	L	L	1	19.0
151	320	D	D	1	19.0
152	321	D	EDSN	3.73	54.7
153	322	H	NSHFYRLQEDA	10.03	93.9
154	323	G	G	1	19.0
155	324	H	HNQ	3.36	51.1
156	325	I	IVAC	5.47	72.3
157	326	R	R	1	19.0
158	327	I	IL	2.31	36.0
159	328	S	S	1	19.0
160	329	D	D	1	19.0
161	330	L	LM	1.6	21.2
162	331	G	G	1	19.0
163	332	L	L	1	19.0
164	333	A	AT	2.21	33.8
165	334	V	CVLMTI	5.37	71.7
166	335	H	DHEKQ	5.54	72.7
167	336	V	FVIML	6.23	77.8
168	337	P	SPKQAL	7.32	84.9
169	338	E	KEDGPVA	7.28	83.9
170	339	G	KGND	4.24	61.4
171	340	Q	KRQED	5.98	75.6
173	341	T	.TMRLPIVK	13.02	100.0
174	342	I	PIVT	4.85	67.8
175	343	K	HKRQ	4.25	62.1
176	344	G	AG.	2.43	37.3
177	345	R	SRMKY	3.78	55.6
178	346	V	VA	2.09	31.5
179	347	G	G	1	19.0
180	348	T	T	1	19.0
181	349	V	HVNGP	3.28	50.5
182	350	G	GA	1.56	20.3
183	351	Y	YF	1.63	22.5
184	352	M	M	1	19.0

185	353	A	AD	2.17	32.5
186	354	P	P	1	19.0
187	355	E	E	1	19.0
188	356	V	VIL	3.65	54.0
189	357	V	LVI	3.74	55.3
190	358	K	SAQKRNDMTL	13.02	100.0
191	359	N	KNHEDG	6.45	78.5
192	360	E	GEQKT	4.03	57.6
193	361	R	TVRKAPE	7.27	83.6
195	362	Y	Y	1	19.0
196	363	T	DTGASR	4.62	65.3
197	364	F	SFLYTM	5.67	73.6
198	365	S	CSGPA	4.77	66.2
199	366	P	APV	2.73	42.1
200	367	D	D	1	19.0
201	368	W	WCY	3.55	52.4
202	369	W	FW	2.49	38.9
203	370	A	SAGT	4.8	66.6
204	371	L	FLVM	4.09	58.8
205	372	G	G	1	19.0
206	373	C	CV	1.63	22.5
207	374	L	MLFST	4.15	60.1
208	375	L	LI	2.83	43.7
209	376	Y	YF	2.89	44.4
210	377	E	KE	1.69	27.7
211	378	M	LMF	2.89	44.4
212	379	I	LIV	3.89	56.6
213	380	A	KRAQED	6.19	77.2
214	381	G	GA	1.63	22.5
215	382	Q	HQKRY	5.19	70.4
216	383	S	SATG	3	47.3
217	384	P	P	1	19.0
218	385	F	F	1	19.0
219	386	Q	RQK	4.96	69.1
223	387	Q	.QKGMDSATR	13.02	100.0
224	388	R	QRYFK	4.55	64.6
225	389	K	HKG	2.24	35.4
226	390	K	KE	2.74	42.8
227	391	K	TK	1.69	27.7
228	392	I	KRIV	4.73	65.9
229	393	K	DKNSE	4.09	58.8

230	394	R	KRWN	4	56.9
231	395	E	LHEK	2.99	46.3
232	396	E	EDV	3.14	48.9
233	397	V	IVML	5.16	69.8
234	398	E	DEKQT	4.83	67.5
235	399	R	KRQEH	7.1	83.0
236	400	L	MLR	3	47.3
237	401	V	TVI	4.92	68.5
238	402	K	LMKRI	7.66	87.1
239	403	E	TENKQSH	8.03	89.1
240	404	V	MVEDTQ	9.54	92.6
241	405	P	NAPTEQS	9.02	91.3
242	406	E	VEP	2.63	40.8
243	407	E	EQVKRATS	8.78	90.7
244	408	Y	LYFW	3.59	53.4
245	409	S	PTSQHE	6.07	76.5
246	410	E	EDSPH	8.96	91.0
247	411	R	STVARKQDE	11.21	96.5
249	412	F	FM	2.07	30.2
250	413	S	STND	4.51	63.3
251	414	P	LTVPQSEDA	9.9	93.2
252	415	Q	EQNDAPK	7.45	85.9
253	416	A	LMATGS	6.47	78.8
254	417	R	KRHI	7.57	86.2
255	418	S	NSGTD	4.57	65.0
256	419	L	LIMVF	6.93	81.4
257	420	C	LCI	2.22	34.4
258	421	S	ESRNKQ	7.25	83.3
259	422	Q	MGQLA	6.86	80.7
260	423	L	LF	1.82	29.6
261	424	L	LP	2.21	33.8
262	425	C	QKHNSCTIAE	11.9	97.1
263	426	K	RK	1.69	27.7
264	427	D	DENSTK	7.06	82.6
265	428	P	VPSAI	6.89	81.0
266	429	A	SENADKGQ	9.96	93.6
267	430	E	KERQF	7.67	87.5
268	431	R	RS	1.68	22.8
269	432	L	L	1	19.0
270	433	G	G	1	19.0
271	434	C	CSMF	3.58	52.7

272	435	R	MKGLHYRQ	10.8	96.1
273	436	G	GSREND	7.6	86.5
274	437	G	NKRGDEV.	10.43	94.5
280	438	S	.GS	13.02	100.0
281	439	A	ASVGM.C	6.81	80.1
282	440	R	DKEQSRA	10.71	95.5
283	441	E	EAGDKM	6.97	81.7
284	442	V	VLIP	5.44	72.0
285	443	K	KMR	2.62	40.5
286	444	E	METQRAKS	8.16	89.4
287	445	H	HNSDQ	6.52	79.1
288	446	P	NEDPVSIH	9.36	92.3
289	447	L	FLIVW	6.03	76.2
290	448	F	F	1	19.0
291	449	K	CKRGHNQS	9.62	92.9
292	450	K	GDSAKNTEQ	10.76	95.8
302	451	L	IMLV	10.04	94.2
303	452	N	DNPSH	4.13	59.8
304	453	F	WF	2.32	36.3
305	454	K	HNQKSRPAG	7.9	88.4
306	455	R	QMHYRKS	7.69	87.8
307	456	L	VLMW	2.61	40.2
308	457	G	YFLGEDNS	8.17	89.7
309	458	A	IQLA.	4.01	57.2
310	459	G	QLRGN	4.82	67.2
311	460	M	KRHMLIP	6.83	80.4
312	461	L	Y.LVIP	6.01	75.9
313	462	E	TP.QEDIM	10.6	94.9
314	463	P	P.	1.7	28.6
315	464	P	P.	1.7	28.6
316	465	F	L.FW	2.91	45.3
317	466	K	VI.KC	7.42	85.5
318	467	P	P.	1.7	28.6
319	468	D	P.DK	2.91	45.3
320	469	P	R.PS	3.3	50.8
321	470	Q	GQEHRSNK	7.7	88.1
322	471	A	ERAVT	4.82	67.2
323	472	I	VI	2.9	44.7
324	473	Y	NY	1.69	27.7
325	474	C	AC	2.4	36.7
345	492	E	NLSPTED	7.29	84.2

346	493	P	DEPTHAKG	8.01	88.7
347	494	T	AGSCTNKDV	12.92	97.4
348	495	D	D	1	19.0
349	496	Q	QEDTKA	7.63	86.8
350	497	D	DQEINKTVA	9.16	91.6
351	498	F	LF	2.2	33.1
352	499	Y	YFC	3.74	55.3
353	500	Q	KERQTASGD	10.65	95.2
354	501	K	MNKQERA	7.42	85.5
355	502	F	F	1	19.0
356	503	A	STPAN	6.29	78.1
357	504	T	LTS	3.26	49.8
358	505	G	TVMG	4.27	62.4
359	506	S	IVSCANT	6.79	79.7
360	507	V	.SV	13.02	100.0

APPENDIX 2

List of oligonucleotide primers

Mutant	Primer pair sequences
GRK5 [NM_005308]	
F36A	(+) 5'-TGGAAGAAATCCTGAAG GCCC CTCACATTAGCCAGTGT (-) 5'-ACACTGGCTAATGTGAGGGGCCTTCAGGATTTCTTTCCA
P37A	(+) 5'-GAAATCCTGAAGTTC GCT CACATTAGCCAGTGT (-) 5'-ACACTGGCTAATGTGAGCGAACTTCAGGATTTC
H38A	(+) 5'-GAAATCCTGAAGTTCCT GCC ATTAGCCAGTGTGAAGAC (-) 5'-GTCTTCACACTGGCTAATGGCAGGGAACCTCAGGATTTC
C42A	(+) 5'-CCTCACATTAGCCAG GCT GAAGACCTCCGAAGG (-) 5'-CCTTCGGAGGTCTTCAGCCTGGCTAATGTGAGG
P61A	(+) 5'-TTATGTGACAAGCAG GCA ATCGGGAGGCTGCTT (-) 5'-AAGCAGCCTCCCGATTGCCTGCTTGTCACATAA
I62A	(+) 5'-TGTGACAAGCAGCCAG CCG GGGAGGCTGCTTTTC (-) 5'-GAAAAGCAGCCTCCCGGCTGGCTGCTTGTCACA
L66A	(+) 5'-CCAATCGGGAGGCT GCT TTCCGGCAGTTTTGT (-) 5'-ACAAAAGTCCGGAAAGCCAGCCTCCCGATTGG
R68A	(+) 5'-GGGAGGCTGCTTTT CGC GAGTTTTGTGAAACC (-) 5'-GGTTTCACAAAAGTGCAGGAAAGCAGCCTCCC
Q69A	(+) 5'-AGGCTGCTTTTCCGG GCG TTTTGTGAAACCAGG (-) 5'-CCTGGTTTTCACAAAACGCCCGGAAAGCAGCCT
D85A	(+) 5'-TACATTAGTTCCT GCC TCCGTGGCAGAATAT (-) 5'-ATATTCTGCCACGGAGGCCAGGAAGTGAATGTA
F166A	(+) 5'-TATCTGGACAGCAT GCT TTTGACCGCTTTCTC (-) 5'-GAGAAAGCGGTCAAAAGCCATGCTGTCCAGATA
R169A	(+) 5'-GACAGCATGTTTTT GAC GCCTTTCTCCAGTGGAAGTGG (-) 5'-CCACTTCCACTGGAGAAAGGCGTCAAAAACATGCTGTC
Q172A	(+) 5'-TTTGACCGCTTTCT CGC TGGATGGATTGGGAA (-) 5'-TTCCAATCCATCCACGCGAGAAAGCGGTCAAA
W173A	(+) 5'-GACCGCTTTCTCCAG GCG AAGTGGTTGGAAAGG (-) 5'-CCTTTCCAACCACTTCGCCTGGAGAAAGCGGTC
L176A	(+) 5'-CTCCAGTGGAAGTGG GCG GAAAGGCAACCGGTG (-) 5'-CACCGGTTGCCTTTCCGCCCACTTCCACTGGAG
P510A	(+) 5'-GGCTCTGTGTCCAT GCA TGGCAAAACGAGATG (-) 5'-CATCTCGTTTTGCCATGCGATGGACACAGAGCC
E514A	(+) 5'-ATCCCATGGCAAAAC GCG ATGATAGAAACAGAA (-) 5'-TTCTGTTTCTATCATCGGTTTTGCCATGGGAT
E517A	(+) 5'-CAAAACGAGATGATAG GCA ACAGAATGCTTTAAG (-) 5'-CTTAAAGCATTCTGTTGCTATCATCTCGTTTTG
T518A	(+) 5'-AACGAGATGATAGAA GCA GAATGCTTTAAGGAG (-) 5'-CTCCTTAAAGCATTCTGCTTCTATCATCTCGTT
Q172A-L176A	(+) 5'-CTC GCG TGGAAAGTGG GCG GAAAGGCAACCGGTG (-) 5'-CACCGGTTGCCTTTCCGCCCACTTCCACGCGAG
E104K	(+) 5'-CTGGGAGAGAAAGGGAAAG AAA ATTATGACCAAGTACCTC (-) 5'-GAGGTACTTGGTCATAATTTTCTTCCCTTTCTCTCCAG
R304H	(+) 5'-TTAGAAGACCTCCAC CAT GAGAACACCGTCTAC

	(-) 5'-GTAGACGGTGTTCTCATGGTGGAGGTCTTCTAA
G439E	(+) 5'-GGCTGCCAGGAGGAGGAGGCTGCAGAGGTCAAG (-) 5'-CTTGACCTCTGCAGCCTCCTCCTCCTGGCAGCC
S484A	(+) 5'-GACATCGAGCAGTTCCGCTACTGTGAAGGGCGTCAAT (-) 5'-ATTGACGCCCTTCACAGTGGCGAACTGCTCGATGTC
T485A	(+) 5'-GACATCGAGCAGTTCTCCGCTGTGAAGGGCGTCAAT (-) 5'-ATTGACGCCCTTCACAGCGGAGAACTGCTCGATGTC
S484A-T485A	(+) 5'-GACATCGAGCAGTTCCGCCGCTGTGAAGGGCGTCAAT (-) 5'-ATTGACGCCCTTCACAGCGGCGAACTGCTCGATGTC
GRK6 [NM_001004106]	
Y166A	(+) 5'-TACCTCGACAGCATCGCCTTCAACCGTTTCCTG (-) 5'-CAGGAAACGGTTGAAGGCGATGCTGTCGAGGTA
L66A-R69A	(+) 5'-CGGCTGGCCTTCCGAGCGTTCTGTGCCACGAGG (-) 5'-CCTCGTGGCACAGAACGCTCGGAAGGCCAGCCG
Q172A-W173A	(+) 5'-AACCGTTTCCTGGCGGCGAAGTGGCTGGAAAGG (-) 5'-CCTTTCCAGCCACTTCGCCGCCAGGAAACGGTT

Alignment generated using MultAlin (146).

GRK5MELENI VANTVILKAR EG..GGGKRK GSKSKWKKEIL KFHPHSQCED LRRITDRDYC SLCDKQPIGR LIFRQFC.ET RPLGECVIQF LDSVAEYEV	35	60	74
GRK6-AMELENI VANTVILKAR EG..GGGNRK GSKSKWRQML QFPHISQCEE RLSLERDYLH SICERQPIGR LIFREFC.AT RPELSRCVAF LDCVAEYEV			
GRK6-BMELENI VANTVILKAR EG..GGGNRK GSKSKWRQML QFPHISQCEE RLSLERDYLH SICERQPIGR LIFREFC.AT RPELSRCVAF LDCVAEYEV			
GRK4-AMELENI VANSILLKAR QG..GYGKKS GSKSKWKEIL TLPPVSQCE LKHSTEKDYS SLCDKQPIGR LIFRQFC.DT KPTLKRHIEF LDBAAEYEA			
GRK4-BMELENI VANSILLKAR QG..GYGKKS GSKSKWKEIL TLPPVSQCE LKHSTEKDYS SLCDKQPIGR LIFRQFC.DT KPTLKRHIEF LDBAAEYEA			
GRK4-CMELENI VANSILLKAR QG..GYGKKS GSKSKWKEIL TLPPVSQCE LKHSTEKDYS SLCDKQPIGR LIFRQFC.DT KPTLKRHIEF LDBAAEYEA			
GRK1	..MDFGSLTV VANSATIAAR GSFDSGSSQP SRDKKYLAKL KUPPLSKCES LRDSLSLEPE SVCLEQPIGK KIQQL.QS ASKHLPALEL WKDIEDYDTA			
GRK7	..MVMGALDNL LANTAYIQAR KPSDCDSKEL QRRR...SL AFLGLQCAE LFKUSLNFH SLCEQPIGR LIFRDEL.AT VFTFRKAATF LEDVQNWELA			
GRK2MADLEAV LADVSYLMAM ESKATPAAR ASKRIILPEP SIERSVMQ.KY LEDRGEVTEB KIF.SQKIGF LIFRDCSLNH LSEARPLVEF YEEIKKYEKL			
GRK3MADLEAV LADVSYLMAM ESKATPAAR ASKRIILPEP SIERSVMQ.KY LAERNEITFD KIF.NQKIGF LIFRDCCLNE INEAVPQVKF YEEIKKYEKL			
N terminus				
GRK5	..LFSACAQSVH EYLGEPPHE YLDSM.FDT LQWKW.ERQ. PVTKNTFRQY QFST..VKGV NLDHTDDDFY SKFSTGCVSI PQWEMETE CFKELNVFEG	160	490	510
GRK6-A	..LFQELTRLPH EYLSVAPFAD YLDSIFNF LQWKW.ERQ. PVTKNTFRQY QFST..VKGV ELEPTQDFY QKATGCVPI PQWEMETE CFQELNVFGL			
GRK6-B	..LFQELTRLPH EYLSVAPFAD YLDSIFNF LQWKW.ERQ. PVTKNTFRQY QFST..VKGV ELEPTQDFY QKATGCVPI PQWEMETE CFQELNVFGL			
GRK6-C	..LFQELTRLPH EYLSVAPFAD YLDSIFNF LQWKW.ERQ. PVTKNTFRQY QFST..VKGV ELEPTQDFY QKATGCVPI PQWEMETE CFQELNVFGL			
GRK4-A	..AFEECTRVAH NYLGEPPHE YQESSIFSF LQWKW.ERQ. PVTKNTFRHY QFSV..VKGI YLDTADEDFY ARFATGCVSI PQWEMESG CFKDINKSES			
GRK4-B	..AFEECTRVAH NYLGEPPHE YQESSIFSF LQWKW.ERQ. PVTKNTFRHY QFSV..VKGI YLDTADEDFY ARFATGCVSI PQWEMESG CFKDINKSES			
GRK4-C	..AFEECTRVAH NYLGEPPHE YQESSIFSF LQWKW.ERQ. PVTKNTFRHY QFSV..VKGI YLDTADEDFY ARFATGCVSI PQWEMESG CFKDINKSES			
GRK1	..LFQQLQATL AHLGAQPFQE YIGSLTFL LQWKW.EAQ. PMGEDWFLDF AST..VKGV ARDKTTEFF QFATGNCPI PQWEMETG CLINMPSEKE			
GRK7	..VTLAKAE..AM AFLQGPFFK FVTSAYDF LQWKLEMQ. PVSDDKFTFEP DFE..VKGV EFDDKQKQFF KNFATGAVPI AQOEIITETG LFEELN...			
GRK2	..LFQPYIEIC QNLRGDVQFK FIESDFTF CQWKNELNI HLTMNDFSVH SDEEDTKGI KULDSQELY RNFLP.TISE RWOQVAET. VFTDINAETG			
GRK3	..LFQPYIEIC ESLRGDIFQK FMESDFTF CQWKNELNI HLTMNDFSVH SDEEDTKGI KULDCQELY KNFLP.VISE RWOQVETP. VTEAVNADTQ			
a9				
a3				
a10				

hGPRK sequence alignment of the N-terminus and helices 3, 9, and 10.

Numbers above sequence correspond to GRK5 residue numbers. Highlighted residues from GRK5 were targeted for mutagenesis in this study. Gene accession numbers for GRKs (1-7) are: NM_005308, NM_001004106, NM_002082, NM_001004105, NM_182982, NM_001004056, NM_001004057, NM_002929, NM_139209, NM_001619, and NM_005160 respectively.

BIBLIOGRAPHY

BIBLIOGRAPHY

1. Krasel, C., J. P. Vilardaga, M. Bunemann, and M. J. Lohse. 2004. Kinetics of G-protein-coupled receptor signalling and desensitization. *Biochem Soc Trans* 32:1029-1031.
2. Benovic, J. L., M. Bouvier, M. G. Caron, and R. J. Lefkowitz. 1988. Regulation of adenylyl cyclase-coupled beta-adrenergic receptors. *Annu Rev Cell Biol* 4:405-428.
3. Johnson, M. 2006. Molecular mechanisms of beta(2)-adrenergic receptor function, response, and regulation. *J Allergy Clin Immunol* 117:18-24; quiz 25.
4. Anderson, G. P. 2006. Current issues with beta2-adrenoceptor agonists: pharmacology and molecular and cellular mechanisms. *Clin Rev Allergy Immunol* 31:119-130.
5. Karoor, V., K. Baltensperger, H. Paul, M. P. Czech, and C. C. Malbon. 1995. Phosphorylation of tyrosyl residues 350/354 of the beta-adrenergic receptor is obligatory for counterregulatory effects of insulin. *J Biol Chem* 270:25305-25308.
6. Karoor, V., and C. C. Malbon. 1996. Insulin-like growth factor receptor-1 stimulates phosphorylation of the beta2-adrenergic receptor in vivo on sites distinct from those phosphorylated in response to insulin. *J Biol Chem* 271:29347-29352.
7. O'Dowd, B. F., M. Hnatowich, M. G. Caron, R. J. Lefkowitz, and M. Bouvier. 1989. Palmitoylation of the human beta 2-adrenergic receptor. Mutation of Cys341 in the carboxyl tail leads to an uncoupled nonpalmitoylated form of the receptor. *J Biol Chem* 264:7564-7569.

8. Fredericks, Z. L., J. A. Pitcher, and R. J. Lefkowitz. 1996. Identification of the G protein-coupled receptor kinase phosphorylation sites in the human beta2-adrenergic receptor. *J Biol Chem* 271:13796-13803.
9. Seibold, A., B. Williams, Z. F. Huang, J. Friedman, R. H. Moore, B. J. Knoll, and R. B. Clark. 2000. Localization of the sites mediating desensitization of the beta(2)-adrenergic receptor by the GRK pathway. *Mol Pharmacol* 58:1162-1173.
10. Tran, T. M., J. Friedman, E. Qunaibi, F. Baameur, R. H. Moore, and R. B. Clark. 2004. Characterization of agonist stimulation of cAMP-dependent protein kinase and G protein-coupled receptor kinase phosphorylation of the beta2-adrenergic receptor using phosphoserine-specific antibodies. *Mol Pharmacol* 65:196-206.
11. Barak, L. S., J. Gilchrist, J. M. Becker, and K. M. Kim. 2006. Relationship between the G protein signaling and homologous desensitization of G protein-coupled receptors. *Biochem Biophys Res Commun* 339:695-700.
12. Dessauer, C. W. 2009. Adenylyl Cyclase-AKAP Complexes: The Next Dimension in cAMP Signaling. *Mol Pharmacol*.
13. Yuan, N., J. Friedman, B. S. Whaley, and R. B. Clark. 1994. cAMP-dependent protein kinase and protein kinase C consensus site mutations of the beta-adrenergic receptor. Effect on desensitization and stimulation of adenylylcyclase. *J Biol Chem* 269:23032-23038.
14. Clark, R. B., M. W. Kunkel, J. Friedman, T. J. Goka, and J. A. Johnson. 1988. Activation of cAMP-dependent protein kinase is required for heterologous desensitization of adenylyl cyclase in S49 wild-type lymphoma cells. *Proc Natl Acad Sci U S A* 85:1442-1446.

15. Green, D. A., and R. B. Clark. 1981. Adenylate cyclase coupling proteins are not essential for agonist-specific desensitization of lymphoma cells. *J Biol Chem* 256:2105-2108.
16. Daaka, Y., L. M. Luttrell, and R. J. Lefkowitz. 1997. Switching of the coupling of the beta2-adrenergic receptor to different G proteins by protein kinase A. *Nature* 390:88-91.
17. Sun, Y., J. Huang, Y. Xiang, M. Bastepe, H. Juppner, B. K. Kobilka, J. J. Zhang, and X. Y. Huang. 2007. Dosage-dependent switch from G protein-coupled to G protein-independent signaling by a GPCR. *EMBO J* 26:53-64.
18. Kunkel, M. W., J. Friedman, S. Shenolikar, and R. B. Clark. 1989. Cell-free heterologous desensitization of adenylyl cyclase in S49 lymphoma cell membranes mediated by cAMP-dependent protein kinase. *FASEB J* 3:2067-2074.
19. Johnson, J. A., R. B. Clark, J. Friedman, R. A. Dixon, and C. D. Strader. 1990. Identification of a specific domain in the beta-adrenergic receptor required for phorbol ester-induced inhibition of catecholamine-stimulated adenylyl cyclase. *Mol Pharmacol* 38:289-293.
20. Hausdorff, W. P., M. Bouvier, B. F. O'Dowd, G. P. Irons, M. G. Caron, and R. J. Lefkowitz. 1989. Phosphorylation sites on two domains of the beta 2-adrenergic receptor are involved in distinct pathways of receptor desensitization. *J Biol Chem* 264:12657-12665.
21. Rich, T. C., T. E. Tse, J. G. Rohan, J. Schaack, and J. W. Karpen. 2001. In vivo assessment of local phosphodiesterase activity using tailored cyclic nucleotide-gated channels as cAMP sensors. *J Gen Physiol* 118:63-78.

22. Xin, W., T. M. Tran, W. Richter, R. B. Clark, and T. C. Rich. 2008. Roles of GRK and PDE4 activities in the regulation of beta2 adrenergic signaling. *J Gen Physiol* 131:349-364.
23. Clark, R. B., T. J. Goka, M. A. Proll, and J. Friedman. 1986. Homologous desensitization of beta-adrenergic receptors in lymphoma cells is not altered by the inactivation of Ni (Gi), the inhibitory guanine nucleotide regulatory protein. *Biochem J* 235:399-405.
24. Trester-Zedlitz, M., A. Burlingame, B. Kobilka, and M. von Zastrow. 2005. Mass spectrometric analysis of agonist effects on posttranslational modifications of the beta-2 adrenoceptor in mammalian cells. *Biochemistry* 44:6133-6143.
25. Krasel, C., M. Bunemann, K. Lorenz, and M. J. Lohse. 2005. Beta-arrestin binding to the beta2-adrenergic receptor requires both receptor phosphorylation and receptor activation. *J Biol Chem* 280:9528-9535.
26. Pan, L., E. V. Gurevich, and V. V. Gurevich. 2003. The nature of the arrestin x receptor complex determines the ultimate fate of the internalized receptor. *J Biol Chem* 278:11623-11632.
27. Koenig, J. A., and J. M. Edwardson. 1997. Endocytosis and recycling of G protein-coupled receptors. *Trends Pharmacol Sci* 18:276-287.
28. Clark, R. B., B. J. Knoll, and R. Barber. 1999. Partial agonists and G protein-coupled receptor desensitization. *Trends Pharmacol Sci* 20:279-286.
29. Krueger, K. M., Y. Daaka, J. A. Pitcher, and R. J. Lefkowitz. 1997. The role of sequestration in G protein-coupled receptor resensitization. *Regulation of beta2-*

- adrenergic receptor dephosphorylation by vesicular acidification. *J Biol Chem* 272:5-8.
30. Tran, T. M., J. Friedman, F. Baameur, B. J. Knoll, R. H. Moore, and R. B. Clark. 2007. Characterization of beta2-adrenergic receptor dephosphorylation: Comparison with the rate of resensitization. *Mol Pharmacol* 71:47-60.
31. Shih, M., F. Lin, J. D. Scott, H. Y. Wang, and C. C. Malbon. 1999. Dynamic complexes of beta2-adrenergic receptors with protein kinases and phosphatases and the role of gravin. *J Biol Chem* 274:1588-1595.
32. Yu, S. S., R. J. Lefkowitz, and W. P. Hausdorff. 1993. Beta-adrenergic receptor sequestration. A potential mechanism of receptor resensitization. *J Biol Chem* 268:337-341.
33. Williams, B. R., R. Barber, and R. B. Clark. 2000. Kinetic analysis of agonist-induced down-regulation of the beta(2)-adrenergic receptor in BEAS-2B cells reveals high- and low-affinity components. *Mol Pharmacol* 58:421-430.
34. Liang, W., Q. Hoang, R. B. Clark, and P. H. Fishman. 2008. Accelerated dephosphorylation of the beta2-adrenergic receptor by mutation of the C-terminal lysines: effects on ubiquitination, intracellular trafficking, and degradation. *Biochemistry* 47:11750-11762.
35. Krupnick, J. G., and J. L. Benovic. 1998. The role of receptor kinases and arrestins in G protein-coupled receptor regulation. *Annu Rev Pharmacol Toxicol* 38:289-319.
36. Pitcher, J. A., N. J. Freedman, and R. J. Lefkowitz. 1998. G protein-coupled receptor kinases. *Annu Rev Biochem* 67:653-692.

37. Premont, R. T., and R. R. Gainetdinov. 2007. Physiological roles of G protein-coupled receptor kinases and arrestins. *Annu Rev Physiol* 69:511-534.
38. Inglese, J., N. J. Freedman, W. J. Koch, and R. J. Lefkowitz. 1993. Structure and mechanism of the G protein-coupled receptor kinases. *J Biol Chem* 268:23735-23738.
39. Pitcher, J. A., J. Inglese, J. B. Higgins, J. L. Arriza, P. J. Casey, C. Kim, J. L. Benovic, M. M. Kwatra, M. G. Caron, and R. J. Lefkowitz. 1992. Role of beta gamma subunits of G proteins in targeting the beta-adrenergic receptor kinase to membrane-bound receptors. *Science* 257:1264-1267.
40. Inglese, J., J. F. Glickman, W. Lorenz, M. G. Caron, and R. J. Lefkowitz. 1992. Isoprenylation of a protein kinase. Requirement of farnesylation/alpha-carboxyl methylation for full enzymatic activity of rhodopsin kinase. *J Biol Chem* 267:1422-1425.
41. Cha, K., C. Bruel, J. Inglese, and H. G. Khorana. 1997. Rhodopsin kinase: expression in baculovirus-infected insect cells, and characterization of post-translational modifications. *Proc Natl Acad Sci U S A* 94:10577-10582.
42. Stoffel, R. H., R. R. Randall, R. T. Premont, R. J. Lefkowitz, and J. Inglese. 1994. Palmitoylation of G protein-coupled receptor kinase, GRK6. Lipid modification diversity in the GRK family. *J Biol Chem* 269:27791-27794.
43. Stoffel, R. H., J. Inglese, A. D. Macrae, R. J. Lefkowitz, and R. T. Premont. 1998. Palmitoylation increases the kinase activity of the G protein-coupled receptor kinase, GRK6. *Biochemistry* 37:16053-16059.

44. Premont, R. T., A. D. Macrae, R. H. Stoffel, N. Chung, J. A. Pitcher, C. Ambrose, J. Inglese, M. E. MacDonald, and R. J. Lefkowitz. 1996. Characterization of the G protein-coupled receptor kinase GRK4. Identification of four splice variants. *J Biol Chem* 271:6403-6410.
45. Vatter, P., C. Stoesser, I. Samel, P. Gierschik, and B. Moepps. 2005. The variable C-terminal extension of G-protein-coupled receptor kinase 6 constitutes an accessorial autoregulatory domain. *FEBS J* 272:6039-6051.
46. Kunapuli, P., V. V. Gurevich, and J. L. Benovic. 1994. Phospholipid-stimulated autophosphorylation activates the G protein-coupled receptor kinase GRK5. *J Biol Chem* 269:10209-10212.
47. Pronin, A. N., C. V. Carman, and J. L. Benovic. 1998. Structure-function analysis of G protein-coupled receptor kinase-5. Role of the carboxyl terminus in kinase regulation. *J Biol Chem* 273:31510-31518.
48. Willets, J. M., R. A. Challiss, and S. R. Nahorski. 2003. Non-visual GRKs: are we seeing the whole picture? *Trends Pharmacol Sci* 24:626-633.
49. Pitcher, J. A., Z. L. Fredericks, W. C. Stone, R. T. Premont, R. H. Stoffel, W. J. Koch, and R. J. Lefkowitz. 1996. Phosphatidylinositol 4,5-bisphosphate (PIP₂)-enhanced G protein-coupled receptor kinase (GRK) activity. Location, structure, and regulation of the PIP₂ binding site distinguishes the GRK subfamilies. *J Biol Chem* 271:24907-24913.
50. Johnson, L. R., M. G. Scott, and J. A. Pitcher. 2004. G protein-coupled receptor kinase 5 contains a DNA-binding nuclear localization sequence. *Mol Cell Biol* 24:10169-10179.

51. Martini, J. S., P. Raake, L. E. Vinge, B. R. DeGeorge, Jr., J. K. Chuprun, D. M. Harris, E. Gao, A. D. Eckhart, J. A. Pitcher, and W. J. Koch. 2008. Uncovering G protein-coupled receptor kinase-5 as a histone deacetylase kinase in the nucleus of cardiomyocytes. *Proc Natl Acad Sci U S A* 105:12457-12462.
52. Barthet, G., G. Carrat, E. Cassier, B. Barker, F. Gaven, M. Pillot, B. Framery, L. P. Pellissier, J. Augier, D. S. Kang, S. Claeysen, E. Reiter, J. L. Baneres, J. L. Benovic, P. Marin, J. Bockaert, and A. Dumuis. 2009. Beta-arrestin1 phosphorylation by GRK5 regulates G protein-independent 5-HT₄ receptor signalling. *EMBO J* 28:2706-2718.
53. Carman, C. V., T. Som, C. M. Kim, and J. L. Benovic. 1998. Binding and phosphorylation of tubulin by G protein-coupled receptor kinases. *J Biol Chem* 273:20308-20316.
54. Pronin, A. N., A. J. Morris, A. Surguchov, and J. L. Benovic. 2000. Synucleins are a novel class of substrates for G protein-coupled receptor kinases. *J Biol Chem* 275:26515-26522.
55. Dinudom, A., A. B. Fotia, R. J. Lefkowitz, J. A. Young, S. Kumar, and D. I. Cook. 2004. The kinase Grk2 regulates Nedd4/Nedd4-2-dependent control of epithelial Na⁺ channels. *Proc Natl Acad Sci U S A* 101:11886-11890.
56. Carman, C. V., J. L. Parent, P. W. Day, A. N. Pronin, P. M. Sternweis, P. B. Wedegaertner, A. G. Gilman, J. L. Benovic, and T. Kozasa. 1999. Selective regulation of G α (q/11) by an RGS domain in the G protein-coupled receptor kinase, GRK2. *J Biol Chem* 274:34483-34492.

57. Carman, C. V., M. P. Lisanti, and J. L. Benovic. 1999. Regulation of G protein-coupled receptor kinases by caveolin. *J Biol Chem* 274:8858-8864.
58. Penela, P., C. Ribas, and F. Mayor, Jr. 2003. Mechanisms of regulation of the expression and function of G protein-coupled receptor kinases. *Cell Signal* 15:973-981.
59. Premont, R. T., S. J. Perry, R. Schmalzigaug, J. T. Roseman, Y. Xing, and A. Claing. 2004. The GIT/PIX complex: an oligomeric assembly of GIT family ARF GTPase-activating proteins and PIX family Rac1/Cdc42 guanine nucleotide exchange factors. *Cell Signal* 16:1001-1011.
60. Penela, P., A. Elorza, S. Sarnago, and F. Mayor, Jr. 2001. Beta-arrestin- and c-Src-dependent degradation of G-protein-coupled receptor kinase 2. *EMBO J* 20:5129-5138.
61. Pronin, A. N., and J. L. Benovic. 1997. Regulation of the G protein-coupled receptor kinase GRK5 by protein kinase C. *J Biol Chem* 272:3806-3812.
62. Horner, T. J., S. Osawa, M. D. Schaller, and E. R. Weiss. 2005. Phosphorylation of GRK1 and GRK7 by cAMP-dependent protein kinase attenuates their enzymatic activities. *J Biol Chem* 280:28241-28250.
63. Palczewski, K., J. Buczylo, P. Van Hooser, S. A. Carr, M. J. Huddleston, and J. W. Crabb. 1992. Identification of the autophosphorylation sites in rhodopsin kinase. *J Biol Chem* 267:18991-18998.
64. Buczylo, J., C. Gutmann, and K. Palczewski. 1991. Regulation of rhodopsin kinase by autophosphorylation. *Proc Natl Acad Sci U S A* 88:2568-2572.

65. Chen, C. K., J. Inglese, R. J. Lefkowitz, and J. B. Hurley. 1995. Ca(2+)-dependent interaction of recoverin with rhodopsin kinase. *J Biol Chem* 270:18060-18066.
66. Pronin, A. N., D. K. Satpaev, V. Z. Slepak, and J. L. Benovic. 1997. Regulation of G protein-coupled receptor kinases by calmodulin and localization of the calmodulin binding domain. *J Biol Chem* 272:18273-18280.
67. Penn, R. B., A. N. Pronin, and J. L. Benovic. 2000. Regulation of G protein-coupled receptor kinases. *Trends Cardiovasc Med* 10:81-89.
68. Lodowski, D. T., J. F. Barnhill, R. M. Pyskadlo, R. Ghirlando, R. Sterne-Marr, and J. J. Tesmer. 2005. The role of G beta gamma and domain interfaces in the activation of G protein-coupled receptor kinase 2. *Biochemistry* 44:6958-6970.
69. Lodowski, D. T., J. A. Pitcher, W. D. Capel, R. J. Lefkowitz, and J. J. Tesmer. 2003. Keeping G proteins at bay: a complex between G protein-coupled receptor kinase 2 and Gbetagamma. *Science* 300:1256-1262.
70. Tesmer, V. M., T. Kawano, A. Shankaranarayanan, T. Kozasa, and J. J. Tesmer. 2005. Snapshot of activated G proteins at the membrane: the Galphaq-GRK2-Gbetagamma complex. *Science* 310:1686-1690.
71. Sallese, M., S. Mariggio, E. D'Urbano, L. Iacovelli, and A. De Blasi. 2000. Selective regulation of Gq signaling by G protein-coupled receptor kinase 2: direct interaction of kinase N terminus with activated galphaq. *Mol Pharmacol* 57:826-831.
72. Sterne-Marr, R., G. K. Dhami, J. J. Tesmer, and S. S. Ferguson. 2004. Characterization of GRK2 RH domain-dependent regulation of GPCR coupling to heterotrimeric G proteins. *Methods Enzymol* 390:310-336.

73. Lodowski, D. T., V. M. Tesmer, J. L. Benovic, and J. J. Tesmer. 2006. The structure of G protein-coupled receptor kinase (GRK)-6 defines a second lineage of GRKs. *J Biol Chem* 281:16785-16793.
74. Singh, P., B. Wang, T. Maeda, K. Palczewski, and J. J. Tesmer. 2008. Structures of rhodopsin kinase in different ligand states reveal key elements involved in G protein-coupled receptor kinase activation. *J Biol Chem* 283:14053-14062.
75. Clark, R. B., and T. C. Rich. 2003. Probing the roles of protein kinases in G-protein-coupled receptor desensitization. *Mol Pharmacol* 64:1-3.
76. Benovic, J. L., A. DeBlasi, W. C. Stone, M. G. Caron, and R. J. Lefkowitz. 1989. Beta-adrenergic receptor kinase: primary structure delineates a multigene family. *Science* 246:235-240.
77. Benovic, J. L., J. J. Onorato, J. L. Arriza, W. C. Stone, M. Lohse, N. A. Jenkins, D. J. Gilbert, N. G. Copeland, M. G. Caron, and R. J. Lefkowitz. 1991. Cloning, expression, and chromosomal localization of beta-adrenergic receptor kinase 2. A new member of the receptor kinase family. *J Biol Chem* 266:14939-14946.
78. Benovic, J. L., and J. Gomez. 1993. Molecular cloning and expression of GRK6. A new member of the G protein-coupled receptor kinase family. *J Biol Chem* 268:19521-19527.
79. Premont, R. T., W. J. Koch, J. Inglese, and R. J. Lefkowitz. 1994. Identification, purification, and characterization of GRK5, a member of the family of G protein-coupled receptor kinases. *J Biol Chem* 269:6832-6841.
80. Kohout, T. A., and R. J. Lefkowitz. 2003. Regulation of G protein-coupled receptor kinases and arrestins during receptor desensitization. *Mol Pharmacol* 63:9-18.

81. Violin, J. D., X. R. Ren, and R. J. Lefkowitz. 2006. G-protein-coupled receptor kinase specificity for beta-arrestin recruitment to the beta2-adrenergic receptor revealed by fluorescence resonance energy transfer. *J Biol Chem* 281:20577-20588.
82. Violin, J. D., L. M. DiPilato, N. Yildirim, T. C. Elston, J. Zhang, and R. J. Lefkowitz. 2008. beta2-adrenergic receptor signaling and desensitization elucidated by quantitative modeling of real time cAMP dynamics. *J Biol Chem* 283:2949-2961.
83. Winstel, R., H. G. Ihlenfeldt, G. Jung, C. Krasel, and M. J. Lohse. 2005. Peptide inhibitors of G protein-coupled receptor kinases. *Biochem Pharmacol* 70:1001-1008.
84. Shenoy, S. K., M. T. Drake, C. D. Nelson, D. A. Houtz, K. Xiao, S. Madabushi, E. Reiter, R. T. Premont, O. Lichtarge, and R. J. Lefkowitz. 2006. beta-arrestin-dependent, G protein-independent ERK1/2 activation by the beta2 adrenergic receptor. *J Biol Chem* 281:1261-1273.
85. Metaye, T., H. Gibelin, R. Perdrisot, and J. L. Kraimps. 2005. Pathophysiological roles of G-protein-coupled receptor kinases. *Cell Signal* 17:917-928.
86. Tran, T. M., R. Jorgensen, and R. B. Clark. 2007. Phosphorylation of the beta2-adrenergic receptor in plasma membranes by intrinsic GRK5. *Biochemistry* 46:14438-14449.
87. Palczewski, K., J. Buczylo, M. W. Kaplan, A. S. Polans, and J. W. Crabb. 1991. Mechanism of rhodopsin kinase activation. *J Biol Chem* 266:12949-12955.
88. Buczylo, J., J. C. Saari, R. K. Crouch, and K. Palczewski. 1996. Mechanisms of opsin activation. *J Biol Chem* 271:20621-20630.

89. Palczewski, K., J. Buczylo, L. Lebiada, J. W. Crabb, and A. S. Polans. 1993. Identification of the N-terminal region in rhodopsin kinase involved in its interaction with rhodopsin. *J Biol Chem* 268:6004-6013.
90. Dhami, G. K., P. H. Anborgh, L. B. Dale, R. Sterne-Marr, and S. S. Ferguson. 2002. Phosphorylation-independent regulation of metabotropic glutamate receptor signaling by G protein-coupled receptor kinase 2. *J Biol Chem* 277:25266-25272.
91. Dhami, G. K., L. B. Dale, P. H. Anborgh, K. E. O'Connor-Halligan, R. Sterne-Marr, and S. S. Ferguson. 2004. G Protein-coupled receptor kinase 2 regulator of G protein signaling homology domain binds to both metabotropic glutamate receptor 1a and Galphaq to attenuate signaling. *J Biol Chem* 279:16614-16620.
92. Noble, B., L. A. Kallal, M. H. Pausch, and J. L. Benovic. 2003. Development of a yeast bioassay to characterize G protein-coupled receptor kinases. Identification of an NH₂-terminal region essential for receptor phosphorylation. *J Biol Chem* 278:47466-47476.
93. Thiyagarajan, M. M., R. P. Stracquatanio, A. N. Pronin, D. S. Evanko, J. L. Benovic, and P. B. Wedegaertner. 2004. A predicted amphipathic helix mediates plasma membrane localization of GRK5. *J Biol Chem* 279:17989-17995.
94. Palczewski, K., H. Ohguro, R. T. Premont, and J. Inglese. 1995. Rhodopsin kinase autophosphorylation. Characterization of site-specific mutations. *J Biol Chem* 270:15294-15298.
95. Higgins, M. K., D. D. Oprian, and G. F. Schertler. 2006. Recoverin binds exclusively to an amphipathic peptide at the N terminus of rhodopsin kinase, inhibiting

- rhodopsin phosphorylation without affecting catalytic activity of the kinase. *J Biol Chem* 281:19426-19432.
96. Torisawa, A., D. Arinobu, S. Tachibanaki, and S. Kawamura. 2008. Amino acid residues in GRK1/GRK7 responsible for interaction with S-modulin/recoverin. *Photochem Photobiol* 84:823-830.
97. Huang, C. C., K. Yoshino-Koh, and J. J. Tesmer. 2009. A surface of the kinase domain critical for the allosteric activation of G protein-coupled receptor kinases. *J Biol Chem* 284:17206-17215.
98. Sterne-Marr, R., J. J. Tesmer, P. W. Day, R. P. Stracquatano, J. A. Cilente, K. E. O'Connor, A. N. Pronin, J. L. Benovic, and P. B. Wedegaertner. 2003. G protein-coupled receptor Kinase 2/G alpha q/11 interaction. A novel surface on a regulator of G protein signaling homology domain for binding G alpha subunits. *J Biol Chem* 278:6050-6058.
99. Day, P. W., J. J. Tesmer, R. Sterne-Marr, L. C. Freeman, J. L. Benovic, and P. B. Wedegaertner. 2004. Characterization of the GRK2 binding site of Galphaq. *J Biol Chem* 279:53643-53652.
100. Krasel, C., S. Dammeier, R. Winstel, J. Brockmann, H. Mischak, and M. J. Lohse. 2001. Phosphorylation of GRK2 by protein kinase C abolishes its inhibition by calmodulin. *J Biol Chem* 276:1911-1915.
101. Cong, M., S. J. Perry, F. T. Lin, I. D. Fraser, L. A. Hu, W. Chen, J. A. Pitcher, J. D. Scott, and R. J. Lefkowitz. 2001. Regulation of membrane targeting of the G protein-coupled receptor kinase 2 by protein kinase A and its anchoring protein AKAP79. *J Biol Chem* 276:15192-15199.

102. Carman, C. V., L. S. Barak, C. Chen, L. Y. Liu-Chen, J. J. Onorato, S. P. Kennedy, M. G. Caron, and J. L. Benovic. 2000. Mutational analysis of Gbetagamma and phospholipid interaction with G protein-coupled receptor kinase 2. *J Biol Chem* 275:10443-10452.
103. Eichmann, T., K. Lorenz, M. Hoffmann, J. Brockmann, C. Krasel, M. J. Lohse, and U. Quitterer. 2003. The amino-terminal domain of G-protein-coupled receptor kinase 2 is a regulatory Gbeta gamma binding site. *J Biol Chem* 278:8052-8057.
104. Mariggio, S., C. Garcia-Hoz, S. Sarnago, A. De Blasi, F. Mayor, Jr., and C. Ribas. 2006. Tyrosine phosphorylation of G-protein-coupled-receptor kinase 2 (GRK2) by c-Src modulates its interaction with Galphaq. *Cell Signal* 18:2004-2012.
105. Sterne-Marr, R., P. A. Leahey, J. E. Bresee, H. M. Dickson, W. Ho, M. J. Ragusa, R. M. Donnelly, S. M. Amie, J. A. Krywy, E. D. Brookins-Danz, S. C. Orakwue, M. J. Carr, K. Yoshino-Koh, Q. Li, and J. J. Tesmer. 2009. GRK2 activation by receptors: role of the kinase large lobe and carboxyl-terminal tail. *Biochemistry* 48:4285-4293.
106. Pao, C. S., B. L. Barker, and J. L. Benovic. 2009. Role of the amino terminus of G protein-coupled receptor kinase 2 in receptor phosphorylation. *Biochemistry* 48:7325-7333.
107. Freeman, J. L., E. M. De La Cruz, T. D. Pollard, R. J. Lefkowitz, and J. A. Pitcher. 1998. Regulation of G protein-coupled receptor kinase 5 (GRK5) by actin. *J Biol Chem* 273:20653-20657.
108. Gan, X., Z. Ma, N. Deng, J. Wang, J. Ding, and L. Li. 2004. Involvement of the C-terminal proline-rich motif of G protein-coupled receptor kinases in recognition of activated rhodopsin. *J Biol Chem* 279:49741-49746.

109. Liggett, S. B., S. Cresci, R. J. Kelly, F. M. Syed, S. J. Matkovich, H. S. Hahn, A. Diwan, J. S. Martini, L. Sparks, R. R. Parekh, J. A. Spertus, W. J. Koch, S. L. Kardia, and G. W. Dorn, 2nd. 2008. A GRK5 polymorphism that inhibits beta-adrenergic receptor signaling is protective in heart failure. *Nat Med* 14:510-517.
110. Eckhart, A. D., T. Ozaki, H. Tevaearai, H. A. Rockman, and W. J. Koch. 2002. Vascular-targeted overexpression of G protein-coupled receptor kinase-2 in transgenic mice attenuates beta-adrenergic receptor signaling and increases resting blood pressure. *Mol Pharmacol* 61:749-758.
111. Gurevich, V. V., and E. V. Gurevich. 2006. The structural basis of arrestin-mediated regulation of G-protein-coupled receptors. *Pharmacol Ther* 110:465-502.
112. Esposito, G., A. Rapacciuolo, S. V. Naga Prasad, and H. A. Rockman. 2002. Cardiac hypertrophy: role of G protein-coupled receptors. *J Card Fail* 8:S409-414.
113. Prasad, S. V., J. Nienaber, and H. A. Rockman. 2002. G-protein-coupled receptor function in heart failure. *Cold Spring Harb Symp Quant Biol* 67:439-444.
114. Rockman, H. A., W. J. Koch, and R. J. Lefkowitz. 2002. Seven-transmembrane-spanning receptors and heart function. *Nature* 415:206-212.
115. Hata, J. A., and W. J. Koch. 2003. Phosphorylation of G protein-coupled receptors: GPCR kinases in heart disease. *Mol Interv* 3:264-272.
116. Kunapuli, P., J. J. Onorato, M. M. Hosey, and J. L. Benovic. 1994. Expression, purification, and characterization of the G protein-coupled receptor kinase GRK5. *J Biol Chem* 269:1099-1105.
117. Benovic, J. L., J. Onorato, M. J. Lohse, H. G. Dohlman, C. Staniszewski, M. G. Caron, and R. J. Lefkowitz. 1990. Synthetic peptides of the hamster beta 2-

- adrenoceptor as substrates and inhibitors of the beta-adrenoceptor kinase. *Br J Clin Pharmacol* 30 Suppl 1:3S-12S.
118. Smrcka, A. V., D. M. Lehmann, and A. L. Dessal. 2008. G protein betagamma subunits as targets for small molecule therapeutic development. *Comb Chem High Throughput Screen* 11:382-395.
119. Jastrzebska, B., M. Golczak, D. Fotiadis, A. Engel, and K. Palczewski. 2009. Isolation and functional characterization of a stable complex between photoactivated rhodopsin and the G protein, transducin. *FASEB J* 23:371-381.
120. Scheerer, P., J. H. Park, P. W. Hildebrand, Y. J. Kim, N. Krauss, H. W. Choe, K. P. Hofmann, and O. P. Ernst. 2008. Crystal structure of opsin in its G-protein-interacting conformation. *Nature* 455:497-502.
121. Morgan, D. H., D. M. Kristensen, D. Mittelman, and O. Lichtarge. 2006. ET viewer: an application for predicting and visualizing functional sites in protein structures. *Bioinformatics* 22:2049-2050.
122. Madabushi, S., H. Yao, M. Marsh, D. M. Kristensen, A. Philippi, M. E. Sowa, and O. Lichtarge. 2002. Structural clusters of evolutionary trace residues are statistically significant and common in proteins. *J Mol Biol* 316:139-154.
123. Yao, H., D. M. Kristensen, I. Mihalek, M. E. Sowa, C. Shaw, M. Kimmel, L. Kavraki, and O. Lichtarge. 2003. An accurate, sensitive, and scalable method to identify functional sites in protein structures. *J Mol Biol* 326:255-261.
124. Lichtarge, O., and M. E. Sowa. 2002. Evolutionary predictions of binding surfaces and interactions. *Curr Opin Struct Biol* 12:21-27.

125. Loudon, R. P., and J. L. Benovic. 1994. Expression, purification, and characterization of the G protein-coupled receptor kinase GRK6. *J Biol Chem* 269:22691-22697.
126. Wilden, U., and H. Kuhn. 1982. Light-dependent phosphorylation of rhodopsin: number of phosphorylation sites. *Biochemistry* 21:3014-3022.
127. Ridge, K. D., J. P. Marino, T. Ngo, E. Ramon, D. M. Brabazon, and N. G. Abdulaev. 2006. NMR analysis of rhodopsin-transducin interactions. *Vision Res* 46:4482-4492.
128. Huang, C. C., K. Yoshino-Koh, and J. J. Tesmer. 2009. A surface of the kinase domain critical for the allosteric activation of G protein-coupled receptor kinases. *J Biol Chem*.
129. Millman, E. E., J. L. Rosenfeld, D. J. Vaughan, J. Nguyen, W. Dai, E. Alpizar-Foster, R. B. Clark, B. J. Knoll, and R. H. Moore. 2004. Endosome sorting of beta 2-adrenoceptors is GRK5 independent. *Br J Pharmacol* 141:277-284.
130. Samama, P., S. Cotecchia, T. Costa, and R. J. Lefkowitz. 1993. A mutation-induced activated state of the beta 2-adrenergic receptor. Extending the ternary complex model. *J Biol Chem* 268:4625-4636.
131. Whaley, B. S., N. Yuan, L. Birnbaumer, R. B. Clark, and R. Barber. 1994. Differential expression of the beta-adrenergic receptor modifies agonist stimulation of adenylyl cyclase: a quantitative evaluation. *Mol Pharmacol* 45:481-489.
132. Pronin, A. N., R. P. Loudon, and J. L. Benovic. 2002. Characterization of G protein-coupled receptor kinases. *Methods Enzymol* 343:547-559.
133. Gether, U., and B. K. Kobilka. 1998. G protein-coupled receptors. II. Mechanism of agonist activation. *J Biol Chem* 273:17979-17982.

134. Munoz, V., and L. Serrano. 1994. Intrinsic secondary structure propensities of the amino acids, using statistical phi-psi matrices: comparison with experimental scales. *Proteins* 20:301-311.
135. Kalisman, N., A. Levi, T. Maximova, D. Reshef, S. Zafriri-Lynn, Y. Gleyzer, and C. Keasar. 2005. MESHI: a new library of Java classes for molecular modeling. *Bioinformatics* 21:3931-3932.
136. Munoz, V., and L. Serrano. 1994. Elucidating the folding problem of helical peptides using empirical parameters. *Nat Struct Biol* 1:399-409.
137. Munoz, V., and L. Serrano. 1995. Elucidating the folding problem of helical peptides using empirical parameters. III. Temperature and pH dependence. *J Mol Biol* 245:297-308.
138. Munoz, V., and L. Serrano. 1995. Elucidating the folding problem of helical peptides using empirical parameters. II. Helix macrodipole effects and rational modification of the helical content of natural peptides. *J Mol Biol* 245:275-296.
139. Houston, M. E., Jr., C. L. Gannon, C. M. Kay, and R. S. Hodges. 1995. Lactam bridge stabilization of alpha-helical peptides: ring size, orientation and positional effects. *J Pept Sci* 1:274-282.
140. Polinsky, A., M. G. Cooney, A. Toy-Palmer, G. Osapay, and M. Goodman. 1992. Synthesis and conformational properties of the lanthionine-bridged opioid peptide [D-AlaL2,AlaL5]enkephalin as determined by NMR and computer simulations. *J Med Chem* 35:4185-4194.

141. Arshady, R., E. Atherton, D. L. J. Clive, and R. C. Sheppard. 1981. Peptide synthesis. Part 1. Preparation and use of polar supports based on poly(dimethylacrylamide). *J. Chem. Soc., Perkin Trans.* 1:529-537.
142. Pearson, D. A., M. Blanchette, M. L. Baker, and C. A. Guindon. 1989. Trialkylsilanes as scavengers for the trifluoroacetic acid deblocking of protecting groups in peptide synthesis. *Tetrahedron Lett.* 30:2739-2742.
143. Jarver, P., and U. Langel. 2006. Cell-penetrating peptides--a brief introduction. *Biochim Biophys Acta* 1758:260-263.
144. Wadia, J. S., and S. F. Dowdy. 2002. Protein transduction technology. *Curr Opin Biotechnol* 13:52-56.
145. Wadia, J. S., and S. F. Dowdy. 2005. Transmembrane delivery of protein and peptide drugs by TAT-mediated transduction in the treatment of cancer. *Adv Drug Deliv Rev* 57:579-596.
146. Corpet, F. 1988. Multiple sequence alignment with hierarchical clustering. *Nucleic Acids Res* 16:10881-10890.

VITA

Faiza Baameur was born on July 5, 1972, in Oran, Algeria. She graduated from Maraval High School in 1988 and attended the University of Oran in Oran, Algeria majoring in Organic Chemistry. She received her Bachelor of Science degree in 1993. In the fall of 1995, she entered the Graduate Program in Physical Chemistry at the University of Oran and received a Master of Science degree in 2000. Faiza joined the Graduate School of Biomedical Sciences at the University of Texas Health Science Center in Houston, TX the fall 2004. She joined the Cell and Regulatory Biology Program as a Pharmacology student and will graduate with her Doctorate of philosophy in December of 2009.

Permanent Address:

4009 McDermid Dr

Houston, TX 77025